universität wien

DIPLOMARBEIT

Titel der Diplomarbeit

„Analysis of senescence markers and impact of drug-induced senescent neuroblastoma cells on tumour cell proliferation and immunomodulation “

Verfasserin

Nelli Frank

angestrebter akademischer Grad

Magistra der Naturwissenschaften (Mag.rer.nat.)

Wien, 2012

Studienkennzahl (lt. Studienblatt):	A 490
Studienrichtung (lt. Studienblatt):	Diplomstudium Molekulare Biologie
Betreuer:	Univ. Prof. Dr. Roland Foisner

Kurzfassung

Zelluläre Seneszenz ist ein Zustand, der durch irreversiblen Proliferationsarrest charakterisiert ist, durch unterschiedliche Arten von intrinsischem und extrinsischem Stress ausgelöst werden kann und des Weiteren mit Tumorsuppression assoziiert ist. Seneszente Zellen bleiben metabolisch aktiv und sezernieren viele Faktoren. Dazu gehören Wachstumsfaktoren und Zytokine, welche die umgebenden Zellen beeinflussen und deren Zellwachstum fördern können.

Das Neuroblastom (NB) ist ein Tumor des vegetativen Nervensystems und der häufigste extrakraniale solide Tumor im Kindesalter. Die Amplifikation des *MYCN* Onkogens ist charakteristisch für aggressive Formen des Neuroblastoms und ein hoch-signifikanter Marker für eine schlechte Prognose. Kürzlich wurde gezeigt, dass in *MYCN* amplifizierten NB-Zellen, die aus Primärtumoren von Stadium 3 oder 4 Patienten stammen, durch 6-8 wöchige Behandlung mit Hydroxyurea *in vitro* Seneszenz induziert werden kann. Nach Behandlung mit Hydroxyurea reduzieren seneszente NB-Zellen ihre *MYCN* Kopien Zahl und den NB-Tumormarker GD2, während die Oberflächenmoleküle CD44 und MHC Klasse I hochreguliert werden.

Das Immunsystem spielt eine wesentliche Rolle in der Vernichtung von Tumorzellen und durch die Produktion von inflammatorischen Faktoren beeinflusst es auch den Krankheitsverlauf. Zytotoxische T-Lymphozyten, natürliche Killerzellen und T-Helferzellen tragen signifikant zur Eradikation von Tumorzellen bei. Es wurde von anderen Arbeitsgruppen gezeigt, dass NB-Zellen nur gering immunogen sind und daher dem Immunsystem ausweichen können. Die Rolle dieser Immunzellen in Therapie-induzierter Seneszenz beim Neuroblastom ist nicht bekannt.

Unser Ziel war es zu analysieren, ob Seneszenz in *MYCN* amplifizierten NB-Zellen durch andere Medikamente, z.B. Camptothecin und Bromdesoxyuridin, *in vitro* schneller induziert werden kann als durch Behandlung mit Hydroxyurea und wie diese Medikamente im Vergleich zu den unbehandelten Kontrollzellen das Wachstumsverhalten, die Proliferation, *MYCN* Kopien Zahl, den GD2 Gehalt und die CD44 und MHC Klasse I Tumormarker Expression verändern. Um zu analysieren, welche molekularen Wege der Seneszenz Induktion durch Behandlung mit den verschiedenen Medikamenten zugrunde liegen, haben wir die p16, p53 und CDK2 Expression mittels Western Blot bestimmt. Weiters haben wir in einer Co-Kultur erforscht, ob seneszente NB-Zellen die Proliferation und die Tumormarker Expression von nicht-seneszenten Zellen in der Umgebung beeinflussen. Darüber hinaus haben wir auch Co-Kulturen mit nicht-seneszenten bzw. seneszenten NB-Zellen und T-Zellen angesetzt, um herauszufinden, ob seneszente NB-Zellen die Proliferation von T-Zellen erlauben.

Wir konnten zeigen, dass Camptothecin und Bromdesoxyuridin Behandlung schon nach 3 Wochen zu Seneszenz in *MYCN* amplifizierten NB-Zellen *in vitro* geführt hat. Dies konnte durch Untersuchung der Morphologie, SA-β-Gal Färbung, Reduktion der *MYCN* Kopien Zahl und des GD2 Levels und einer Hochregulierung von CD44 und MHC I gezeigt werden. Diese Eigenschaften waren ähnlich wie bei den spontan seneszenten und Hydroxyurea behandelten seneszenten NB-Zellen. Weiterhin weisen unsere Daten, im Hinblick auf $CD8^+$ und $CD4^+$ T-Zellen, auf eine immunstimulierende Rolle der seneszenten NB Tumorzellen hin. Die Induktion von Seneszenz in *MYCN* amplifizierten NB-Zellen, durch Behandlung mit Medikamenten in geringen Konzentrationen, zeigt Potential im Hinblick auf Einschränkung des Tumorwachstums, Inhibierung des aggressiven Phänotyps in NB-Zellen und Erhöhung der Immunogenität von NB Tumorzellen. Diese Eigenschaften, die durch die Seneszenz Induktion ausgelöst werden, könnten in der klinischen Anwendung wichtig sein, um ein Tumorrezidiv in NB Patienten zu verhindern.

Abstract

Cellular senescence, a state of permanent cell-cycle arrest, can be triggered by various types of intrinsic and extrinsic stress and is associated with tumour suppression. However, senescent cells remain metabolically active and produce many secreted factors, such as growth factors and cytokines, which affect nearby cells and may also promote their proliferation. Neuroblastoma (NB) is a tumour derived from cells of the sympathetic nervous system and comprises the most common extra cranial solid tumour of childhood. Amplification of the *MYCN* oncogene characterizes aggressive NBs and is a prediction marker for poor outcome. Recently, it was shown that *in vitro* 6-8 weeks hydroxyurea treatment is a potent senescence inducing application in *MYCN* amplified neuroblastoma cell lines, derived from the primary tumour of stage 3 or 4 patients. Senescent NB-cells decrease *MYCN* copy number and the NB tumour marker GD2, while the surface molecules CD44 and MHC class I are upregulated upon hydroxyurea treatment. The immune system plays an important part in eradication of tumour cells, but also by producing inflammatory signals and thus influencing disease progression. Cytotoxic T-lymphocytes, Natural killer cells and $CD4^+$ T-cells significantly contribute to tumour cell erradication. It has been shown, that NB-cells are low immunogenic and therefore evade the immune system. The role of these immune cells in therapy-induced senescence in neuroblastoma is not known.

We aimed to analyze, whether senescene in *MYCN* amplified NB-cells can be induced faster than with hydroxyurea by using drugs such as camptothecin and bromodeoxyuridine and how those drugs change the growth behaviour, proliferation, *MYCN* copy number, GD2 level and tumour marker expression CD44 and MHC class I compared to control cells. In order to analyse the underlying cellular pathways leading to senescence by these different drug treatments we have evaluated p16, p53 and CDK2 by western blot. Furthermore, we studied whether senescent NB-cells modulate proliferation and tumour marker expression of nearby non-senescent cells in co-culture. Additionally, we co-cultured T-cells with non-senescent and senescent NB-cells to see whether senescent NB-cells allow T-cell proliferation.

We could show, that camptothecin and bromodeoxyuridine treatment induced senescence already after 3 weeks in *MYCN* amplified NB-cells *in vitro*, proved by morphology, SA-β-Gal staining, *MYCN* copy number reduction, GD2 level decrease and CD44 and MHC I upregulation which was similar to spontaneous senescent and hydroxyurea treated senescent NB-cells. Moreover, our data suggest an immune-stimulatory role of senescent tumour cells with respect to $CD8^+$ and $CD4^+$ T-cells.

Inducing senescence in *MYCN* amplified neuroblastoma cells by low-dose drug-treatment *in vitro* has the potential to restrict tumour growth, inhibit the aggressive phenotype in NB-cells and render tumour cells immunogenic. These features of senescence induction could be important in clinical applications to prevent tumour relapse in NB patients.

Table of content

Kurzfassung 3
Abstract 5
Table of content 6
1 Introduction 9
1.1 Neuroblastoma 9
1.1.1 Amplification of the *MYCN* proto-oncogene 11
1.1.2 MYCN expression and function 12
1.2 Senescence 12
1.2.1 General features and biomarkers 12
1.2.2 Theories of Senescence 14
1.2.2.1 Replicative Senescence 14
1.2.2.1.1 Telomere shortening 15
1.2.2.2 Premature Senescence 15
1.2.2.2.1 Senescence induced by extrinsic signals 16
1.2.2.2.2 Oncogene-induced senescence 16
1.2.2.2.3 Tumour suppressor loss-induced senescence 17
1.2.3 Senescence Signalling Pathways 17
1.2.4 Senescence as a barrier to tumourigenesis 19
1.2.5 Senescence and aging 20
1.2.6 Senescence in anticancer therapy 22
1.3 Senescence in *MYCN* amplified neuroblastoma cell lines 22
1.3.1 Drug-induced senescence by hydroxyurea treatment *in vitro* 23
1.3.2 GD2 level and CD44 expression 23
1.4 Immune evasion and antitumoural immune response against neuroblastoma 24
2 Materials and Methods 27
2.1 Cell Culture 27
2.1.1 Treatment with Hydroxyurea, Bromodeoxyuridine and Camptothecin 27
2.1.2 Cell Counting 27
2.1.3 Co-culture of Hydroxyurea induced senescent cells and control cells 28
2.1.4 Co-culture of control, spontaneous or drug induced senescent cells and T-cells 29
2.1.4.1 Isolation of peripheral blood mononuclear cells 29
2.1.4.2 Column-based isolation of T-cells from PBMCs 29
2.1.4.3 CFSE labelling 30
2.1.4.4 Anti-CD3 Titration 30
2.1.4.5 Co-cultivation of T-cells and NB-cells 30
2.1.4.6 Co-cultivation of T-cells with conditioned medium of NB-cells 31

2.1.4.7 Co-cultivation of T-cells and NB-cells in transwell plates 31
2.2 Flow Cytometry 32
2.2.1 Immunostaining of GD2, CD44 and MHC I for FACS analysis 33
2.2.2 Immunostaining of CD45, CD4, CD8, CD25 for FACS analysis 33
2.3 Microscopy 34
2.3.1 Senescence-associated β-galactosidase activity assay 34
2.3.2 Cytospin preparation 34
2.3.3 Double-target Fluorescent in situ hybridization to analyse *MYCN*-status 34
2.3.4 Probe (*MYCN* and 2p) labelling by nick translation 35
2.3.5 GD2 and CD44 Immunostaining on cytospins 36
2.4 Protein Analysis 36
2.4.1 Western Blot 36
2.5 Statistics 38
3 Aim of the study 39
4 Results 41
4.1 Characteristics of induced senescent neuroblastoma cells *in vitro* 41
4.1.1 Growth behaviour and cell morphology 41
4.1.2 SA-β-Gal Activity 43
4.1.3 *MYCN* copy number 45
4.1.4 Analysis of GD2 level, CD44 and MHC I expression 49
4.1.4.1 Immunofluorescence staining of GD2 and CD44 49
4.1.4.2 Flow-cytometry analysis of GD2, CD44 and MHC I 49
4.1.5 Analysis of the senescence pathway 53
4.2 Functional Analysis: Proliferation in co-cultures of senescent and non-senescent neuroblastoma cells 55
4.3 Functional Analysis: Immunomodulation 57
4.3.1 Anti-CD3 Titration 57
4.3.2 Co-culture of T-cells and neuroblastoma cells 59
4.3.3 T-cells cultured with conditioned medium from neuroblastoma cells 61
4.3.4 Co-culture of T-cells and neuroblastoma cells in a transwell plate 63
5 Discussion 66
5.1 Characteristics of drug induced senescent neuroblastoma cells *in vitro* 66
5.2 Functional Analysis: Co-culture of senescent and non-senescent neuroblastoma cells 70
5.3 Functional Analysis: Immunomodulation of T-cells through neuroblastoma cells 71
References 74
List of abbreviations 85
Curriculum Vitae 86
Acknowledgements 87

1 Introduction

1.1 Neuroblastoma

Neuroblastoma (NB) is an embryonal tumour of the sympathetic nervous system that derives from multi-potent neural crest cells. It accounts for 7–10% of all childhood cancers, and it is the most common extra cranial solid tumour of childhood [1]. The disease is diagnosed at the median age of about 18 months. 40% are diagnosed by one year, 75% by four years and 98% by 10 years of age. The cause of neuroblastoma is unknown, but it seems unlikely that environment plays a significant role [2]. Neuroblastoma is a disease of the sympathicoadrenal lineage of the neural crest. For this reason tumours can arise anywhere within the sympathetic nervous system. Most tumours develop within the abdomen and more than half of these are located in the adrenal medulla. Other common sites of tumour appearance are the neck, the chest and the pelvis. Depending on the site of the primary tumour, the metastases and the involved metabolic changes, the disease shows a wide diversity of signs and symptoms [3].

The various stages of neuronal differentiation of tumour cells show some prognostic significance. Most neuroblastomas are poorly differentiated and consist of small, round cells with scant cytoplasm called neuroblasts, which represent either immaturity or aggressiveness. However some tumours, the ganglioneuroblastomas, show histological differentiation. They are characterized by a mixture of mature or maturing ganglion cells and neuroblasts without neural differentiation. In the most differentiated and benign type of tumours, the ganglioneuroma, clusters of mature neurons surrounded by a dense stroma of Schwann cells are found [4-6].

The clinical hallmark of neuroblastoma is heterogeneity, meaning the tumour has a diverse spectrum of clinical presentation, prognosis and genomic features. Some tumours show spontaneous regression, particularly in infants, or they differentiate into a benign ganglioneuroma even without therapy [7]. Others display a very malignant phenotype that is poorly responsive to current intensive therapies and metastasize in advanced stages, mostly in children of more than one year of age [5]. According to age at diagnosis, the stage of disease and tumour biology the likeliness of tumour progression and survival varies broadly [8, 9]. Correlations between clinical outcome and some genetic features, such as oncogene amplification, DNA-content (ploidy status) or allelic loss have been identified. For instance, one marker for favourable clinical outcome and good survival rates is near-triploidy [10]. 55% of primary neuroblastomas are triploid or near-triploid, meaning they have between 58 and 80 chromosomes [11]. These tumours have almost always whole chromosome gains and only in rare cases structural rearrangements [12]. Furthermore, benign types of tumours usually have a high expression of neurotrophin receptor TrkA, which probably mediates apoptosis or differentiation in neuroblastoma. Patients with this kind of neuroblastomas are

usually younger than one year of age, more likely have localized tumours and altogether have a good prognosis. In contrast unfavourable tumours are mostly near-diploid (35-57 chromosomes) or near-tetraploid (81-103 chromosomes) [11] and are characterized by deletions of 1p36 (in 30% of NB) or 11q23 (in 40% of NB) [13-16], an unbalanced gain of 17q21 [17-19] and amplification of the oncogene *MYCN* [12, 20, 21]. Contrary to TrkA, a high TrkB expression together with its ligand brain-derived neurotrophic factor (BDNF) may lead to a survival pathway in aggressive tumours, especially in *MYCN* amplified (MNA) tumours. These patients are more likely older than one year and they have a poor prognosis. Further studies have shown that also deletions on chromosome 3p, 4p, 9p and 12p have prognostic significance [22-24].

In 1986 the International Neuroblastoma Staging System (INSS) was proposed (and revised in 1993) classifying neuroblastoma according to its anatomical presence at diagnosis [25]. Since then most cancer centres have used the INSS to stage neuroblastoma. The stages are described in table 1.

Stage	Description
1	The tumour is in only one area and all the tumour that can be seen is completely removed during surgery
2A	The tumour is in only one area and all the tumour that can be seen cannot be completely removed during surgery
2B	The tumour is in only one area and all tumours that can be seen may be completely removed during surgery. Cancer cells are found in the lymph nodes near the tumour.
3	The tumour cannot be completely removed during surgery and has spread from one side of the body to the other side and may also have spread to nearby lymph nodes; or the tumour is in only one area, on one side of the body, but has spread to lymph nodes on the other side of the body; or the tumour is in the middle of the body and has spread to tissues or lymph nodes on both sides of the body, and the tumour cannot be removed by surgery.
4	The tumour has spread to distant lymph nodes, the skin, or other parts of the body
4-S	The child is younger than 1 year and the cancer has spread to the skin, liver and/or bone marrow; and the tumour is in only one area and all of the tumour that can be seen may be completely removed during surgery, and/or cancer cells may be found in the lymph nodes near the tumour

Table 1| **The International Neuroblastoma Staging System** (content is taken from the website of the National Cancer Institute)

Next to the stage of neuroblastoma, several other factors also affect prognosis, including the age of the child, tumour histology, tumour cell ploidy, cytogenetic abnormalities and *MYCN*

gene status. These factors are used to determine the risk group of neuroblastoma patients. Due to the heterogenous behaviour of the tumour patients are categorized into a low-, intermediate- or high-risk group [26] to predict the outcome of therapy and select appropriate patient treatment strategies. Patients with low-risk neuroblastoma are mostly cured through surgery without treatment [27] whereas patients with intermediate-risk are treated with surgery and chemotherapy [28]. For high-risk patients there are several therapies including surgery, radiation therapy, chemotherapy, bone marrow or haematopoietic stem cell (HSC) transplantation. Following HSC-transplantation high-risk neuroblastoma patients are frequently treated with 13-cis-retinoic acid and immunotherapy with monoclonal antibodies targeting GD2, which is the predominant tumour-specific antigen in NB-cells, and/or cytokines (GM-CSF or IL-2) [27-30]. Despite these therapies, a lot of patients, particularly with high-risk neuroblastoma, suffer relapse mostly in bone or bone marrow [28]. The 3-year survival ranges from 99%, for tumours with good prognosis, to only 30% for aggressive tumours [5].

Although a subset of patients with neuroblastoma shows a predisposition to develop this disease, most neuroblastomas develop spontaneously through gain or loss of alleles, ploidy changes or amplification of oncogenes [5].

1.1.1 Amplification of the *MYCN* proto-oncogene

The overall incidence of *MYCN* amplification in neuroblastoma is about 22% [5] and amplification of this oncogene is linked to aggressiveness of the disease [21]. 40% of the patients with advanced disease and only 5-10% of the patients with low stage disease have a *MYCN* amplification [20]. The *MYCN* gene like the *c-MYC* gene is a member of the *MYC*-related oncogene family. It was first found in neuroblastoma cell lines as amplified DNA that shows a homology to viral *myc* [31, 32]. *MYCN* maps to the distal short arm of chromosome 2. When amplified, it is mainly located on extrachromosomal double-minutes (dmin) or infrequently in intrachromosomal homogeneously staining regions (hsr) which are both manifestations of gene amplification [33, 34]. The amplified part can vary in size and comprises a large region from chromosome 2p24 including the *MYCN* locus. This region is excised to form an extrachromosomal circular element (dmin) [34]. Under selective pressure, hsrs are generated through integration of the amplified DNA back into the genome [35]. *MYCN* is the only gene from this region showing consistent amplification, but other genes can be co-amplified as well. Until now, three genes have been found to be frequently co-amplified with *MYCN* in neuroblastomas: *DDX1, N-cym* and *NAG*. Moreover these genes frequently show an increased expression when co-amplified in NB-cell lines, assuming a contribution to the NB tumour phenotype [36-38]. In addition to neuroblastoma, *MYCN* amplification or overexpression exists also in several other cancers that are often of neuroendocrine or embryonic origin. These tumours are for instance retinoblastoma [39],

glioblastoma, Wilms´ tumour [40] and medulloblastoma [41]. It is still not completely understood why amplification of *MYCN* is associated with the aggressive type of neuroblastoma. However, *MYCN* amplification mostly correlates with MYCN overexpression on the protein level [42].

1.1.2 MYCN expression and function

MYCN like the other MYC family proteins is a transcription factor that influences expression of many target genes and therefore controls important cellular processes like proliferation, apoptosis, differentiation, protein synthesis and metabolism [28]. MYC transcription factors have a conserved structure consisting of a transcriptional activation domain of the N-terminus and a C-terminus basic helix-loop-helix leucine zipper domain, which is important for dimerization, DNA binding and transcription regulation [43]. MYC proteins form a protein complex with their binding partner MAX. This MYC-MAX dimer acts as a transcriptional activator [44]. However, MYCN can also repress the expression of genes, for instance it regulates genes involved in cell adhesion. Despite many similar properties of c-MYC and MYCN proteins like dimerization with MAX and binding to DNA, they differ significantly in their pattern of expression in normal tissues. In adult human and mice, *c-MYC* expression is present in all proliferating tissues while *MYCN* expression is very low or even absent. *MYCN* expression is restricted only to certain tissues in the developing embryo [45-48], for instance there are high levels in the neuroepithelium. In contrast to that *c-myc* is expressed in many tissues but is almost absent in this highly proliferative tissue. MCYN is also found in the developing intestine, kidney, heart and lung [46, 49]. Despite expression pattern differences, *MCYN* can functionally replace *c-MYC* in murine development [50]. In *Th-MYCN* transgenic mice, an animal model for neuroblastoma in which the *MYCN* expression is under the control of the tyrosine hydroxylase promoter, MYCN has been shown to promote proliferation and prevent differentiation of neuronal progenitors during embryonic development leading to the formation of hyperplastic lesions [51]. This study suggests that *MYCN* expression has to be down-regulated in order to allow differentiation into mature neurons.

1.2 Senescence

1.2.1 General features and biomarkers

Cells that are exposed to stress, respond either by apoptosis, by transient growth arrest or by entry into senescence. The cell fate is dependent on the cell type and the kind and level of stress. Senescence was first described by Hayflick and Moorhead (1961) in normal human fibroblasts *in vitro*. It was defined as the state of irreversible long-term cell cycle arrest that cells enter when they reach the end of their replicative lifespan [52]. This arrest in the G1/G0

phase of the cell cycle is an indispensable marker for identifying all types of cellular senescence *in vitro* as well as *in vivo* [53]. Germline, cancer and certain stem cells possess in contrast an indefinite replicative capacity [54].

Further, senescent cells lose the ability to respond to growth factors [55] and they undergo a dramatic change in morphology. Senescent cells alter their original shape and, depending on the trigger, they can increase their volume, acquire a flattened cytoplasm, become multinucleated and increase adhesion to the extracellular matrix while losing cell-cell contacts [56]. Cells that have undergone senescence almost stop to proliferate, but remain in a viable, metabolic active state for months *in vitro* [57]. In addition, many (but not all) cell types become resistant to certain apoptotic signals when they acquire senescence [58]. The underlying mechanisms are not completely understood, but expression changes in proteins that either inhibit or promote apoptosis might be a cause for resistance in some cells [59]. In other cell types, the tumour suppressor p53 is supposed to prefer transactivation of genes that arrest cell proliferation, rather than genes that lead to apoptosis [60].

A commonly used senescence biomarker is acidic senescence-associated β-galactosidase (SA-β-gal) [61], which has a highly increased activity in senescent cells. This happens presumably due to an expansion of the lysosomal compartment, which leads to an increase in SA-β-gal activity [62]. During senescence also the gene expression alters and therewith the secretome of senescent cells. Factors such as cytokines and chemokines are secreted, affecting the microenvironment and the surrounding cells [63, 64]. These profound changes in the secretome of cells entering the senescent stage are termed the senescence-associated secretory phenotype (SASP) [65]. However, the gene expression changes occurring in senescent cells are specific and mostly conserved within individual cell types [66].

Gene expression changes can be explained in part through alterations in the structure of chromatin [63]. After treatment with a DNA binding dye senescent cells often display remarkable punctate staining regions different from the overall homogenous patterns of cycling human cells. These DNA regions are termed senescence-associated heterochromatic foci (SAHF), which are highly condensed chromatin regions that are proposed to enforce cellular senescence by silencing genes involved in proliferation. SAHF are notably enriched in trimethylated lysine 9 of histone H3 (H3K9), and associate with a group A protein and heterochromatin protein 1 [67-69]. However, not all cell types of senescent cells show SAHFs. Therefore the establishment of cellular senescence is not dependent on the formation of SAHFs. Moreover, not all stimuli leading to senescence in cells concomitantly induce SAHFs, e.g. in human skin fibroblasts SAHFs are preferentially formed after oncogene induced senescence, but not after telomere shortening, exposure to ionizing radiation, treatment with H_2O_2 or hydroxyurea [70].

Hayflick and Moorhead (1961) suggested that the proliferation of normal cells is limited trough the loss of determined cellular factors during several cell divisions. Nowadays, cellular senescence is considered to be a response triggered by a combination of at least three mechanisms, which are telomere shortening, accumulation of DNA damage and derepression of the *INK4a/ARF* locus (Fig. 1). To which extent these mechanisms contribute to the senescence process depends on the cell type and the culture conditions [71].

Oncogene activation *in vivo* often leads to cellular senescence suggesting that the senescence pathway may be as important as apoptosis for protection against cancer. Further, senescence has been linked to organismal aging [71-74].

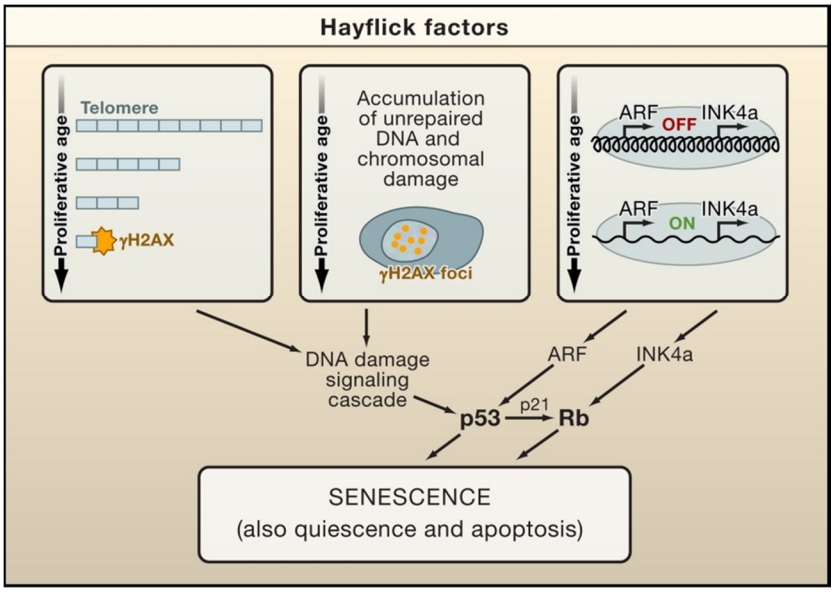

Figure 1 | Hayflick factors record the proliferative history of cells and tissues

The three best-known Hayflick factors—telomere shortening, accumulation of DNA damage, and derepression of the INK4a/ARF locus—are summarized together with their main effectors, the tumour suppressors p53 and retinoblastoma (Rb) (taken from Collado et al, 2007 [71])

1.2.2 Theories of Senescence

Senescence can be subdivided into “replicative senescence”, referring to a senescence process that occurs following extended proliferation, most likely triggered by a cell-intrinsic mechanism, and “stress-induced premature senescence”, referring to senescence triggered by extrinsic and intrinsic stress.

1.2.2.1 Replicative Senescence

During the process of cell proliferation telomeres are progressively shortened from one cell division to another, driving the cells to undergo replicative senescence when the telomeres reached a critical length.

1.2.2.1.1 Telomere shortening

Telomeres, the ends of linear chromosomes, consist of repetitive DNA elements and protect DNA ends from degradation and recombination [75, 76]. Telomeres become gradually shorter with every cell division round, because the replication machinery is incapable to copy the ends of linear molecules. This phenomenon is called the end replication problem. The telomere length gives information about cell division and cell cycle arrest [77]. In the end, telomeres reach a critical short length and behave like double-stranded DNA breaks. Consequently, the tumour suppressor protein p53 is activated and either starts the telomere-initiated senescence, also called replicative senescence, or cell apoptosis [76, 78]. Telomerase is a ribonucleoprotein with DNA polymerase activity and has the ability to elongate telomeres, thereby avoiding the effect of the end replication problem. In contrast to stem cells, telomerase is not expressed in human somatic cells. This fact makes most primary human cells unable to maintain their telomeres to inhibit a DNA damage response (DDR), which explains their limited life span [79]. In contrast, most human cancer cells possess the ability to maintain or elongate their telomeres, basically through a high telomerase expression [80] or a mechanism termed alternative lengthening of telomeres (ALT) [81]. This maintenance of telomere length permits cancer cells to proliferate indefinitely.

It is a common practice to immortalize primary human cells *in vitro* through the ectopic expression of the catalytic subunit of the telomerase holoenzyme (hTERT), which elongates telomeres. Further, there are studies showing that mice deficient in telomerase activity are significantly resistant to cancer induced by genetic defects or carcinogenic treatment [77]. These facts underline that telomere shortening plays an important role in cellular senescence [82].

1.2.2.2 Premature Senescence

Cells that possess endogenous telomerase activity maintain their telomere length but still can acquire a senescent status. Thus, there must be other triggers able to shorten the intrinsic replicative lifespan of a cell and inducing a senescence phenotype. Cells can initiate the senescence program not only through replicative senescence, but also due to diverse stressors including oxidative stress, reactive oxygen species (ROS), inactivation of tumour suppressor genes or activation of oncogenes. This type of senescence is termed premature senescence, since the cell proliferation capacity is limited prior to the effect of telomere shortening. The distinction between replicative and premature senescence does not necessarily describe two independent cellular mechanisms, but the fact that different stresses can cause a common cellular response.

1.2.2.2.1 Senescence induced by extrinsic signals

Cellular senescence can be triggered by extrinsic stress such as DNA-damaging treatments or agents (e.g. γ-irradiation, bleomycin or actinomycin D) [83, 84] or through oxidative stress (e.g. treatment with H_2O_2) [85, 86].

In cell culture, ionizing radiation does not induce apoptosis of human fibroblasts, but rather a senescence-like arrest [87]. Chemotherapeutic substances have been shown to induce cell cycle arrest and senescence *in vitro*, for instance treatment of human colon cancer cells with a low concentration of camptothecin or treatment of human erythroleukemia cells with hydroxyurea lead to senescence [88-90].

These *in vitro* findings have been supported by several reports on senescent tumour cells *in vivo.* In everyday clinical treatment of human cancers, tumour cells are forced into senescence. Studies reported that cell lines derived from different human solid tumours show senescence-like morphological changes and SA-β gal expression after ionizing radiation and treatment with various chemotherapeutic substances [89].

Even without drug treatment some of the tumour cell lines, which are said to be immortal, display the senescent phenotype in a significant minority of the cells (10–20%) [91]. This finding suggests that tumour cells could senesce spontaneously and that this process could occur in response to environmental changes of the cell [89]. In fact, inadequate culturing conditions *in vitro* can cause premature senescence. Cells have to acclimate to an artificial environment, when they are explanted and cultured. *In vitro*, other concentrations of nutrients and growth factors exist. Cells have to adapt to the absence of neighbouring cells and factors from the extracellular matrix. Further, cells are influenced by the oxygen levels surrounding them [92]. It is widely assumed that rather ROS than oxygen itself is involved in senescence. ROS are produced by mitochondria and ROS levels are elevated in senescent cells [93]. Each of the above mentioned conditions can induce a culture shock initiating stress-induced senescence independent of telomere length.

1.2.2.2.2 Oncogene-induced senescence

The concept of oncogene-induced senescence emerged with the study of Serrano et al. (1997), in which normal cells were forced to express high levels of an oncogenic version of HRAS, whereupon these cells entered the cell cycle arrest and changed their morphology indistinguishable from replicative senescent cells. This phenomenon is called oncogene-induced senescence (OIS). In contrast to replicative senescence it cannot be prevented by the ectopic expression of hTERT, which elongates telomeres, confirming that OIS is independent from telomere shortening [94]. Two well-known tumour suppressors were shown to be up-regulated and to play an important role in leading those cells into the cell cycle

arrest. These factors are INK4A, which activates the RB family, and ARF, which activates p53 [95].
Moreover, OIS is for instance induced by aberrant activation of oncogenes like Ras, BRAF or Myc [96]. Although overexpression of oncogenes primarily induces apoptosis or senescence, certain oncogenes (e.g. Myc) can also suppress these processes. Myc even suppresses Ras-induced senescence. Hence Myc and Ras may neutralize their anti-tumourigenic activity, allowing the tumour to proliferate. Thus, not only activation but also inactivation of some oncogenes can result in senescence and tumour regression [97, 98].

1.2.2.2.3 Tumour suppressor loss-induced senescence

Similarly to oncogene overexpression or mutation, shown for PTEN and NF1, the loss of a tumour suppressor in cells can also activate the senescence pathway. Mouse embryonic fibroblasts (MEFs) deficient for PTEN undergo senescence while p53 is concomitantly induced. Additional deletion of p53 allows the cell to bypass the effect of PTEN loss [99]. Likewise, NF1 depletion induces senescence *in vitro* and simultaneously there is a decrease in the activity of ERK and AKT [100].

These different senescence triggers are not independent from one another. Extrinsic stresses may affect intrinsic factors e.g. oxidative stress may affect the accumulation of DNA damage and accelerate telomere shortening. A population of cells may suffer from multiple stressors, which can lead to a complex cumulative effect [101].

1.2.3 Senescence Signalling Pathways

A variety of stressors can initiate cells to adopt a senescent phenotype. This observation supports the theory that senescence is a general response mechanism, which is not restricted to a certain type of stress. Furthermore, a number of changes in morphology and function occur upon activation of senescence. These changes can be assigned to specific molecular pathways.

In general, two pathways are responsible for the establishment and maintenance of growth arrest during senescence: the p53 and the retinoblastoma protein (pRb) pathway (Fig. 2).
The INK4a/ARF locus encodes the proteins $p16^{INK4a}$ and $p14^{ARF}$ ($p19^{ARF}$ in mouse). Both proteins possess anti-proliferative activity and interact with the p53 and pRb tumour suppressor pathway, although they use different molecular effectors [102, 103]. $p16^{INK4a}$ inhibits the assembly of cyclin dependent kinase 4/6 (CDK4, CDK6) and cyclin D (CycD) and thus the activated complex, which otherwise would phosphorylate pRb and pRb-related proteins (p107 and p130). Without the phosphorylation of pRb and related proteins the

transcription of E2F target genes is inhibited. E2F is essential for the transition from G1 to S-phase and mitosis. Hence, this process prevents the progression of the cell cycle, because $p16^{INK4a}$ maintains the active unphosphorylated state of pRb, which inhibits cell growth [102].

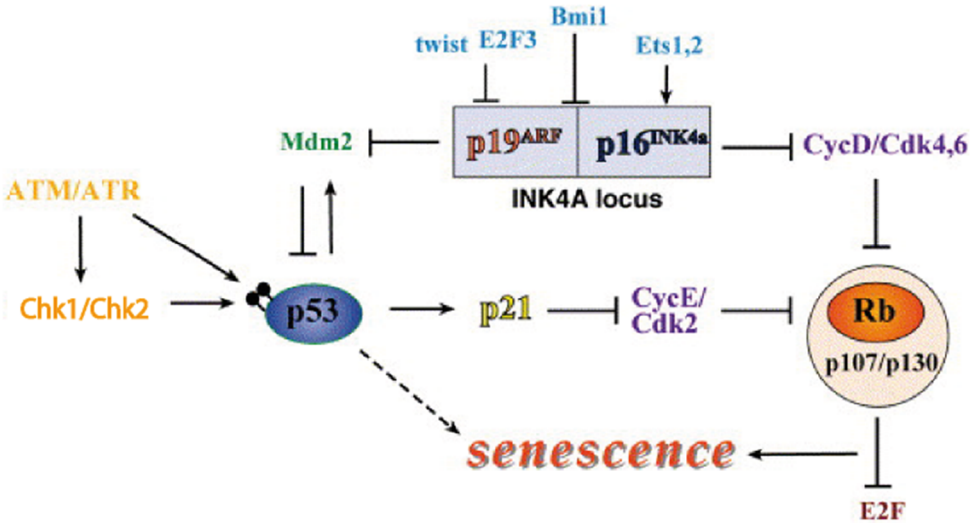

Figure 2 | The molecular circuitry of senescence

p53 and Rb are the main activators of senescence. p53 can activate senescence by activating Rb through p21 and other so far unknown proteins, and also, in human cells, can activate senescence independently of Rb. Rb activates senescence by shutting down the transcription of E2f target genes. Rb is activated either by p21 or by the p16INK4a product. p53 activation is achieved by phosphorylation, performed by the ATM/ATR and Chk1/Chk2 proteins, and by the p14/p19ARF product of the INK4a locus, which sequesters Mdm2 in the nucleolus. The transcriptional control of the INK4a products is not fully elucidated, indicated are some of these regulators (adapted from Ben-Porath et al, 2005 [101]).

The other product of the INK4a/ARF locus, $p14^{ARF}$, stabilizes p53 by binding to MDM2, which otherwise would target p53 for degradation. The tumour suppressor p53 can induce an important downstream factor, the cell cycle inhibitor $p21^{CIP1}$, that blocks the phosphorylation of pRb by modulating CDK2/cyclin E complexes and thus initiate a cell cycle arrest. However, beside the induction of senescence, p53 activation can also cause apoptosis. The reason, why a cell decides for the one or the other way is not yet understood [102].

The activation of p53 can also be induced through the DDR signalling cascade sensing and repairing DNA damage. It is activated through phosphatidylinositol 3-kinase-like protein kinases such as ATR and ATM. These kinases phosphorylate chromatin modifying proteins such as γH2AX, adapter proteins (NBS1), and further kinases such as CHK1 and CHK2, which are downstream in this pathway and in turn activate p53 by phosphorylation [104].

Activation of p53 or $p16^{INK4a}$ or simultaneous activation of both pathways respectively, results in inhibition of pRb phosphorylation. So, p53 and $p16^{INK4a}$ can be seen as a processing unit transforming different incoming stress signals (e.g. telomere shortening, irradiation, DNA-damaging agents, ROS) into a common adequate cellular response.

In addition, p38-MAPK proteins have been shown to be important in mediating senescence caused by oxidative stress and high levels of RAS. Activation of the p38MAPK/NF-κB pathway also plays an essential role in the induction of the SASP, which needs several days to develop after a DDR [102].
Taken together, the cyclin-dependent kinase inhibitors (CKIs) p16 and p21 are two critical senescence regulators. Their expression is elevated in most types of senescent cells and their function is to block the activity of Cdks, which in turn leads to an up-regulated Rb activity and thereby induces senescence [105].

Additionally, the CKI p27 is also regarded as an important effector of cellular senescence which is part of a third pathway, the PTEN/$p27^{Kip1}$ pathway (Fig. 3) [106]. Loss of the tumour suppressor PTEN occurs in a variety of human cancers. PTEN, a phosphatase, catalyses the conversion of PIP_3 into PIP_2. The proto-oncogene, PI3-kinase counteracts this action of PTEN. Overexpression of PTEN, as well as the effect of PI3K inhibitors result in up-regulation of the CKI p27 [107], which occurs by protein stabilization in response to decreased PIP_3 levels.
Human fibroblasts treated with PI3K inhibitors accelerate the onset of cellular senescence and senescent human fibroblasts display an accumulation of p27 [108]. Further, p27 levels are often significantly diminished in human tumours especially in advanced stages [109].

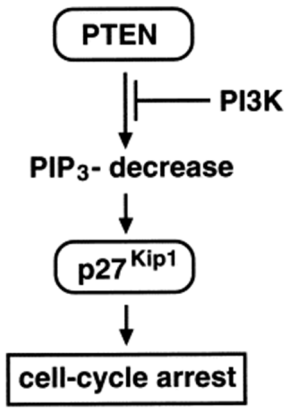

Figure 3 | The PTEN/p27Kip1 pathway (taken from Bringold, F. and M. Serrano, 2000 [106])

1.2.4 Senescence as a barrier to tumorigenesis

Senescent tumour cells were identified in pre-malignant stages of tumours (e.g. in lung adenomas and melanocytic nevi), but in their corresponding malignant stages senescence was absent. This observation suggests a role for senescence as a barrier to tumour progression [110]. When a normal cell acquires mutations in several cancer-causing genes, it can become malignant. Nowadays, senescence is anticipated to play an important role in the tumour suppression process in at least three ways. First, the tumour growth is stopped by

senescence associated proliferation arrest. Second, this proliferation arrest provides genetic stability by suppressing accumulation of additional oncogenic alterations during replication and mitosis. Third, senescent cells alert the immune system by secreting immune regulators to clear incipient cancer cells (Fig. 4) [111].

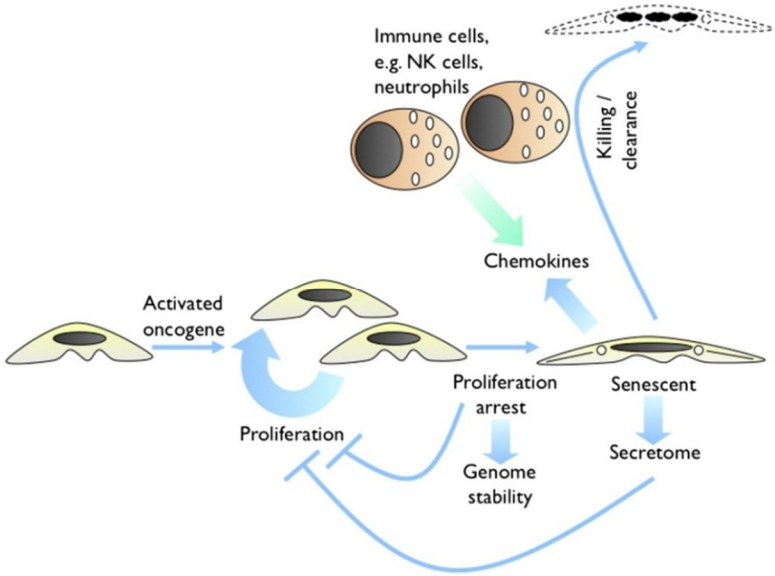

Figure 4 | Senescence as a tumour suppressor mechanism

Acquisition of an activated oncogene or inactivation of a tumour suppressor initially causes a proliferative burst. Ultimately, senescence kicks in to arrest proliferation of the cells harbouring the oncogenic event. Proliferation arrest is reinforced through the secretome. Senescence-associated proliferation arrest is likely to arrest tumour progression by preventing proliferation of neoplastic cells and suppressing accumulation of additional genetic alterations (genome stability). In addition, senescence recruits the innate immune system to clear the genetically altered cells that threaten the host with malignant disease (taken from Adams, P.D., 2009 [111]).

In order to reach the potential to divide unlimitedly and to be able to transform into tumours, cells have to escape senescence. This step is one of the hallmarks of cancer cells [112]. In line with the aspect that the mechanism of senescence acts as a tumour suppressor, well-known tumour suppressors as p53, p16, pRb, p21 and Arf are also regulators of senescence [112-114]. Deletion of some senescence regulators such as p53, Arf, p16 and p27 causes progression of tumours to a malignant stage [115, 116]. So, there is a causal link between malignant transformation and the loss of mediators of senescence.

1.2.5 Senescence and aging

Cellular senescence, although preventing initial stages of cancer, is also involved in organismal aging and even promotes the degenerative and cancerous pathologies of aging. Looking at physiological aging, an increase of molecular senescence biomarkers, such as

DNA damage, SA-β-gal, expression of p16INK4a and telomere shortening has been reported in some aging tissues [61, 117]. In addition, studies have shown increased levels of senescent cells in tissues of age-associated pathologies, such as osteoarthritis, atherosclerosis and liver cirrhosis [118-120].

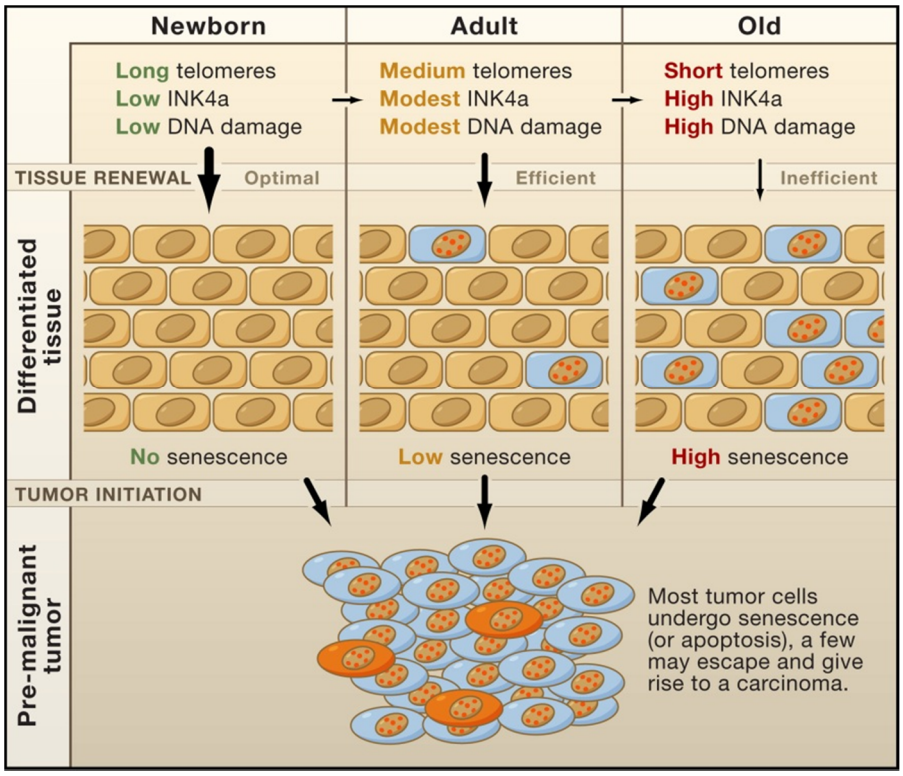

Figure 5 | Senescence of stem cells and committed cells

Multiple mechanisms operate on stem cells and on committed cells to produce senescence. Telomere shortening, derepression of the INK4a/ARF locus, and the accumulation of DNA damage operate during the lifespan of the organism on stem cells (left side, from top to bottom), as well as on committed cells derived from the stem cells on their way to generating a differentiated tissue (from left to right). The final result is age-dependent loss of stem cell functionality (represented by a thin arrow in the top right) and an age-dependent increase in the number of senescent cells in differentiated tissues (represented as blue cells). Tumours may arise at any point in life, but the stress signals characteristic of tumours will engage the senescence program. This tumour-specific senescence constitutes an important barrier to tumour progression (taken from Collado et al, 2007 [71].

There are two mechanisms that explain how cellular senescence may probably contribute to aging: accumulation of senescent cells in tissues during the aging process and loss of stem cell function by limiting the regenerative potential of stem cells (Fig. 5) [71]. As a result, these two factors could lead to impaired tissue homeostasis and function and consequently to aging of the organism.

1.2.6 Senescence in anticancer therapy

Current anti-tumour chemotherapeutics are designed to kill cancer cells. The problem is that these therapies are often limited by pro-survival alterations present in cancer cells and that they are also toxic to normal cells. By attacking cancer cells from a different angle senescence-inducing drugs might offer an opportunity to reduce the toxicity of chemotherapy in healthy tissue.

As aforementioned, senescence can be induced by DNA damage. This suggests that DNA damaging chemotherapeutic drugs may activate the senescence mechanism in tumour cells and in this way could contribute to the success of cancer treatment [83, 84, 121]. Studies in human breast cancer patients show positive staining for senescence markers in a high percentage of tumours. Furthermore, senescence induction in these tumours is associated with p53 and p16 activation. There was no induction of senescence in tumours before chemotherapy, which indicates that senescent cells are formed as a response to chemotherapy [122]. Likewise, chemotherapy induced senescence was found in biopsies from patients with lung and prostate cancer [65, 123]. For the reduction of tumour growth drugs inducing senescence might prove effective either alone or in a therapy combined with classic therapeutic approaches.

In vitro, several human cancer cell lines undergo the senescence process when treated with moderate doses of classical chemotherapeutic drugs, but go into apoptosis when treated with higher doses [124, 125]. Cellular senescence as an end point of tumour therapy might be important for the development of new drugs for therapeutic treatments or as prognostic markers, respectively [110].

1.3 Senescence in *MYCN* amplified neuroblastoma cell lines

In cultures of *MYCN* amplified primary neuroblastoma cell lines, senescent cells arise spontaneously at varying frequencies [125]. These cells are morphologically distinct from the majority of neuronal-type cells (N-cells): Senescent NB-cells show typical morphological characteristics of senescent cells, such as enlarged cytoplasm. Further they stop proliferation and show strong adherence to plastic surfaces. Due to their spontaneous appearance and their morphology these cells were named spontaneous flat (F)-cells [126].

In contrast, N-type cells are small, light-refractile cells with neuronal features. Many N-cells possess usually short, thin processes, but some of them have also long processes searching connection to cells over a longer distance. They grow densely and form focal accumulations.

Although morphologically different, both cell types share the same tumour-specific genetic aberrations, such as 1p loss or 17q gain [125, 127, 128]. However, they differ in the *MYCN* copy number status. Only 2-12% *MYCN* amplified cells were found in the F-cell population,

compared to 95% *MYCN* amplified cells in N-cells [126]. The reduced *MYCN* copy number is probably a result of micronucleus formation and expulsion of *MYCN* copies from the nucleus into the cytoplasm, where DNA is degraded in the lysosomal compartment. This mechanism has been suggested to contribute to senescence-onset in NB-cells [126].

1.3.1 Drug-induced senescence by hydroxyurea treatment *in vitro*

Hydroxyurea (HU) is an “old” drug and used to treat patients with melanoma, chronic myelocytic leukaemia and metastatic cancer of the ovaries. HU is also given in combination with radiation treatment for head and neck cancer. Further, it is given to patients with sickle-cell anaemia to prevent them from crisis.

Studies have shown that treatment with low concentrations of hydroxyurea (HU) accelerates the expulsion of amplified genes in several tumour cell lines [129, 130]. Previous data have shown that low dose treatment with HU in *MYCN* amplified neuroblastoma cells result in an accelerated entrance into the senescence pathway. After 6-10 weeks HU induction the number of cells decreased and mostly only senescent cells remained in cell culture. More than 95% of cells stained positive for SA-β-Gal, the most accepted senescence marker. 3-4 weeks after treatment start proliferation state dropped to 25% according to bromodeoxyuridine uptake and enlarged flat cells, F-cells, with increased granularity developed. After 5-8 weeks of treatment only cells having strongly reduced *MYCN* copy number were present in the culture. For some the number even went down to one copy per cell. Concurrently, CD44 and MHCI were up-regulated on the surface of HU-treated NB-cells. Moreover, telomeres were shorter and telomerase activity could not be detected after 8 weeks of HU induction. Thus, HU induced senescent F-cells and spontaneous senescent F-cells show similar features, such as up-regulation of CD44, MHCI and SA-β-Gal positivity [125].

Therefore, previous studies of our research group show that in the most aggressive MNA neuroblastomas the formation of senescent F-cells can be induced via low dose HU treatment within 6-10 weeks, which results in loss of their malignant properties [125].

1.3.2 GD2 level and CD44 expression

The tumour-associated antigen disialoganglioside GD2 is present in high density on the surface of NB-cells [131]. In normal human tissues, expression of GD2 is restricted to neurons, peripheral sensory nerve fibres and skin melanocytes [132]. Thus, GD2 is a useful target for identification and treatment of tumour cells with monoclonal antibodies. We have previously found, that in NB primary cell lines N-cells express GD2, whereas senescent F-cells are GD2 negative [125, 126].

The transmembrane glycoprotein CD44 is involved in cell-cell interactions and attachment to extracellular matrix mainly through hyaluronic acid. It has many isoforms generated through alternative splicing or alterations in glycosylation [133]. Expression of CD44 can be regulated by differentiation or mitogenic factors [134]. In malignancies of the hematopoietic system, CD44 variant expression in general is an unfavourable prognostic factor and is associated with tumour progression and dissemination [135]. Similar observations were made in breast and colon carcinomas [136, 137]. In contrast, CD44 expression in NB is related to low risk stages, differentiated NB tumours, with a favourable prognosis, while tumours negative for CD44 are progressive and metastatic with poor prognosis [138]. Furthermore, there is a strong relationship between the lack of CD44 expression and amplification of *MYCN* in NB [139]. In general, NB-cell lines do not express CD44 as they are mostly derived from aggressively growing high risk NB. In primary NB-cell lines derived from stage 3+4 patients we have previously reported that N-cells are CD44 negative, whereas senescent F-cells show a high expression of CD44 [125]. Upon treatment with HU we have observed that the number of CD44 positive cells increases and that these cells show different stages of micronuclei formation with packed *MYCN* signals or already reduced *MYCN* copies after expulsion. Cells that have expulsed supernumerary copies of *MYCN* also express MHC class I [125, 126]. This molecule is usually almost absent in neuroblastoma cells [140].

1.4 Immune evasion and antitumoural immune response against neuroblastoma

The immune system not only detects and eliminates pathogens that may do harm to the organism, but also serves as a guardian against transformed cells that may lead to cancer.
Most tumours are poorly immunogenic and consequently evade immune recognition and elimination. This is also a problem in aggressive neuroblastoma [141]. NB tumours have evolved several different ways to avoid or suppress an immune response, especially by targeting pathways required for the initiation of a successful T-cell, dendritic cell- and/or NK-mediated tumour-specific immune response. Critical pathways that can be affected are: antigen processing and presentation via the MHC class molecules of proteins, TLR-mediated activation of antigen presenting cells, expression of ligands for activating NK immunoreceptors, and expression of co-stimulatory molecules and cytokines. In general, processing and presentation of tumour antigens by MHC class I molecules requires antigen degradation by the immuneproteasome. The resulting peptides are translocated into the lumen of the endoplasmatic reticulum by the TAP transporter assisted by chaperons. The

peptide is then loaded onto mature MHC class I molecules and subsequently transferred to the cell surface[142].

NB-cell lines and primary tumours display low or absent expression of MHC class I and II molecules and defects in in β2-microglobulin (β2m), a subunit of MHC I [143, 144]. Primary NB tumours lack or show reduced expression of components of the immuneproteasome complex (PSMB10) and of the translocation machinery (tapasin (TAPBP), TAP1 or TAP2). These defects explain reduced peptide loading on MHC class I molecules, their instability and failure to be expressed on the cell surface [145] and therewith to a restricted or no recognition by CTL which mediate antigen-specific cytotoxic functions following peptide recognition on MHC class I molecules [146].

Another immuno-suppressive mechanism of NB-cells is shedding of gangliosides, such as GD2. Gangliosides are cell-membrane associated glycosphingolipids and are over-expressed frequently in tumour cells. They are shed into the local microenvironment and plasma of tumour-bearing patients and inhibit antigen-processing and presentation, lymphocyte proliferation, Th-cell differentiation and activation of mast cells as well as differentiation and activation of antigen presenting cells (DC and monocytes) [147-155].

Furthermore, neuroblastoma cells potentially evade the immune system by releasing immunosupressive molecules, such as IL-10 and TGFβ, which prevents activation and expansion of tumour-infiltrating lymphocytes [156]. Finally, costimulatory molecules such as CD40, CD80, CD86 and others are down-regulated in NB-cell lines and primary NB tumours. The absence of CD40 in primary neuroblasts indicates that NB-cells may evade the programmed cell death mediated by CD40/CD40L interaction [157].

There are still a lot of questions in the field of immune response against NB-cells. It has been suggested that NK cells may target NB-cells much better than CTL, because of their low MHC class I expression [158, 159]. Indirectly, also NKT cells may mediate cytotoxicity against NB-cells by secreting IL-2, which activates NK cells [160]. Furthermore, the potential role of B-cells in NB progression is not yet clear and T regulatory cells (Tregs), positive for CD4, CD25 and Foxp3, have not been evaluated in NB tumours [161].

Attempts have been made to enhance immunogenicity in NB and to induce a tumour cell-specific immune response in patients by immunotherapy [162, 163]. However, the only proven beneficial immunotherapy for NB high-risk patients is a chimeric anti-GD2 mAb (ch14.18) alone or combined with IL-2 or GM-CSF. It is given to patients after they have received intensive chemotherapy, irradiation, and surgery [164]. Other anti-neuroblastoma T cell therapy trials, such as vaccines and adoptive cell therapy, are still in early development and not yet proven to be successful.

The role of the immune system in mediating anti-tumour responses upon drug-induced oncogene inactivation and concomitant senescence in neuroblastoma is not known. Recently, it was reported by our group that MHC I surface expression is up-regulated on neuroblastoma cell lines by long-term (>8 weeks) low dose hydroxyurea treatment *in vitro* [125]. This finding and our preliminary studies suggest that hydroxyurea treated neuroblastoma cells allow $CD8^+$ and $CD4^+$ T-cell activation. Similarly, Rakhra K et al. have reported that in c-MYC-dependent tumours $CD4^+$ T-cells are required for tumour regression upon oncogene inactivation in mice [165]. Also cells of the innate immune system have been implicated in senescence induction in malignant B-cell lymphoma via a strongly increased secretion of various cytokines, among them TGFβ [166]. Moreover, a study on liver cancer showed that mice with an impaired immune surveillance of senescent hepatocytes developed cancer, while in mice with normal active Th-cells senescent cells were removed before cancer could develop [167].

Strategies to overcome the immunosuppressive behaviour of NB tumour cells and therewith enhance the anti-tumour immunotherapy still have to be developed. Thus our research focuses on inducing senescence in NB-cells derived from high risk patients by drug treatment and to study the resulting immunogenic changes of these senescent cells.

2 Materials and Methods

2.1 Cell Culture

All cell culture work was performed under sterile conditions. Cells were analysed with an Axiovert 40C inverted microscope (Zeiss, Austria) and photographed with PixeLINK software (Ottawa, USA).

The two Neuroblastoma cell lines STA-NB-10 and NB-Ma were cultured in RPMI 1640 GlutaMAX (Gibco-BRL, Grand Island, New York, USA) supplemented with 10% fetal calf serum (FCS Gold, PAA Laboratories GmbH, Pasching, Austria), 2,5% HEPES (PAA Laboratories GmbH), 1% Sodium-Pyruvate (PAA Laboratories GmbH) and 0,8% Penicillin (10.000 U/ml)/Streptomycin (10 mg/ml) (PAA Laboratories GmbH). Cultivation took place at 37°C supplied with 5% CO_2 and 90% relative humidity in an incubator. Cell passaging was done when cells were 80-90% confluent (on average once a week).

To harvest the cells, they were washed first with phosphate-buffered saline (PBS, PAA Laboratories GmbH) and then incubated with 1.5 ml of Accutase (PAA Laboratories GmbH) at 37°C for 3-5min (for control cells) or 15-20 minutes (for spontaneous and induced senescent cells). Detached cells were resuspended in medium and either splitted into a new flask or used for experiments.

To receive pure cultures of spontaneous senescent cells, N-cells were detached via Accutase treatment for 3-5 min and removed from the flask, thereby leaving only spontaneous senescent cells which could be further cultivated.

2.1.1 Treatment with Hydroxyurea, Bromodeoxyuridine and Camptothecin

Subconfluent cultures of STA-NB-10 and NB-Ma cells were treated either with 150 µM Hydroxyurea (Sigma-Aldrich, Austria) for 8-10 weeks or 20 µM Bromodeoxyuridine (Sigma-Aldrich, Austria) or 5 nM Camptothecin (Sigma-Aldrich, Austria) for 3-5 weeks. Medium was renewed and drugs were added once a week. Medium of control cells was changed weekly and cells were passaged if necessary.

2.1.2 Cell Counting

Cells were counted with the Bürker-Türk counting chamber. Detached cells were resuspended in a definite volume of PBS or medium. 10 µl of cell suspension was mixed with 10µl of Trypan blue to distinguish viable and non-viable cells (non-viable cells are stained blue). 10 µl of this suspension was pipetted into the Bürker-Türk counting chamber and viable cells were counted in each of the four corner squares.

Viable cell concentration was calculated using the formula: cells/ml = t x tb x 1/4 x 10^4

t = total viable cell count of four corner squares
tb = correction for the trypan blue dilution (counting dilution was 1/tb)
1/4 = correction to give mean cells per corner square
10^4 = conversion factor for counting chamber

2.1.3 Co-culture of Hydroxyurea induced senescent cells and control cells

HU induced senescent cells were detached via Accutase treatment (described in chapter 2.1) and total cell number was calculated after counting cells in a Bürker-Türk counting chamber (described in chapter 2.1.2). Cells were washed with PBS, resuspended in PBS and Cell Proliferation Dye eFluor670 (CPD, eBioscience, Austria) was added (1µl per 1x10^7 cells/ml). Incubation took place at 37°C for 10 min in an incubator. 5 ml FCS were added and incubated for 5 min at RT to stop the reaction. Cells were washed two times with PBS, resuspended in medium, transferred back to a culture flask and incubated for two days at 37°C in an incubator. At the experimental day (day 0) CPD labelled HU induced senescent cells and control cells were harvested, counted and resuspended in medium (5x10^5 cells/ml). If necessary, wells were coated with fibronectin (Roche Diagnostics GmbH, Mannheim, Germany) for 30 min at 37°C in an incubator. Fibronectin has been removed before seeding the cells. Wells were filled either with control cells, HU induced senescent cells or with both cell types for co-culturing in duplicates or triplicates, respectively. Cells were seeded in 96-well plates (1x10^5 cells/well in 200 µl medium), 24-well plates (2x10^5 cells/well in 1 ml medium) or 12-well plates (2x10^5 cells/well in 3 ml medium), incubated at 37°C in an incubator and analysed at the respective time points. Supernatants were collected and frozen at -20°C. Cells were washed one time with PBS, harvested with Accutase and resuspended in an appropriate volume of medium. Cell Counting was done in a Bürker-Türk counting chamber and an aliquot of each condition (control cells, HU induced senescent cells and co-culture) has been used for preparation of 4 cytospins (2.5x10^4 cells/cytospin) which were frozen at -20°C. 1x10^5 cells were first washed and then resuspended in 50 µl FACS buffer. Surface marker GD2, MHC class I and CD44 were stained for FACS analysis (chapter 2.2.1).

In the first experiment, for each time point two wells (duplicates) of a 96-well plate with flat bottom were seeded either with control cells, HU treated senescent cells (1x10^5 cells/well = 200 µl) or for the co-culture with both types of cells (5x10^4 cells per cell type/well = 100µl/cell type). For the second and third experiment wells were coated with fibronectin before cells were seeded, control cells were cultured in 24-well plates (2x10^5 cells/well) and wells were filled up to 1 ml with medium. For HU treated senescent cells and the co-culture a 12-well plate has been used with 2x10^5 cells/well in 3 ml medium.

2.1.4 Co-culture of control, spontaneous or drug induced senescent cells and T-cells

For all experiments with T-cells either 96-well plates with round bottom (NuncTM, Roskilde, Denmark) or 24-well plates with flat bottoms (IWAKI Europe, Willich, Germany) were coated with anti-mouse IgG1 antibody (Sigma Aldrich, Vienna, Austria) for 2 hours at 37°C before use. For each setup, T-cells were thawed and seeded on the same day.

2.1.4.1 Isolation of peripheral blood mononuclear cells

Fresh Buffy Coat (Österreichisches Rotes Kreuz) was diluted 1:2 with room temperature PBS. For density gradient centrifugation diluted blood was cautiously layered over 10-15 ml Ficoll (LSM 1077 Lymphocyte, PAA, Pasching, Austria) and centrifuged for 30min at 300g at 20°C without brake. Peripheral blood mononuclear cells (PBMCs) formed a ring in the interphase which was carefully transferred into a new tube and washed twice with PBS. Cells were resuspended in 50ml MACS buffer (PBS/0.5% BSA/2 mM EDTA) and 50µl were aliquoted for cell number measurement with a Sysmex Cell counter (Sysmex Europe, Norderstedt, Germany).
For freezing of PBMCs, $1x10^8$ cells were centrifuged, resuspended in 5ml medium and mixed with 5ml FCS/ 20% DMSO. This cell suspension was transferred into cryo tubes (1ml/tube=$1x10^7$ cells). Samples were frozen step-wise by cooling for 1-2 hours at -20°C and sub-sequent transfer to -80°C. To store cells for a longer period, they were moved to a liquid nitrogen tank.

2.1.4.2 Column-based isolation of T-cells from PBMCs

T-cells were isolated from human PBMCs by depletion of non-T cells (negative selection) using the Human Pan T Cell Isolation Kit II (Miltenyi Biotec, Bergisch Gladbach, Germany). Pre-cooled solutions were used and cells were kept on ice, unless otherwise mentioned. All volumes of reagents used were calculated for 10^7 cells. Cells were centrifuged at 300 g for 10 min at 4°C and resuspended in 1,6 ml MACS buffer. Non-T cells were indirectly magnetically labelled with 200µl of biotin-conjugated monoclonal antibodies, as primary labelling reagent. The Pan T-Cell Biotin-Antibody Cocktail contains antibodies directed against CD14 (macrophage marker), CD16 (Natural killer cells), CD19 (B-cell marker), CD36 (platelet marker), CD56 (Natural killer cells), CD123 (plasmacytoid dendritic cell and basophil marker) and Glycophorin A (erythroid cell marker). Incubation took place for 10 min at 4°C. 1.2 ml MACS buffer was added before cells were labelled with 400 µl anti-biotin monoclonal antibodies conjugated to MicroBeads, the secondary labelling agent, for 15 min at 4°C. Cells were washed with MACS buffer (10−20 x labelling volume) and centrifuged at 300 g for 10 min. The cell pellet was resuspended in 3 ml MACS buffer. LS columns were placed in the

magnetic field of a suitable MACS Separator and columns were prepared by rinsing with 3 ml MACS buffer. Cell suspension was applied onto the columns (1 ml/column) and the effluent was collected as fraction with unlabelled cells. Columns were washed with 3x with 3 ml MACS buffer each and the entire effluent was collected in the same tube as before. This fraction represented the enriched T-cell fraction. T-cells were diluted 1:2 in medium and FCS/ 20% DMSO. This cell suspension was aliquoted into cryo tubes ($1x10^7$ cells/tube) and frozen at -80°C. Aliquots before (PBMCs) and after (T-cells) depletion were taken to look for purity of the enriched T-cells by flow cytometry.

2.1.4.3 CFSE labelling

T-cells were thawed and washed twice with PBS at 1200 rpm, 7 min at 4°C before they were resuspended in PBS (10^7 cells/ml). 1 nM CFSE (Sigma-Aldrich, St Louis, MO, USA) was added, gently mixed and incubated for 10 min at 37°C. 5 ml FCS were added and incubated at RT for 5 min. Cells were washed twice with medium, 50 µl were removed after the first washing step for cell number measurement with the sysmex cell counter and cells were resuspended in medium, respectively.

2.1.4.4 Anti-CD3 Titration

Frozen T-cells were thawed, washed one time with PBS, resuspended in PBS and labelled with CFSE. The cell number was defined with the sysmex cell counter and the cell suspension was diluted with medium. Cell suspensions were mixed with anti-CD3 antibody (Sigma-Aldrich, Germany) at 10 ng/ml, 25 ng/ml, 100 ng/ml and 250 ng/ml, respectively. The negative control contained no anti-CD3 antibody and for positive control 1 µg/ml Staphylococcal enterotoxin B (SEB, Sigma-Aldrich, St Louis, MO, USA) was added. Each condition was set up in triplicates in a 96-well plate ($5x10^4$ cells/well) which was incubated at 37°C for 3, 4, 5 and 6 days, respectively. For FACS analyses, cells were transferred into micronic tubes (Szabo-Scandic, Vienna, Austria), washed and resuspended in 50 µl FACS buffer. 4 µl DAPI-solution (2 µl/ml dilution in 1xPBS, Sigma-Aldrich, Germany) was added and proliferation of T-cells was analysed with the BD LSRII Flow Cytometer (Becton Dickinson, USA) and using the FACS-Diva software.

2.1.4.5 Co-cultivation of T-cells and neuroblastoma cells

Three replicate wells were set up for each experimental group (control, spontaneous senescent cells, HU treated-, CPT treated- and BrdU treated senescent cells) together with T-cells at three NB:T-cell ratios, 1:1,1:5 and 1:10. T-cells were thawed, CFSE labelled and adjusted to $5x10^5$ cells/ml in medium. 10 ng/ml anti-CD3 was added and $5x10^4$ cells/well were transferred into IgG coated 96-well plates. The number of T-cells/well was always the

same, while the number of NB-cells was adapted depending on the NB:T-cell ratios. For negative control T-cells were not stimulated with anti-CD3 and for positive control T-cells were stimulated with 1 µg/ml SEB.
Control, spontaneous senescent cells, HU treated-, CPT treated- and BrdU treated senescent cells were harvested, counted with the Bürker-Türk counting chamber and diluted with medium to appropriate concentrations in order to obtain the three different NB:T-cell ratios (end volume 200 µl/well). All surrounding empty wells were filled with PBS. Plates were incubated for 6 days at 37°C in an CO2-incubator. Co-culture supernatants were collected and frozen at -20°C and cells were analysed for T- cell proliferation (CFSE) and CD45, CD4, CD8 and CD25 with the BD LSRII Flow Cytometer (see chapter 2.2.2).

2.1.4.6 Co-cultivation of T-cells with conditioned medium of neuroblastoma cells

Control, spontaneous senescent cells, HU treated-, CPT treated- and BrdU treated senescent cells were plated in duplicates or triplicates, respectively, in a 96-well plate ($5x10^4$ cells/well) one day before T-cells were plated for co-cultivation. Cells were incubated over night at 37°C in an incubator.
T-cells were thawed, CFSE labelled and transferred into an IgG coated 96-well plate ($5x10^4$ cells/well). Plates with NB-cells were shortly centrifuged, conditioned medium was transferred onto T-cells and anti-CD3 antibody was added (5 ng/ml). For negative control T-cells were not stimulated with anti-CD3 and for positive control T-cells were stimulated with 1 µg/ml SEB.

Conditioned medium was transferred and anti-CD3 was added only on day 0 (for “1x transfer”) or daily, respectively. For daily supernatant transfer, wells with NB-cells were refilled with medium, incubated over night at 37°C and supernatant was transferred again onto T-cells the next day. This procedure was repeated every day until analysis. Plates were incubated for 6 days at 37°C and cells were analysed for T- cell proliferation (CFSE) and CD45, CD4, CD8 and CD25 with the BD LSRII Flow Cytometer (see chapter 2.2.2).

2.1.4.7 Co-cultivation of T-cells and neuroblastoma cells in transwell plates

Transwell plates (12 mm transwell with 0.4 µm Pore Polyester Membrane Insert, Corning) allow the co-culture of two different kind of cells without direct cell-cell contact, but with an exchange of cytokines produced by the cells through an microporous membrane.

T-cells were thawed and CFSE labelled. In the lower compartment of a flat 24-transwell plate coated with anti-IgG $2x10^5$ T-cells were added. In the upper compartment, $1x10^5$ NB-cells (control, spontaneous senescent cells, HU treated-, CPT treated- and BrdU treated

senescent cells) were seeded. Wells contained 700 µl medium in total and 5 ng/ml anti-CD3 was added. In addition, NB-cells and T-cells were plated together in the lower compartment without a transwell insert ("direct contact"). Reactions were set up in duplicates. Plates were incubated for 6 days at 37°C in an incubator and cells were analysed for T- cell proliferation (CFSE) and immuno-stained for CD45, CD4, CD8 and CD25, followed by FACS analysis with the BD LSRII Flow Cytometer (see chapter 2.2.2).

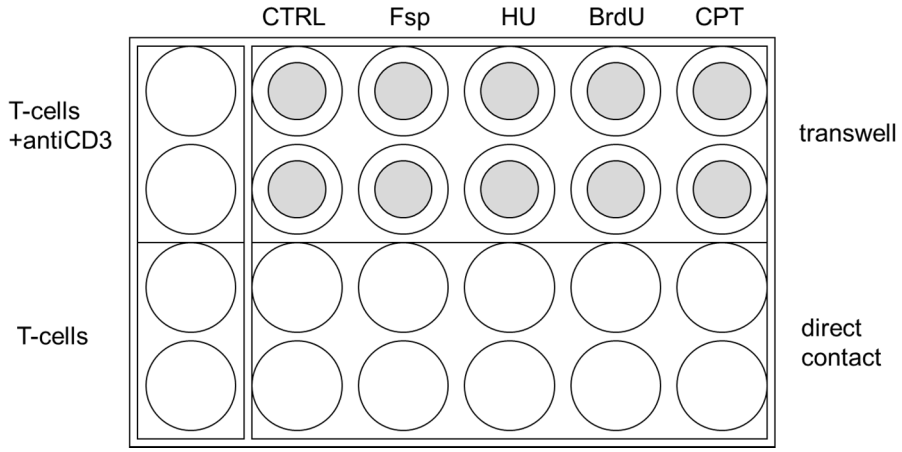

Figure 6 | Co-culture of different types of NB-cells and T-cells in transwells and in direct contact.

2.2 Flow Cytometry

The BD LSRII Flow Cytometer was equipped with three lasers (solid state lasers 405nm and 488nm, He-Ne laser 635nm). The BD LSRFortessa cell analyser was equipped with four lasers (355nm, 405nm, 488nm and 640nm). The cytometer performance was checked weekly using SPHERO^{TM} Ultra Rainbow fluorescent particles (Sperotech, Libertyville, US). For data evaluation the BD FACS DiVa^{TM} (Becton Dickinson) software was used. Depending on the antibodies used, appropriate gating strategies were defined.

A washing step is defined by adding 400µl FACS buffer (PBS, 0.05% sodium azide, 0.1% BSA), centrifugation at 1200rpm at 4°C for 5 minutes and discarding the supernatant. Samples were kept on ice throughout the staining procedure. DAPI solution (2µl/ml DAPI in 1xPBS solution, Sigma-Aldrich, Germany) was added 5 minutes before measurement at the flow cytometer.

2.2.1 Immunostaining of GD2, CD44 and MHC I for FACS analysis

For analysis of CD44, MHC I and GD2 (chapter 4.1.4.2: Flow-cytometry analysis of GD2, CD44 and MHC I and chapter 4.2: Functional Analysis- Co-culture of senescent and non-senescent NB-cells) 10^5 cells were washed with FACS buffer and resuspended in 50µl FACS buffer. For the first staining step, 6 µl of 1:20 pre-diluted anti-GD2-FITC, 5 µl anti-CD44-PE and 3 µl anti-MHC I-biotin were added (see table 1). The cell suspension was mixed and incubated for 20 min at 4°C. Cells were washed with FACS buffer and resuspended again in 50 µl FACS buffer before the second staining step. 10 µl anti-streptavidin-PerCP were added, mixed and incubated for 20 min at 4°C. After a further washing step, cells were resuspended in 50 µl FACS buffer, 4 µl DAPI solution was added and cells were analysed for cell proliferation and CD44, MHC I and GD2 using the BD LSRFortessa flow cytometer (Becton Dickinson).

2.2.2 Immunostaining of CD45, CD4, CD8, CD25 for FACS analysis

For analysis of CD45, CD4, CD8 or CD25 (chapter 4.3: Functional analysis-immunomodulation) 10^5 cells were harvested, washed with FACS buffer and resuspended in 50 µl FACS buffer. Cells were stained with 2,5 µl anti-CD4-PerCP, 2 µl anti-CD8-APCeFluor 780, 2,5 µl anti-CD25-PE and 2,5 µl anti-CD45-APC (table 1), respectively. The cell suspension was mixed and incubated for 20 min at 4°C. Cells were washed with FACS buffer, resuspended again in 50 µl FACS buffer, 4 µl DAPI solution was added and cells were analysed for CFSE and CD45, CD4, CD8 or CD25 using the BD LSRII Flow Cytometer.

Ab specificity	Conjugate	Dilution	Used volume [µl]	Company
GD2	FITC	1:20	6	*
CD44	PE	1:10	5	BD Bioscience**
MHC I	Biotin	-	3	Abcam***
Streptavidin	PerCP	1:100	10	BD Bioscience**
CD4	PerCP	-	2,5	BD Bioscience**
CD8	APCeFluor 780	-	2	eBioscience****
CD25	PE	-	2,5	eBioscience****
CD45	APC	-	2,5	eBioscience****

Table 1 | Antibodies used for flow cytometry (*purified anti-GD2 antibody, chimeric ch14.18, was kindly provided by Prof. Dr. med. Handgretinger, Universitätsklinikum Tübingen, Germany/ ** BD Bioscience, San Jose, CA, USA / *** Abcam, Cambridge, UK / **** eBioscience, San Diego, CA, USA)

2.3 Microscopy

2.3.1 Senescence-associated β-galactosidase activity assay

Cells were grown in a 6-well plate at a density of $5x10^5$ cells/well. After washing cells one time with PBS the senescence detection kit (BioVision, Mountain View, USA) was used to stain for SA-β Gal activity. 1 ml Fixative Solution per well was added for 15 min at room temperature. Meanwhile the Staining Solution Mix (1 ml/well) containing 940 µl Staining solution, 10 µl Staining Supplement and 50 µl X-gal in DMF (20 mg/ml) was prepared. After cells were washed two times with PBS, they were covered with the freshly prepared Staining Solution Mix and incubated overnight at 37°C in an incubator. Next day, cells were rinsed with PBS, analysed with an Axiovert 40C inverted microscope (Zeiss, Austria) and photographed with PixeLINK software (Ottawa, USA). 200 cells positive for SA-β Gal activity (blue-staining) were counted.

2.3.2 Cytospin preparation

Cells were harvested with Accutase, resuspended in PBS and kept on ice until usage. Slide carriers, cytospin funnels, filter cards and slides were assembled and placed into the cytocentrifuge (Shandon, Cheshire, United Kingdom). Filters were pre-wetted with 50 µl of 0,9% sodium chloride solution and centrifuged at 600 rpm for one minute. 50-200 µl ($1-4x10^4$ cells per slide) of the cell suspension was distributed onto each slide by centrifuging 8 minutes at 500 rpm. Filter and funnel were carefully removed without damaging the cells and the slide was air dried at least for one hour. Preparations were either used immediately or stored at RT for up to two weeks. To store cytospins for a longer period they were frozen at -20°C in appropriate boxes.

2.3.3 Double-target Fluorescent in situ hybridization to analyse *MYCN*-status

The cell spot on cytospin slides was marked on the back of the slide using a diamond scribe. Slides were fixed in precooled (4°C) 4% paraformaldehyde (Roti-Histofix 4%, Roth, Karlsruhe, Germany) for 10-15 min. Then they were washed twice with 1xPBS for 5 min at RT, dehydrated in an Ethanol series (70%, 90%, 95% Ethanol; for each 2 minutes) and air dried in a rack. 1 µl of the nick-labeled probes, *MYCN*-dig and 2p-bio, were applied to the cells and a cover glass was sealed with rubber cement (Fixogum, Marabu, Tamm, Germany). For denaturation of target DNA and probe, slides were placed on a heating plate (Präzitherm, Störcktronic) at 78°C for 8 min. Hybridization was achieved through incubation in a moist chamber in a Haereus incubator at 37°C over-night. Next day, slides were washed for 5 minutes in 2 x SSC at RT. Then they were placed two times 15 min into a tank with pre-warmed 50% formamide in 2 x SSC at 42°C (in a water bath) and two times for 7 min into a

tank with pre-warmed 2 x SSC at 42°C. For detection of the probes, antibodies against digoxigenin, and biotin were diluted in the same 2-3% BSA/PBS solution and 100 µl was applied to the hybridized area. The dilution factor used for mouse Cy3-conjugated Anti-biotin (Dianova GmbH, Hamburg, Germany) was 1:800 and for sheep FITC-conjugated anti-digoxigenin antibody (Roche Diagnostics GmbH, Mannheim, Germany) 1:200. Incubation was performed in a moist chamber at 37°C for 30-45 min followed by two washing steps (each 7 min) in 4 x SSC supplemented with 0.1% Tween20 at 42°C . Secondary antibodies in 2-3% BSA/PBS solution were incubated in a moist chamber at 37°C for 30 min. Goat Cy3-conjugated anti-mouse (Dianova GmbH, Hamburg, Germany) was diluted 1:500 and rabbit FITC-conjugated anti-sheep (Dianova GmbH, Hamburg, Germany) was diluted 1:200. The washing procedure described above was repeated and slides were dehydrated again through an ethanol series followed by air drying in the dark. Preparations were mounted with 10 µl Vectashield (Vector, Burlingame, Ca, USA) supplemented with DAPI and covered with a cover slip that was sealed with rubber cement (Marabu). Analysis was performed with an Axioplan fluorescence microscope (Zeiss, Austria) and images were processed with the Isis software (MetaSystems, Altlussheim, Germany).

2.3.4 Probe (*MYCN* and 2p) labelling by nick translation

The bacterial clones 08–103-1 (chromosome 2p) and RP11-355-H10 (AC010145, *MYCN*) were obtained from Dr. M. Rocchi (Resources for Molecular Cytogenetics, University of Bari, Italy). 2 µg of extracted template DNA was combined with either DIG-Nick Translation Mix (Roche, Vienna, Austria) containing 0.08 mM digoxigenin-11-dUTP for *MYCN* labelling or Biotin-Nick Translation Mix (Roche, Vienna, Austria) containing 0.08 mM biotin-16-dUTP for 2p labelling. The total volume was adjusted to 40 µl with ddH_2O. Incubation took place in a water bath at 16°C for 90 min. Afterwards probe labelling and size (*MYCN*: 200 Kb) was verified by running 5 µl of the respective sample mixed with 1 µl loading buffer in a 1,2% agarose gel at 100 V and 500 mA. Meanwhile the probes were stored on ice to allow further nick labelling.

The reaction was stopped by addition of 30 µg of COT human DNA (Roche Diagnostics GmbH, Mannheim, Germany), a volume of NaAc (3M, pH 5.5, Merck, Darmstadt, Germany) calculated as 1/10 of the probe volume plus the COT DNA volume and 2.5 times the volume of the solution of 100% Ethanol (Merck, Darmstadt, Germany). Labelled DNA probes were precipitated through a 30 min incubation reaction at -80°C followed by 30 min centrifugation at 13000 rpm at 4°C in a Hereaus Biofuge pico. The supernatant was discarded and the pellet resuspended in 70% Ethanol. The following centrifugation was done for 15 min at 13000 rpm at 4°C. After the supernatant was again removed, the DNA pellet dried for 5 min at RT. Finally, the probe was resuspended in 40 µl of a hybridization mix (master mix contains 200 µl distilled water, 200 µl formamide, 100 µl 20x SCC and 200 µl dextransulfate)

and the DNA dissolved at 37°C in an thermomixer (Eppendorf, Germany). Probes were stored at 4°C.

2.3.5 GD2 and CD44 Immunostaining on cytospins

Cytospin slides were fixed in precooled (4°C) 4% paraformaldehyde (Roti-Histofix 4%, Roth, Karlsruhe, Germany) for 15 min. After washing two times with 1xPBS for 5 min each at RT, slides were incubated with the primary antibodies for 30-45 min at 37°C in a humid chamber. The mouse anti-human CD44 antibody (Bender MedSystems, Vienna, Austria) was diluted 1:50 and the anti-human GD2-FITC antibody (purified anti-GD2 ch14.18 delta was kindly provided by Prof. Dr. med. Handgretinger, Universitätsklinikum Tübingen, Germany. FITC labelling of anti-GD2 was done in our group) 1:100 in 2-3% filtered BSA. After the slides were again washed two times with 1xPBS for 5 min each at RT, the Cy3-labeled goat-anti-mouse secondary antibody (Dianova GmbH, Hamburg, Germany) was applied at a 1:500 dilution with 2-3% filtered BSA for 30-45 min in a humid chamber at 37°C. After two washing steps in 1xPBS, slides were stained with a 2 µl/ml DAPI (Sigma-Aldrich, Germany) in 1xPBS solution for 1 min at RT. Slides were again washed two times for 5 min in 1x PBS to remove the DAPI solution. Finally, cells were covered with Vectashield (Vector, Burlingame, Ca, USA) and an adequate cover slip was sealed with Fixogum rubber cement (Marabu). Slides were examined with an Axioplan fluorescence microscope (Zeiss, Austria) and pictures were taken with a high resolution CCD camera with the ISIS software (MetaSystems, Altlussheim, Germany).

2.4 Protein Analysis

2.4.1 Western Blot

Cells were harvested, centrifuged at 1200 rpm for 10 min and washed once with PBS before shock freezing the pellet in liquid nitrogen. After thawing, the cell pellets were lysed with RIPA buffer (50 mM Tris.HCl pH7.4, 1% NP-40, 0.5% Na-deoxycholate, 0.1% SDS, 150 mM NaCl, 2 mM EDTA, 50 mM NaF) containing phosphatase inhibitor sodium orthovanadate (Sigma S6508-10G) and protease inhibitor (Complete ETDA free, Roche) and dispersed by sonication (3 sec, 9 Cycles, 50% Power). Tubes were kept on ice during sonication to prevent heating of the sample. Afterwards, tubes were centrifuged for 15 min at 13.000 rpm and 4°C and the supernatant, containing the protein extract, was transferred to a fresh tube. Protein concentration of each sample was determined with a Bradford Assay (Biorad Protein Assay). The sample volume corresponding to 60 µg protein was calculated. All samples were filled up to the same volume with RIPA buffer, mixed with 4x loading buffer and boiled for 5 min at 95°C. Samples were centrifuged for 2 min at full speed and loaded on a 8,5% or 10%

SDS PAGE (Sodium Dodecyl Sulfate PolyAcrylamide Gel Electrophoresis) gel (see table 3) depending on the size of the protein to be assayed. Additionally 5 µl of pre-stained Page Ruler was loaded in one slot. The gels were submerged in 1x running buffer and the gel was run at 40V until samples reached the separating gel. Then the voltage was increased to 100V for 1.5 hours. Proteins on the gel were blotted onto a nitrocellulose membrane with 0.2µm pore size. Gel and membrane were sandwiched between sponge and paper and clamped together avoiding air bubbles. Blotting was achieved in 1x transfer buffer for 1.5 hours at 220 mA. The proteins were visualized through staining with Ponceau for 7-8 min to determine if they have migrated uniformly and evenly. The Ponceau staining was scanned. Unspecific binding sites were blocked with 1x blocking solution (Roche) for at least 30 min under agitation at RT. The membrane was incubated with the primary antibodies diluted in 0.5% blocking solution over night at 4°C shaking. The blots were washed 2 times for 10 min with TBST and 2 times for 10 min with 0.5% blocking solution. Secondary antibodies were diluted in 0.5% blocking solution and pipetted on the membrane. Incubation was performed for one hour at room temperature in the dark under agitation. Antibodies and the concentrations used are depicted in table 4. Membranes were washed three times for 10 min with TBST and once for 10 min with TBS. Measurement of the fluorescence was performed with the LI-COR ODYSSEY system. Chemiluminescence was detected using the Femto-chemiluminescence detection kit (Thermo Scientific, USA), light-sensitive films and a film developer.

RIPA buffer	PBS containing 5mM EDTA, 1% NP40, 1% deoxycholate, and 2% SDS, with 1x protease inhibitor mix
10x running buffer	30,3g Tris base pH 8,3, 144g Glycine, 10g SDS in 1L dH_2O
1x running buffer	1:10 dilution of 10x running buffer
10x transfer buffer	140g Glycine, 30g Tris base 1L dH2O
1x transfer buffer	100 ml 10xTransferbuffer, 700ml dH2O and 200ml Methanol
Maleic Acid Buffer	5,8g Maleic Acid (100mM), 4,38g NaCl (150mM), adjust pH to 7,5 with NaOH and steril filter
10x Blocking Solution	10g Blocking Reagent in 100ml Maleic Acid Buffer (autoclaved)
1x / 0,5x Blocking Solution	1:10 / 1:20 dilution of 10x Blocking solution with TBS
10x TBS	60,57g Tris-HCl pH 7,5 and 43,83 g NaCl (1,5M) in 500ml dH_2O
1x TBS	1:10 dilution of 10x TBS
1x TBST	1:10 dilution of 10x TBS + 1ml Tween-20 in 1L

Table 2 | Buffers and solutions used for Western Blot

Reagent	Stacking Gel 8,5%	Stacking Gel 10%	Seperating Gel
30 % Acrylamide mix *	1,4 ml	1,65 ml	0,415 ml
Aqua dest.	2,28 ml	2,025 ml	1,7 ml
Tris (1.5 M, pH 8.8)	1,25 ml	1,25 ml	-
Tris (1 M, pH 6.8)	-	-	0,315 ml
20% SDS	25 µl	25 µl	12,5 µl
10% APS	50 µl	50 µl	25 µl
TEMED	3 µl	3 µl	2,5 µl

Table 3 | Recipes for Stacking and Running Gel. * Rotiphorese Gel 30, Carl Roth, Germany

1. Ab against	dilution	species	Company	2. Ab against	dilution	Company
Cdk2 (M2)	1:500	rabbit	Santa Cruz biotechnology	GαRb red	1:10.000	LI-COR
GAPDH	1:1000	mouse	Santa Cruz biotechnology	GαM green	1:10.000	LI-COR
n-Myc	1:50	mouse	Abcam	GαM green	1:10.000	LI-COR
p16 (F-12)	1:100	mouse	Santa Cruz biotechnology	αRb-HRP	1:10.000	Femto-Kit
p53 (DO-1)	1:1000	mouse	Santa Cruz biotechnology	GαM green	1:10.000	LI-COR
phospho p53 (Ser15)	1:350	rabbit	Cell Signaling	αRb-HRP	1:10.000	Femto-Kit

Table 4 | Antibodies used for Western Blot

2.5 Statistics

Data are presented as means ± standard deviation above and below the mean. Statistical analysis was conducted using Microsoft Office Excel 2010. A paired, 2-tailed Student *t* test was used to determine the statistical significance of differences between two analysed groups. Values of $P < 0.05$ were considered significant.

3 Aim of the study

(1) In the first part of our study, we aimed to analyse whether camptothecin and bromodeoxyuridine have the ability to induce senescence faster than hydroxyurea in *MYCN* amplified neuroblastoma cells *in vitro* and whether these treated cells differ in morphology, growth behaviour, *MYCN* status and marker expression from control and spontaneous senescent F-cells.

We have recently observed that long-term low-dose-treatment with the chemotherapeutic agent hydroxyurea (HU) induces senescence in primary neuroblastoma cell lines *in vitro*. Senescence induction with HU takes 8-10 weeks. To find other drugs which are able to induce senescence in a shorter period of time we tested camptothecin (CPT) and bromodeoxyuridine (BrdU) on *MYCN* amplified (MNA) neuroblastoma cells. We investigated changes in morphology, which could be indications of senescence, by microscopy. Next, we stained treated and untreated NB cultures for SA-β-Gal to confirm the senescence induction in HU, CPT and BrdU treated NB-cells and to quantify the number of senescent cells in these cultures. *MYCN* copy number was analysed by fluorescent in situ hybridization (FISH) in order to investigate, whether HU, CPT and BrdU treatment leads to a reduction of *MYCN* amplification in the nucleus, and therefore would acquire the characteristic of a less aggressive type of NB-cells. Furthermore we examined the abundance of the NB tumour marker GD2, known to be low after HU treatment, and expression of CD44, known to be up-regulated after HU treatment, by immunofluorescence and FACS in control, spontaneous senescent and drug induced senescent cells. We previously described that NB-cell lines, negative for MHC I, up-regulate MHC I surface expression in spontaneously occuring senescent cells and in response to HU. We then wanted to know, if expression of the MHC class I molecule changes also after treatment with CPT and BrdU and therefore analysed the differently treated NB-cells via FACS. To study candidate pathways involved in senescence of spontaneous senescent cells and drug induced senescent cells we analysed the expression and in part the phosphorylated/activated forms of key mediators of senescence by Western Blot.

(2) In the second part of our study, we asked whether senescent neuroblastoma cells modulate the proliferative capacity and tumour marker expression of non-senescent neuroblastoma cells *in vitro.*

The senescence-associated secretory phenotype (SASP) has been described as the secretion of numerous cytokines, growth factors and proteases by normal and tumourigenic

(premature) senescent cells. SASP components have been shown to trigger both beneficial and unfavourable effects, probably depending on the cell type and physiological context. For instance, some secreted factors can induce proliferation arrest and senescence in malignant cells to prevent tumour development. However, SASP can also stimulate regeneration and repair of tissues after damage and thus can promote proliferation in nearby cells. These ambivalent facts raised the question, whether senescent NB-cells modulate the proliferative capacity and the expression pattern of GD2, CD44 and MHC I in non-senescent neuroblastoma cells *in vitro*. To investigate this, we assessed a co-culture experiment with control and HU treated senescent NB-cells. Cells were counted and expression of GD2, CD44 and MHC I was monitored by FACS staining, in weekly intervals.

(3) In the last part of our study, our aim was to test whether senescent neuroblastoma cells differ from non-senescent neuroblastoma cells in their capability to stimulate T-cell proliferation/activation *in vitro*.

Previous publications have reported that neuroblastoma cells are poorly immunogenic. For instance they lack MHC I expression and thus inhibit T-cell activation *in vitro* and *in vivo.* As senescence leads to a change of the expression profile in NB-cells, we posed the question:
Do senescent NB-cells allow T-cell proliferation *in vitro*?
Functional analyses were carried out to test the response of $CD4^+$ and $CD8^+$ T-cells to senescent versus non-senescent NB-cells. We co-cultured T-cells and NB-cells (either control cells, spontaneous senescent cells, HU-, CPT- or BrdU induced senescent cells) for 6 days and looked for the percentage of cells that had proliferated within the $CD4^+$ and $CD8^+$ fraction by FACS analysis. Further, we wanted to know, if secreted or cell bound factors play a role. Thus we analysed if the supernatant of NB-cells is sufficient to trigger an effect on T-cell proliferation. For this, on the one hand conditioned medium of NB-cells has been transferred to T-cells, and on the other hand co-cultures in transwell plates have been carried out and again proliferation of cells within the $CD4^+$ and $CD8^+$ population was measured by FACS analysis. Additionally, we looked for the T-cell activation marker CD25 in the transwell experiment.

4 Results

4.1 Characteristics of induced senescent neuroblastoma cells *in vitro*

In this part of our study we wanted to investigate whether CPT and BrdU treatment of MNA neuroblastoma cell lines lead to senescence, as shown in long-term HU treated NB-cells, *in vitro*. Further we wanted to know, if those drug treated NB-cells are similar to spontaneous senescent F-cells and HU treated senescent cells and whether they differ in morphology, growth behaviour, SA-β-Gal staining, *MYCN* copy number and GD2, CD44 and MHC I expression compared to control cells.

The two neuroblastoma cell lines STA-NB 10 and NB-Ma, used in this study, have been established from high risk tumours of neuroblastoma patients, which show MNA appearing as dmin. We have described previously, that low dose treatment with the micronuclei-inducing drug HU over 6-8 weeks induces senescence, apoptosis and differentiation in MNA NB-cell lines [125]. In order to identify a drug, which induces senescence in a shorter period of time, several NB-cell lines were treated with potential senescence inducing drugs. Short term cell survival was measured by MTT assay at day 3 and day 5 and IC50 values were determined. Based on this assay, we investigated the effect of camptothecin (CPT) and bromodeoxyuridine (BrdU) at IC50 concentrations (determined at day 5) on the two neuroblastoma cell lines STA-NB 10 and NB-Ma in a longterm experiment.
CPT is an anticancer drug, which targets the enzyme topoisomerase I and arrests cells in G2 phase. Treatment with CPT has been shown to trigger rapid apoptosis in some cell types (e.g. HeLa) [168]. However low doses of CPT can also induce a senescence-like-phenotype as observed in a human colon cancer cell line [88].
BrdU is a thymidine analogue that is incorporated into replicating DNA. Originally, it was designed to disturb DNA synthesis in cancer cells [169]. BrdU has been shown to induce a senescence-like phenotype in normal and immortal mammalian cells *in vitro* [170, 171] and in NB-cell lines [172]. Therefore it was chosen as positive control for *in vitro* experiments.

4.1.1 Growth behaviour and cell morphology

To look for changes of morphology and growth behaviour of drug treated NB-cells and compare them to control cells and spontaneous senescent F cells, control cells (CTRL) of the cell lines STA-NB 10 and NB-Ma were treated either with 150 µM HU, 5 nM CPT or 20 µM BrdU for 3-10 weeks, respectively (Fig. 7).
Control cells primarily consist of N-cells, small cells with scant cytoplasm and neurite outgrowth (Fig. 7A). Sporadically, spontaneous F-cells, cells with flat morphology and high granularity, were found in the control populations (Fig. 7A), but their frequency was

significantly lower than in drug treated populations (Fig. 7C-E). Spontaneous senescent F-cells were purified as described in materials and methods. In both cell lines spontaneous F-cells showed a senescent morphology and strongly slowed down their proliferation (Fig. 7B).

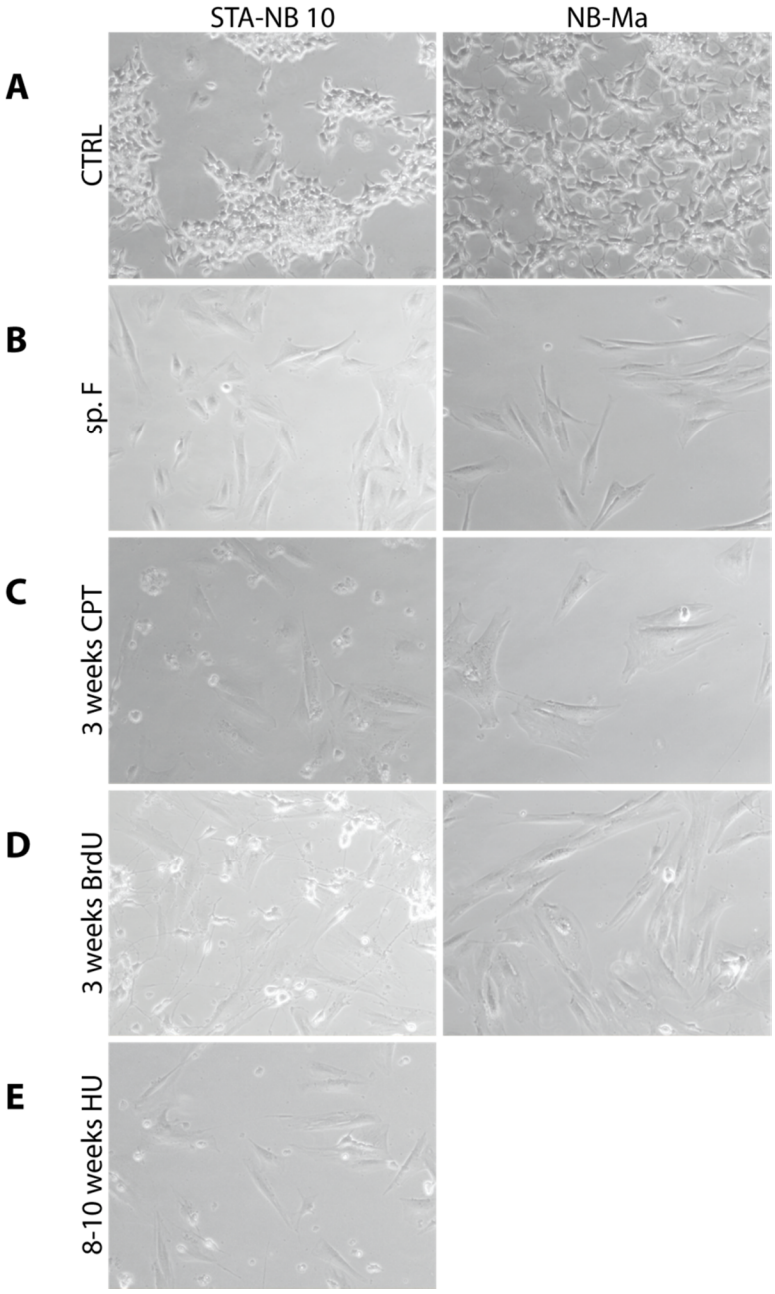

Figure 7 | Morphology of STA-NB 10 and NB-Ma cells before and after drug treatment
Images of control cells (CTRL), spontaneous senescent F-cells (sp.F), 3 weeks CPT treated cells, 3 weeks BrdU treated cells and 8-10 weeks HU treated cells were taken using phase contrast microscopy.
(×10 magnification)

HU treatment of STA-NB 10 cells led to a decrease of N-cells in the culture. In the first week after induction many cell debris were present in the medium, but there were still a lot of N-cells in the culture. After continuous induction with HU more and more senescent F-cells appeared in the culture while the amount of N-cells further went down. Further, some of the remaining N-cells clustered and developed long outgrowths connecting other N-cell clusters

in the surrounding. These neurite networks resembled typical structures of differentiating neuroblastoma cells. After 8-10 weeks of weekly HU induction only a few sporadic N-cells remained next to a high number of senescent F-cells (Fig. 7E). HU treatment of NB-Ma was not included in this diploma study, but was done at a later time point in the group of Peter Ambros.

Upon CPT treatment both cell lines responded similar. In the first week a high number of N-cells died, but after 2-3 weeks the frequency of senescent F-cells increased, nevertheless compared to HU treated cells there were less F-cells present per culture flask. The cells became more granulated and larger compared to the HU treated cells. After 3 weeks, mainly F-cells were present in the culture (Fig. 7C).

Similarly, treatment with BrdU led initially to cell death in both cell lines. 2-3 weeks later the number of N-cells had decreased strongly and large adherent senescent F-cells were observed (Fig. 7D). After BrdU treatment the morphology and density of F-cells was more similar to HU treated cells than to the CPT treated cells. The proportion of the three cell types (N-cells, F-cells and differentiating cells) varied between different flasks and different inducing drugs, but generally cells with neurite extensions declined over time.

4.1.2 SA-β-Gal Activity

Senescence-associated β-galactosidase (SA-β-Gal) is the most consistent and widely used marker for senescent cells, which is defined as beta-galactosidase activity detectable at pH 6.0 in senescent cells [61]. SA-β-Gal activity is typically measured by staining with the substrate X-gal, which forms a perinuclear blue precipitate upon cleavage [173]. Thus senescent cells can be recognized due to their blue appearance after SA-β-Gal staining.

To prove senescence in NB-cells, SA-β-Gal activity was assayed on: control cells, spontaneous senescent F-cells, 3 weeks CPT treated cells, 3 weeks BrdU treated cells and 8-10 weeks HU treated cells (Fig. 8).

In both NB-cell lines the small N-cells were found to be SA-β-Gal negative, whereas F-cells were mostly positive for SA-β-Gal staining. Control flasks contained only 0-3% SA-β-Gal positive senescent cells (Fig. 8A and Fig. 9). Interestingly, the percentage of SA-β-Gal positive cells in spontaneous senescent F-cells differed strongly between the two NB-cell lines. In the STA-NB 10 cell line only 12% of SA-β-Gal positive cells were found (Fig. 8B, left panel and Fig. 9), while in the NB-Ma cell line 86% of the cells showed the blue SA-β-Gal staining (Fig. 8B, right panel and Fig. 9).

All drug induced senescent NB-cells of both cell lines acquired a strong blue SA-β-Gal staining indicating that they entered the senescent pathway (Fig. 8C-E). CPT induced cells showed 94-98% and BrdU induced cells displayed 88-90% SA-β-Gal positive cells. With 76% the HU induced STA-NB 10 cells showed slightly less SA-β-Gal positive cells compared to

cells treated with CPT or BrdU (Fig. 9). The SA-β-Gal results are in accordance to the senescence morphology observed in these cells.

For reasons of simplicity pre-senescent and senescent cells are summarized under the term senescent cell or senescent F-cell.

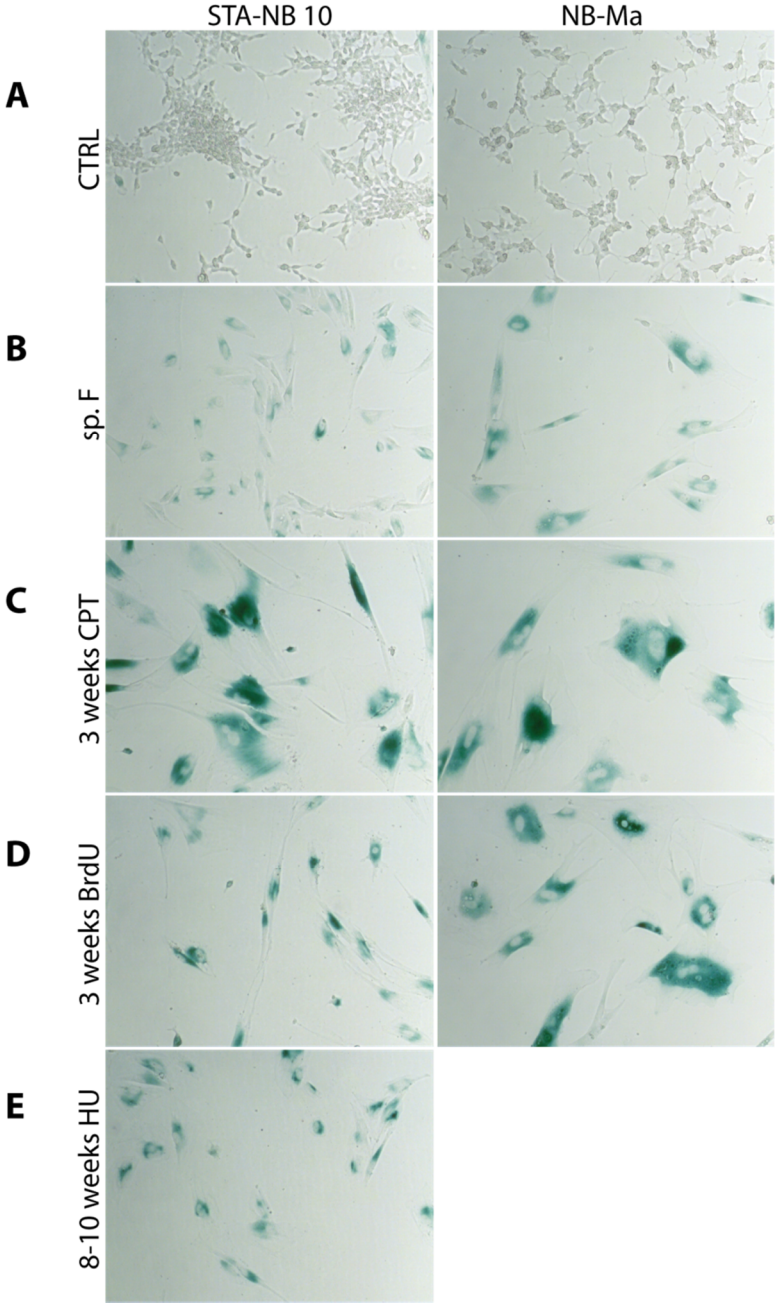

Figure 8 | SA-β Gal staining of STA-NB 10 and NB-Ma cells before and after drug treatment
Control cells (CTRL), spontaneous senescent F-cells (sp.F), 3 weeks CPT treated cells, 3 weeks BrdU treated cells and 8-10 weeks HU treated cells were stained for SA-β Gal. Cell images were taken using bright field microscopy. (×10 magnification)

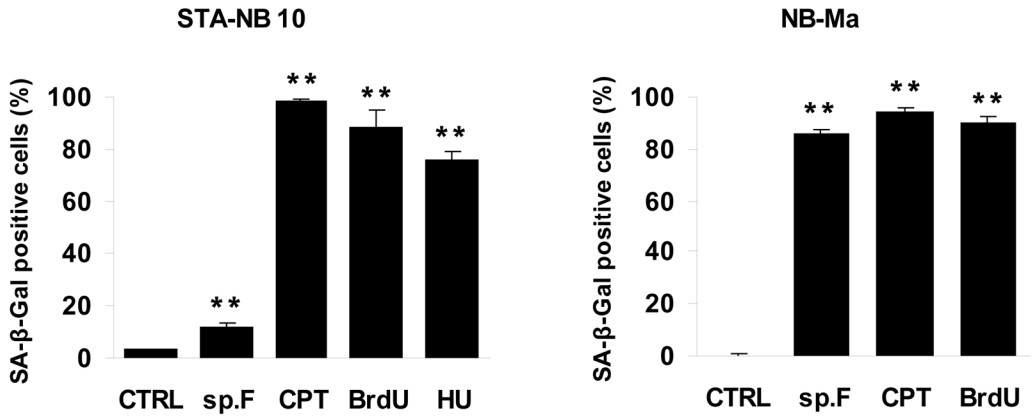

Figure 9 | Quantification of SA-β Gal positive cells in STA-NB 10 and NB-Ma cells

The percentage of SA-β-Gal positive cells in cultures of control cells (CTRL), spontaneous senescent F-cells (sp.F), 3 weeks CPT treated cells, 3 weeks BrdU treated cells and 8-10 weeks HU treated cells was determined by counting blue stained cells. In total 200 cells each were counted under the bright field microscope (mean ± s.d. of number counted by three persons; ** shows significance at the P ≤ 0.01 level compared to CTRL).

4.1.3 *MYCN* copy number

To investigate, if HU, CPT and BrdU treatment lead to a reduction of *MYCN* amplification in the nucleus, which would indicate that NB-cells turn into non-amplified cells known to be less aggressive in NB tumours, *MYCN* copy number was analysed by fluorescence in situ hybridization (FISH).

FISH was used to evaluate *MYCN* status in neuroblastoma [174]. This technique was applied on cytospin preparations of control cells, spontaneous senescent F-cells and treated cells, respectively (Fig. 10 and Fig. 11). A probe specific for the short arm of chromosome 2 (2p) was used as reference probe for *MYCN* FISH. Cells with *MYCN* amplification, which is defined as at least 4-times increased *MYCN* copy number compared to the 2p reference probe, were counted and the percentage of MNA cells was calculated for each condition and cell line (Fig. 12).

In control cell preparations of STA-NB 10 and NB-Ma the small round shaped nuclei contained strongly amplified *MYCN* copies (Fig. 10A and Fig. 11A). Visual inspection revealed a high number of green signals spread over the whole nucleus. In contrast, there were only two red signals for the reference probe indicating chromosome 2 disomy. Altogether, 90-92% of the control cells were *MYCN* amplified (Fig. 12).
In spontaneous F-cells of both cell lines most nuclei are bigger and more elongated compared to control nuclei. These cells had much less *MYCN* copies in both cell lines and

the *MYCN* signals were often found in clusters at the border of the nucleus (Fig. 10B and Fig. 11B).

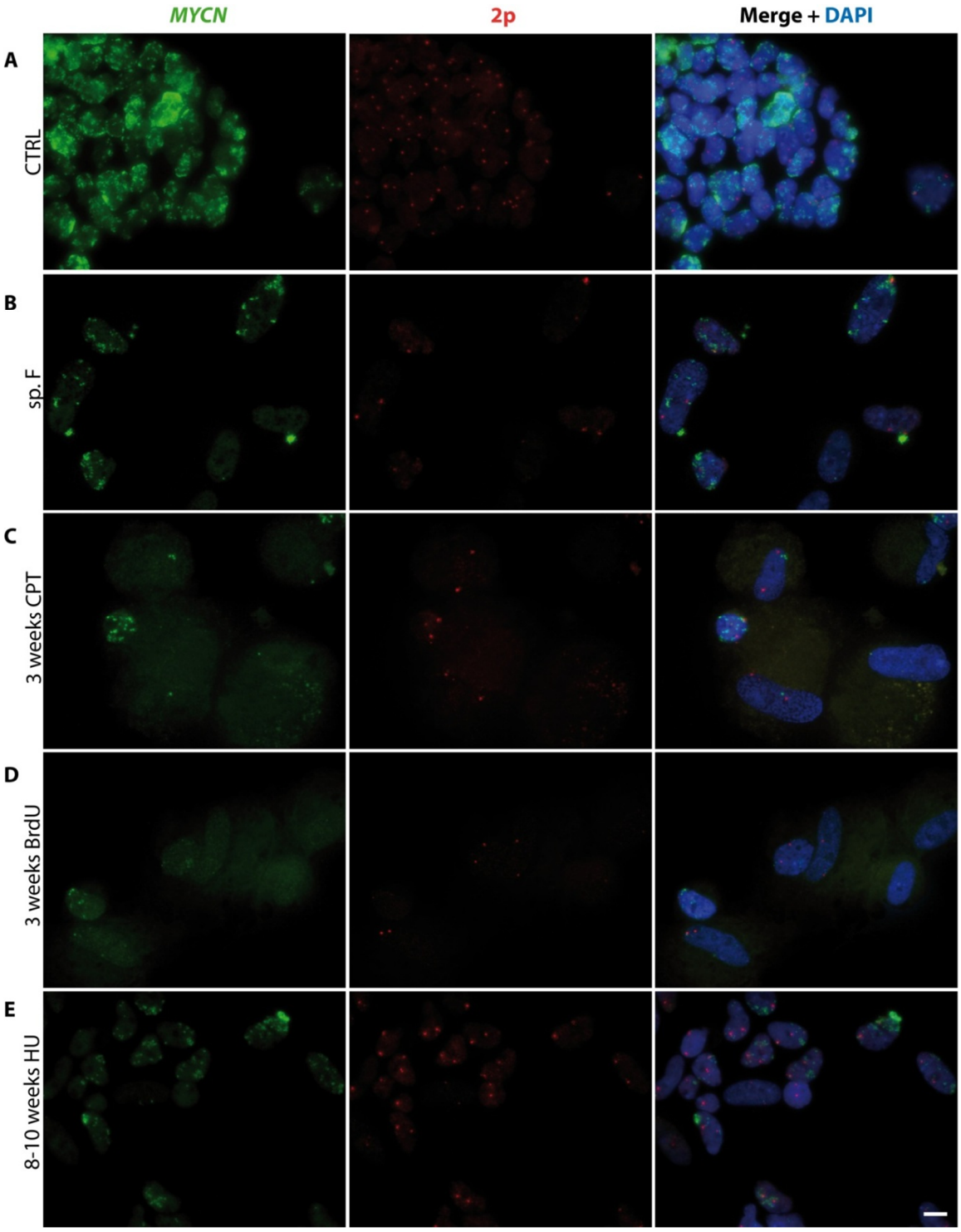

Figure 10 | *MYCN* copy number analysis in cells of STA-NB 10

FISH for *MYCN* (green) and 2p reference (red) and DAPI staining (blue) for nucleus identification on control cells (CTRL), spontaneous senescent F-cells (sp. F), 3 weeks CPT treated cells, 3 weeks BrdU treated cells and 8-10 weeks HU treated cells. (White bar=10 µM)

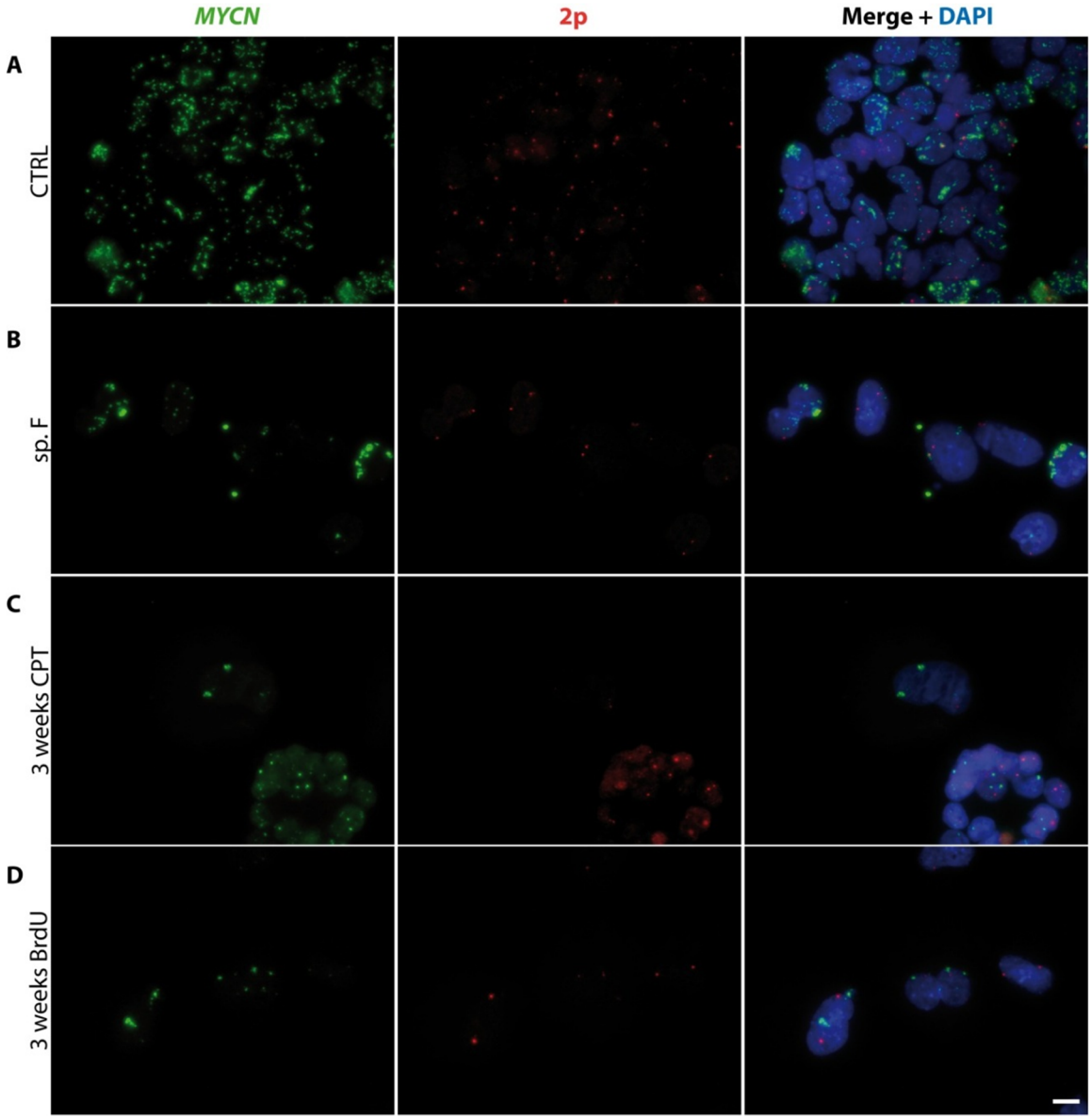

Figure 11 | *MYCN* copy number analysis in cells of NB-Ma

FISH for *MYCN* (green) and 2p reference (red) and DAPI staining (blue) for nucleus identification on control cells (CTRL), spontaneous senescent F-cells (sp. F), 3 weeks CPT treated cells, 3 weeks BrdU treated cells and 8-10 weeks HU treated cells. (White bar=10 µM)

Further, DAPI positive micronuclei densely packed with *MYCN* copies were frequently seen in the proximity of a nucleus. The percentage of cells having MNA was clearly decreased to 53-59% in spontaneous senescent F-cell populations (Fig. 12).

Similar to spontaneous senescent F-cells the nuclei of CPT, BrdU and HU treated senescent cells were larger than the nuclei of control cells. Notably, senescent cells display a higher autofluorescence in the cytoplasm due to the formation of autofluorescent lysosomal storage bodies known as lipofuscin [175].

CPT treated senescent cells showed a reduced number of *MYCN* copies (Fig. 10C and Fig. 11C). 47% of the CPT treated STA-NB 10 cells (Fig. 12, left panel) and 59% of the CPT treated NB-Ma cells (Fig. 12, right panel) were *MYCN* amplified. There remained still some N-cells in the culture when the cytospins were prepared, thus a direct comparison of N-cells (small round nuclei with many *MYCN* copies) and induced senescent F-cells (larger nuclei with less *MYCN* copies) can be seen on some slides (Fig. 10C).

FISH on BrdU treated cells was technically difficult, as BrdU incorporation probably hampers proper binding of the FISH probes. Thus MYCN and 2p signals were missing in the majority of nuclei and it was not possible to accurately quantify cells with MNA (BrdU treated STA-NB 10 are absent in Fig. 12, left panel). Nevertheless, in the small number of cells with both probes present, a reduction of *MYCN* copies was observed (Fig. 10D). In the NB-Ma cell line FISH on BrdU treated cells was successful showing a drastic reduction of the *MYCN* copy number in the majority of nuclei. The number of cells with supernumerical *MYCN* copies dropped down to 56% (Fig. 12, right panel).

As expected FISH on HU treated senescent STA-NB 10 cells revealed a low copy number of *MYCN* in the nuclei (Fig. 10E). Only 40% of cells with MNA remained in the cell population after HU treatment (Fig. 12, left panel). In summary, spontaneous senescent F-cells and cells treated with CPT, BrdU and HU revealed a strong reduction of MNA cells compared to control cells.

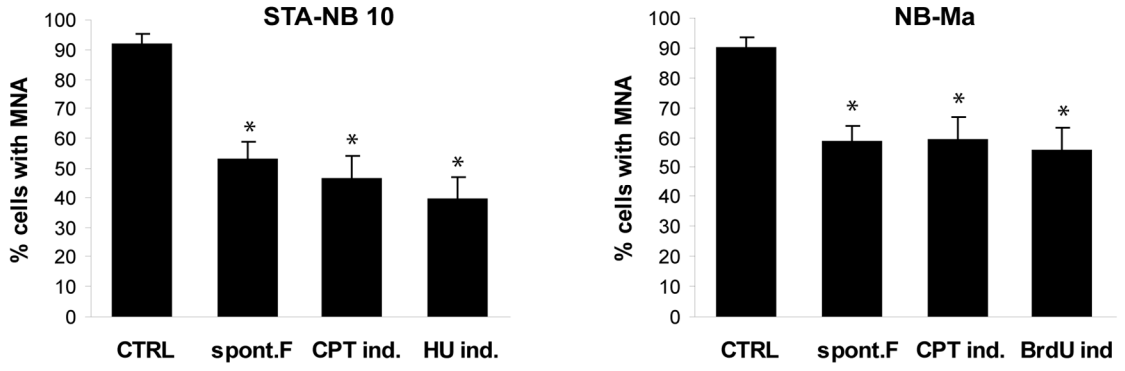

Figure 12 | Quantification of cells with *MYCN* amplification in STA-NB 10 and NB-Ma cells

The percentage of MNA cells in control cells (CTRL), spontaneous senescent cells and drug induced senescent cells was evaluated by counting nuclei with 4-times increased *MYCN* FISH signals compared to the 2p signal within 100 nuclei in total. All data are mean values ± s.d. of the number of MNA cells counted by two persons (* shows significance at the $P \leq 0.05$ level compared to CTRL; n=3).

4.1.4 Analysis of GD2 level, CD44 and MHC I expression

We have previously shown that in primary NB-cultures N-type cells show high levels of the NB tumour marker GD2 and lack CD44 and MHC I staining. In contrast, GD2 is down-regulated and CD44 and MHC I are up-regulated in spontaneous senescent F-cells and after HU treatment [125]. To study whether CPT and BrdU treated senescent cells differ in marker expression from control, spontaneous senescent F-cells and HU treated senescent cells, we first analysed GD2 and CD44 on cytospin preparations by immunofluorescence staining and second, studied and quantified cells containing these markers by FACS fluorescence together with MHC I.

4.1.4.1 Immunofluorescence staining of GD2 and CD44

Control cells of both cell lines were strongly positive for GD2 and completely negative for CD44 with the exception of some sporadic F-cells between the N-cells (Fig. 13 and Fig. 14). In contrast, spontaneous senescent F-cells and all drug treated senescent cells (no matter which drug was used for treatment) showed the opposite immunostaining with almost no signal for GD2 and a strong signal for CD44. Similar to the FISH images, a higher cytoplasmic autofluorescence was visible in senescent cells compared to control cells. However this yellow/greenish staining could be clearly distinguished from a normal mostly membrane-associated GD2 signal. In HU induced STA-NB 10 cells (Fig. 13) a few strong GD2 (green) stained N-type cells were visible next to strongly CD44 (red) stained senescent cells, exemplifying that GD2 and CD44 expression are exclusive on the majority of cells (Fig. 13 and Fig. 14).

4.1.4.2 Flow-cytometry analysis of GD2, CD44 and MHC I

To determine the percentage of cells positive for MHC I, CD44 or GD2 in untreated and drug treated senescent NB-cells, cells were immunostained and analysed by flow-cytometry. First we analysed the cells in forward scatter (FSC) versus side scatter (SSC). Next we gated for DAPI negative cells to omit dead cells. Viable cells were then depicted in a MHC I versus GD2 dot plot. Thereafter MHC I positive and MHC I negative cells were plotted for CD44 versus GD2, respectively (Fig. 15).

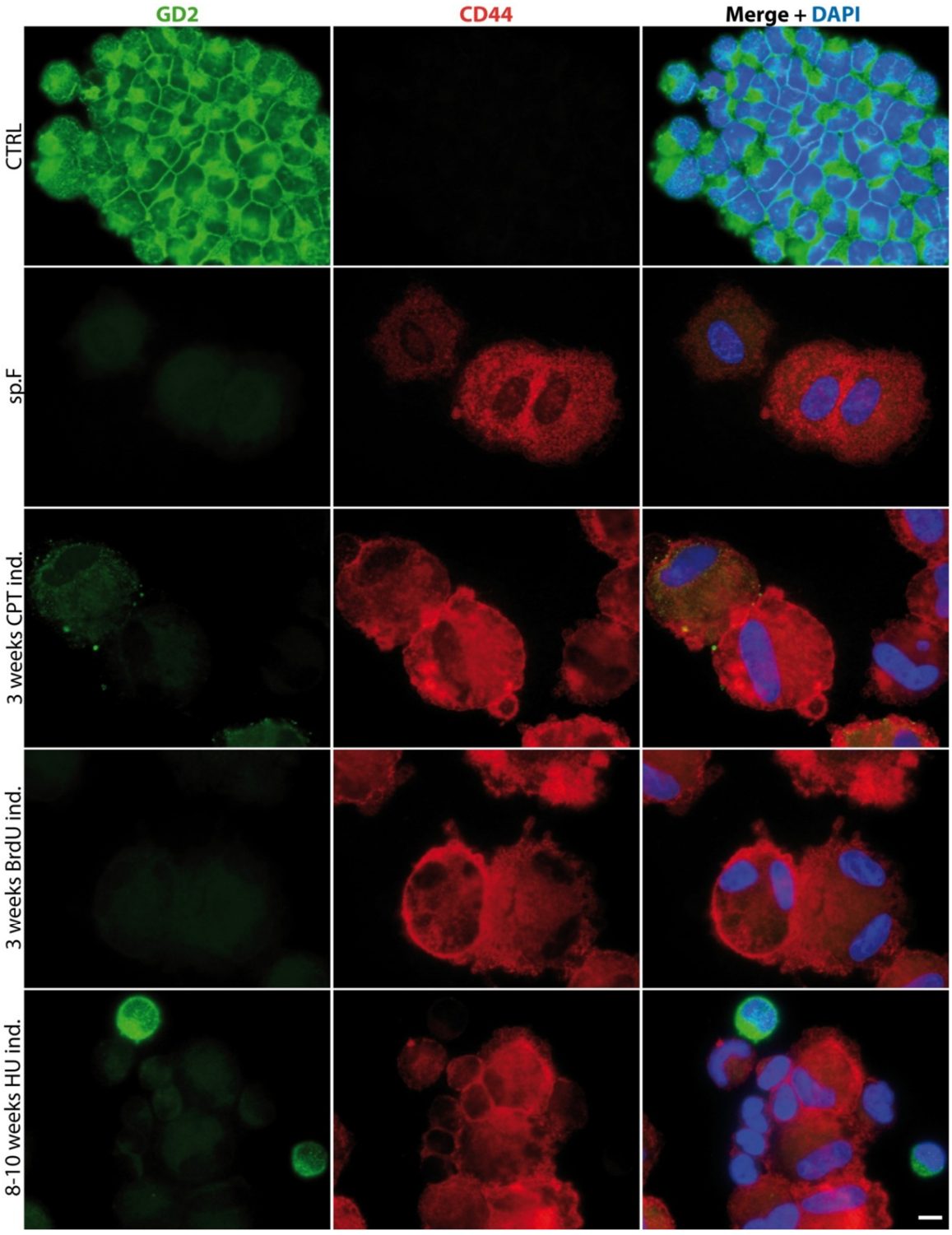

Figure 13 | STA-NB 10 cells were stained for DAPI, GD2 and CD44

Control cells (CTRL), spontaneous senescent F-cells (sp.F), CPT-, BrdU- and HU treated senescent cells were immunostained with anti-GD2-FITC (green), anti-CD44-TRITC (red) and DAPI on cytospin preparations. (White bar=10 µM)

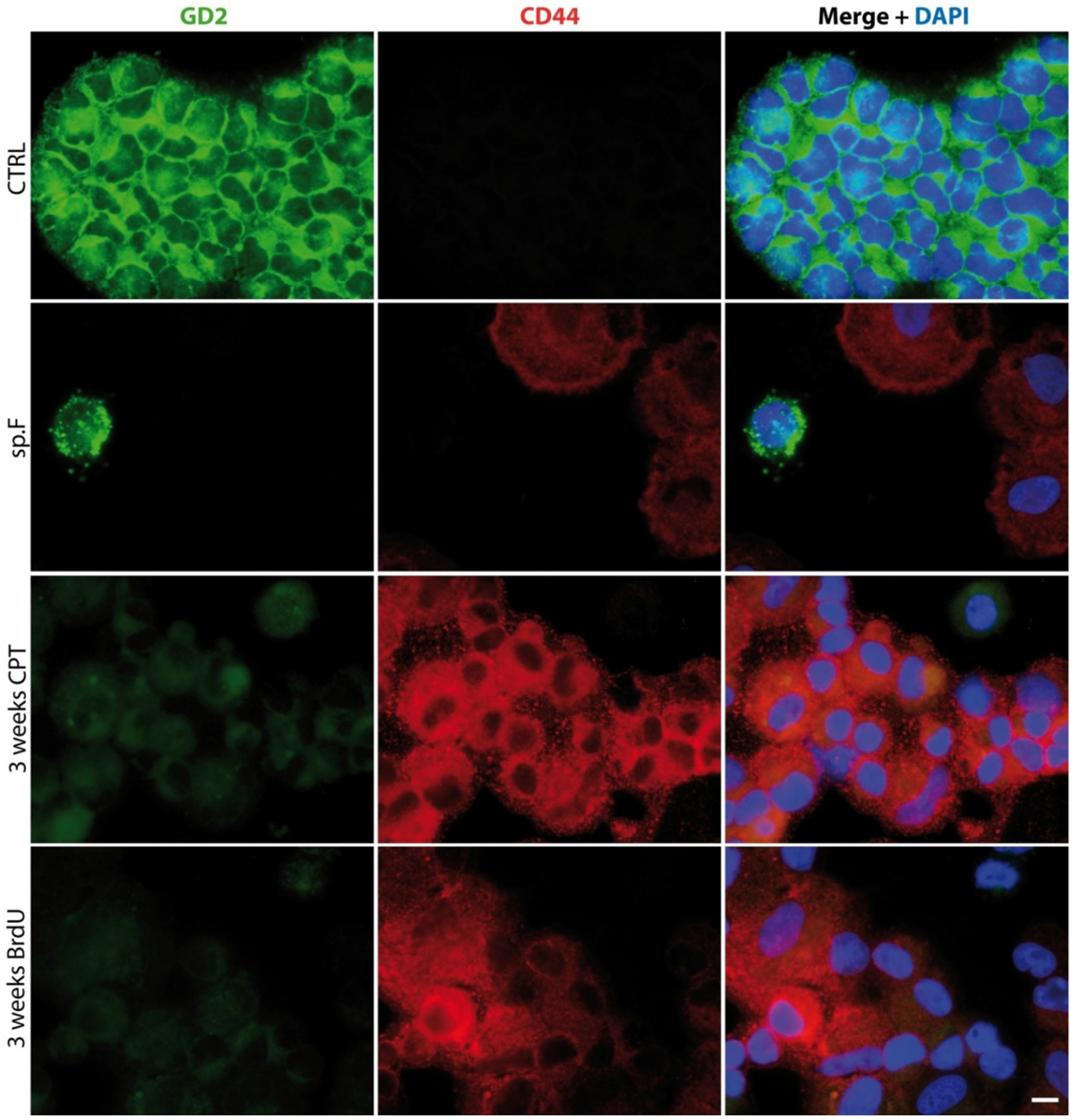

Figure 14 | NB-Ma cells were stained for DAPI, GD2 and CD44

Control cells (CTRL), spontaneous senescent F-cells (sp.F), CPT- and BrdU- treated senescent cells were immunostained with anti-GD2-FITC (green), anti-CD44-TRITC (red) and DAPI on cytospin preparations. (White bar=10 µM)

Senescent cells, both spontaneous and drug induced, showed higher SSC values, indicating higher granularity, compared to control cells (Fig. 15, left panel). Interestingly, CPT treated senescent cells displayed an even higher SSC and FSC, a measure for cell size, compared to all other conditions (Fig. 15, left panel). Further, control cells showed more dead cells and cell debris ($DAPI^+$) compared to senescent cells (Fig. 15, second panel from left). The gate for $DAPI^-$ cells has been adapted for spontaneous senescent F-cells and all drug treated senescent cells, due to their higher autofluorescence.

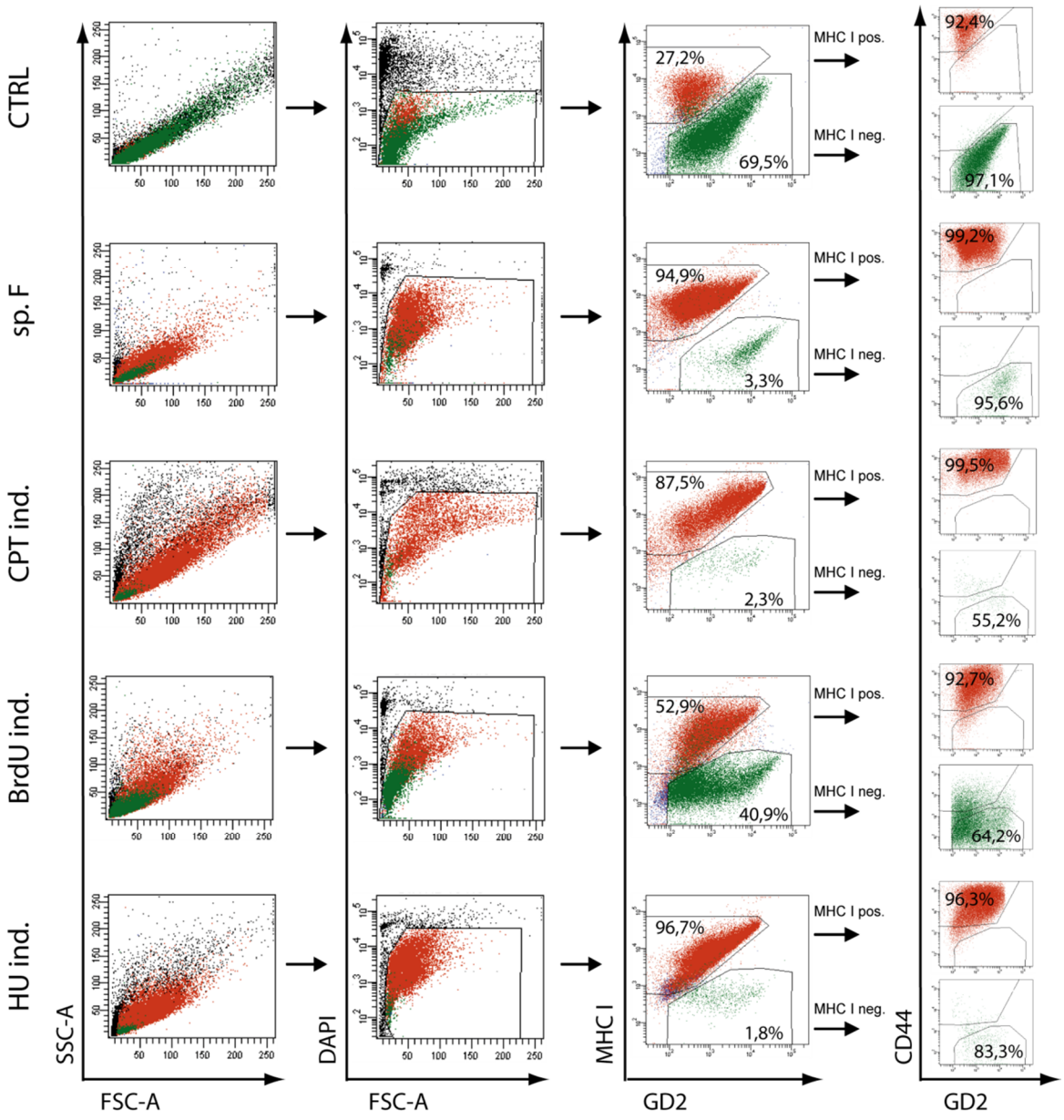

Figure 15 | STA-NB 10 cells were stained for DAPI, GD2, CD44 and MHC1 and analysed by FACS
Cells were gated on DAPI negative cells to exclude dead cells. In the next step these cells were gated on $MHCI^+$ and $MHCI^-$ cells, which were then separately displayed in a dot plot with CD44 on the y-axis and GD2 on the x-axis. Analysis was performed using the BD LSRFortessa cytometer. Data were evaluated using the BD FACS DiVa software. (One representative experiment of 3 is shown)

In the STA-NB 10 cell line more MHC I^+ $CD44^+$ cells can be seen in spontaneous senescent F-cell cultures (ranged between 70-97%), HU treated cells (ranged between 94-99%), CPT treated cells (~87%) and BrdU treated cells (~52%) compared to control cells (ranged between 3-27%). After BrdU treatment a high number of MHC I^- $GD2^+$ cells could be

detected in the culture (ranged between 43-49%) (Fig. 15, second panel from right and Fig. 16, left panel).

Similar results were found in the NB-Ma cell line. The percentage of MHC I^+ $GD2^-$ cells was clearly higher in spontaneous senescent F-cells (ranged between 43-84%), CPT treated (58-93%) and BrdU treated (82-91%) cells compared to control cells (2-7%) (Fig. 16, right panel).

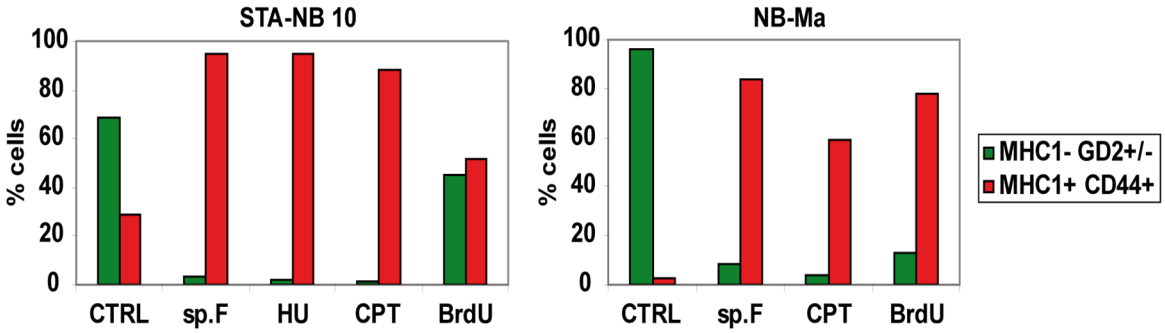

Figure 16| Quantification of MHC I^- $GD2^{+/-}$ and MHC I^+ $CD44^+$ cells by FACS analysis

The diagrams show the percentage of indicated cell populations in control (CTRL), spontaneous senescent F-cells (sp.F), CPT-, BrdU- and HU treated STA-NB 10 and NB-Ma cell lines. (Results from one representative experiment out of 3 are shown)

For all conditions, the majority (>92%) of MHC I^+ cells was $CD44^+$ (representing senescent F-cells). In control and spontaneous senescent F-cells almost all MHC I^- cells were CD44 low/intermediate (>95%). Notably, the percentage of $CD44^-$ cells within the MHC I^- $GD2^{+/-}$ cells was reduced in treated cells (55% in CPT ind., 64% in BrdU ind. and 83% in HU ind. cells). Thus not all MHC I^- cells were also $CD44^-$ (Fig.15, right panel).

In summary, we could show that treating MNA neuroblastoma cells for 3 weeks with CPT and BrdU turned them into enlarged adherent cells which became senescent. Thus, senescence induction of MNA NB-cells with CPT and BrdU was faster compared to HU induction, which took 8-10 weeks. Further, we could confirm senescence in all drug treated NB-cells by SA-β-Gal staining. Moreover, both cell lines displayed a decrease of *MYCN* copy number in spontaneous senescent cells and all drug treated senescent cells. Finally, we could see that GD2 level was reduced and CD44 and MHC I expression was increased in spontaneous senescent cells and all drug treated senescent cells compared to control cells.

4.1.5 Analysis of the senescence pathway

To study which senescence pathway is activated in spontaneous senescent cells and in HU, CPT and BrdU treated senescent STA-NB 10 cells we analysed the expression of the key mediators of the senescence pathways such as CDK2, p16, p53 and phospho-p53 (Ser15)

(as phosphorylation of p53 is associated with activation) by western blotting of whole cell lysates. Additionally, we studied the MYCN protein level to see whether the expression changes with the reduction of *MYCN* copy number in spontaneous senescent cells, HU-, CPT- and BrdU-treated senescent cells (Fig. 17).

MYCN expression was detected only in control cells, but not in senescent cells, which is in line with the reduced *MYCN* copy number seen in senescent cells. The CDK2 level was markedly down-regulated in all senescent cells compared to control cells. Furthermore, an accumulation of p16 could be observed in spontaneous senescent cells and in CPT and BrdU induced cells but not in HU induced cells which showed p16 levels similar to that in control cells. The expression of phospho-p53 was slightly up-regulated in spontaneous senescent cells and cells becoming senescent upon CPT treatment (Fig. 17; the upper strong band which can be seen in control cells is an unspecific band). The amount of total p53 was slightly higher in control cells (Fig. 17).

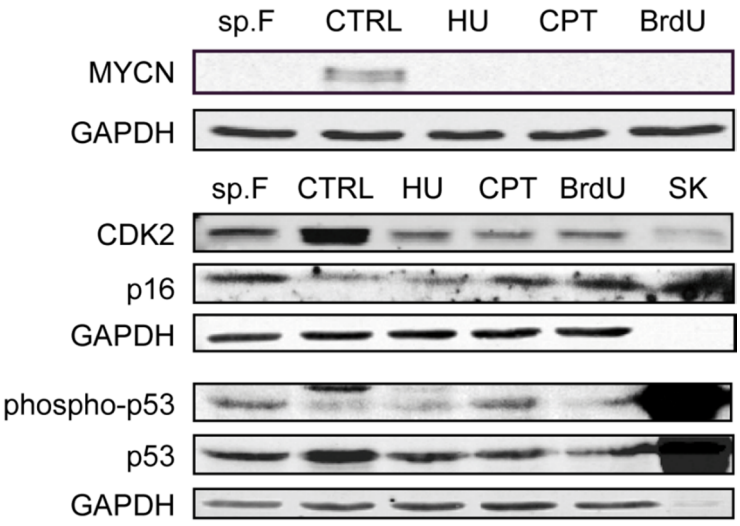

Figure 17| Western Blot of samples obtained after drug treatments of STA-NB 10 cells

Control cells (CTRL), spontaneous senescent F-cells (sp.F), HU induced, CPT induced and BrdU induced cells were collected and whole cell lysates were taken for Western blot. SK-N-MC (SK) cells (Ewing Sarcoma cell line) were additionally analysed and used as control for p53. Antibodies against MYCN, CDK2, p16, phospho-p53 and p53 were used. GAPDH demonstrates the loading control as it is constitutively expressed in almost all tissues at high levels.

4.2 Functional Analysis: Proliferation in co-cultures of senescent and non-senescent neuroblastoma cells

To observe whether senescent NB-cells modulate the growth behaviour and tumour marker expression of non-senescent neuroblastoma cells and vice versa we co-cultured control cells and HU induced senescent cells in one well. In addition, control cells and senescent cells were grown separately in distinct wells to compare the results with those of the co-culture.
Senescent cells were labelled with CPD, a cell dye, incorporating in the cell membrane, in order to be able to distinguish them via FACS from control cells which were CPD negative. We preferred to stain senescent cells instead of control cells with CPD because senescent cells should keep the CPD labelling longer than control cells due to their very low proliferation rate. Control cells proliferate faster, so their CPD intensity halves with every cell division. Cell number and expression of GD2, CD44 and MHC I was monitored at day 0, 2, 7, and 14. Supernatants were collected and frozen for future studies. Cytospins were prepared and frozen for future stainings.

In the first experiment, for each time point two wells (duplicates) of a 96-well plate with flat bottom were seeded either with control cells or HU treated senescent cells ($1x10^5$ cells/well) or for the co-culture with both types of cells ($5x10^4$ cells per cell type/well). For the second and third experiment wells were pre-coated with fibronectin and control cells were seeded in 24-well plates ($2x10^5$ cells/well). HU induced senescent cells and the co-culture was seeded in 12-well plates.

In experiment 1 control and senescent cells had a similar proliferation curve until day 7 (Fig. 18A). At the beginning cells showed little proliferation, then the number of cells fell to a lower cell number than on day 0. Cells in the co-culture proliferated and reached a three times higher cell number compared to day 0. Most of the cells dyed after day 7, thus there are no data for later time points. In the second and third experiment, bigger wells were used to ensure that the cells obtain enough medium for cell growth and wells were coated with fibronectin before seeding for better cell-attachment to the bottom of the wells. Both experiments ended after the analysis on day 14.
In experiment 2 the same cell number was observed on day 0 and on day 2. Moreover, cells proliferated between day 2 and 14. Control cells expanded 2.5 fold until day 7 and 4 fold until day 14. In HU treated senescent cultures the cell number stayed constant until day 7 and then increased their cell number 2.5 fold until day 14. Cells in the co-culture expanded very fast until day 7, but then died until the next analysis on day 14 and reached the same cell number as on day 0. Experiment 3 showed nearly the same trend until day 2. Thereafter, control cells started to proliferate and had a 4 fold higher cell number on day 14 compared to

day 0. Senescent cells did not proliferate, some cells even died. Cells in the co-culture doubled until day 7 and stayed almost the same until day 14. In summary, it was not possible to cultivate cells in co-culture for more than 2 weeks at this experimental setup. Further, all three experiments yielded different proliferation curves which were not conclusive.

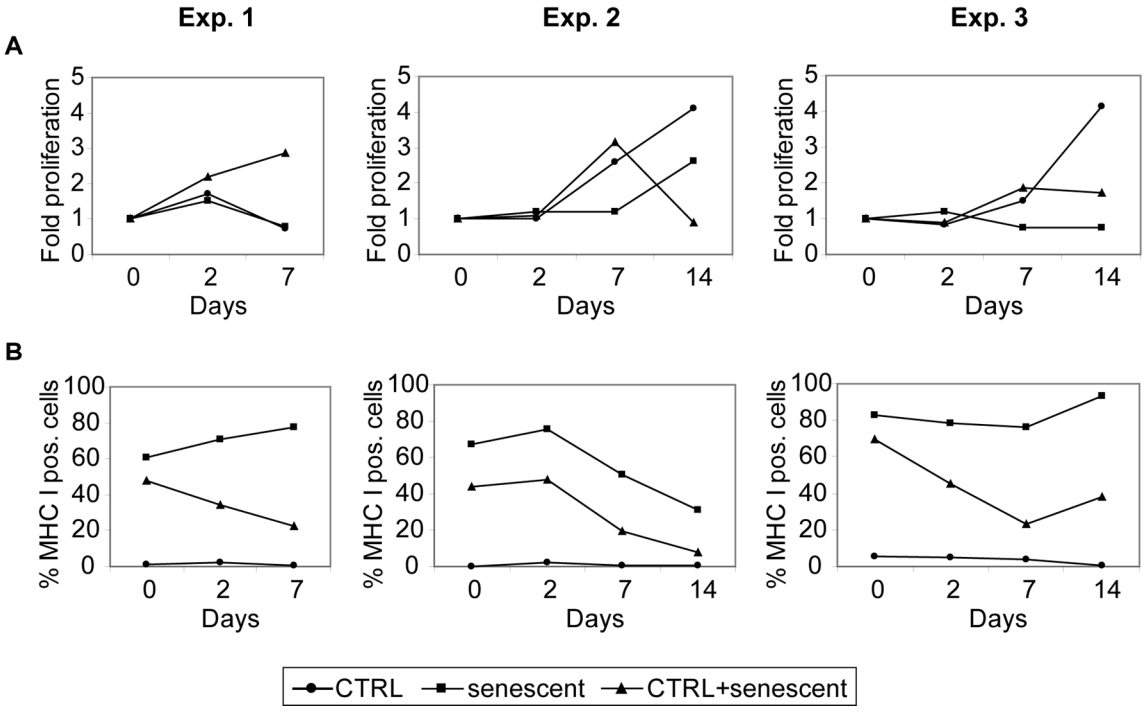

Figure 18 | Co-culture of control cells and HU induced senescent cells from the STA-NB 10 cell line
Control cells and senescent cells were cultivated separately and in co-culture to measure proliferation (A) and MHC I expression (B) of cells in each condition after 2, 7 and 14 days. Results of three independent experiments are shown.

CPD negative control cells contained mainly N-cells, but also a small population of F-cells which were shifted to the right side presumably because of their higher auto fluorescence (Fig. 19). The majority (80%) of the senescent cells were clearly CPD positive. The other part of the senescent cells was neither CPD negative nor clearly CPD positive. In comparison to the N-cells of the control cells they were more distributed and shifted to the right. As expected a mixture of these two populations was visible in the co-culture: Two defined populations, CPD negative and CPD positive are clearly distinguishable, representing control and CPD labelled senescent cells. This picture changed when cells that were longer in co-culture were analysed. Cells which were CPD positive on day 0 moved to the left and interfered with the unstained cells. Therefore, it was not possible to definitely separate CPD positive and negative cells. Thus the CPD staining was not accounted for further analysis.

Instead, we analysed MHC I positive, CD44 positive, GD2 negative cells in the total DAPI negative (alive) population. Percentages of MHC I positive cells in control, senescent and control plus senescent cells are shown in figure 18 B (results of three independent experiments). In all three experiments control cells contained only 0-5% MHC I positive cells and this did not change throughout the whole experimental period. Senescent cultures started with 60-83% and cells in the co-culture well with 44-70% MHC I positive cells. Regarding senescent cells, there was an increase from 60% to 78% MHC I positive cells in experiment 1. In experiment 2 MHC I positive cells increased little (from 67% to 76%) before the percentage dropped to 31% until day 14. In contrast, in experiment 3 MHC I positive cells decreased from 83% to 76% until day 7 and then increased to 93% until day 14. Notably, co-cultured cells showed a decrease of MHC I positive cells in all experiments.

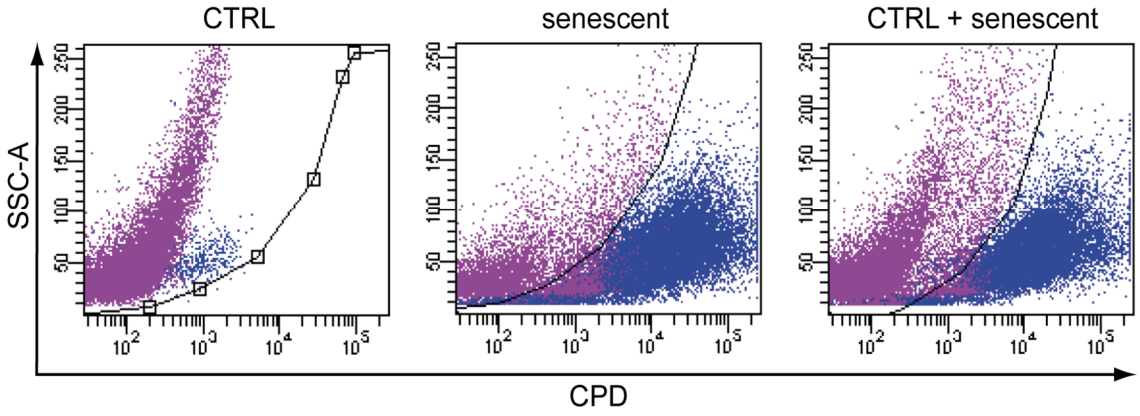

Figure 19 | CPD staining

One example of a co-culture experiment on day 0, when looking for the CPD staining by FACS is shown. Control cells (CTRL, unstained), senescent cells (CPD stained) and control+ senescent cells (both cell types mixed together in a 1:2 ratio) were first gated for DAPI negative cells to eliminate dead cells before they were visualized in a SSC versus CPD plot.

4.3 Functional Analysis: Immunomodulation

Neuroblastoma cells are poorly immunogenic. For instance they lack MHC I expression and thus inhibit T-cell activation *in vitro* and *in vivo*. As senescence leads to a change of the expression profile in NB-cells, we wanted to study whether senescent NB-cells modulate T-cell proliferation *in vitro*.

4.3.1 Anti-CD3 Titration

Mature T-cells recognize and react to the antigen/ MHC complex through their antigen-specific receptors (TCR). T-cells can be antigen independently activated upon *in vitro* stimulation via antibodies to the TCR. In order to test a possible influence of senescent or

control NB-cells on T-cell activation, we aimed to activate T-cells by using an anti-CD3 antibody. Thus, anti-CD3 was titrated in a CFSE based T-cell proliferation assay. For this purpose a titration study using different concentrations of an anti-CD3 (10 ng/ml, 25 ng/ml, 100 ng/ml and 250 ng/ml) was performed and proliferation was measured on day 3, day 4, day 5 and day 6 (descripted in detail in chapter 2.1.4.4).

With every cell division CFSE labelled cells halve their CFSE intensity. Therefore cells that have proliferated can be seen as peaks with a lower CFSE intensity (shifted to the left) in a count vs. CFSE plot and every peak is equivalent to one cell division (Fig. 20, right panel).

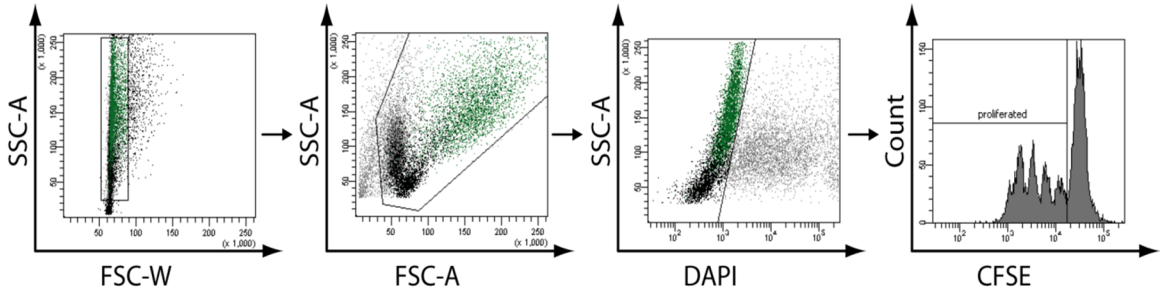

Figure 20 | Gating-Strategy for CFSE labelled proliferating T-cells

First we gated for single cells and then excluded cell debris in the FSC-SSC plot. Next, gates were set to exclude DAPI positive (dead) cells. Finally, a gate for T-cells that have proliferated was defined (the peak on the very right side represents non-proliferating cells).

Proliferation of T-cells was determined at day 3 to day 6 upon activation with 10 - 250 ng/ml anti-CD3 (Fig. 22). When using 10 ng/ml, on day 3 no proliferation was detected. On day 4 T-cells started to proliferate and on day 6 already more than half of the T-cells showed proliferation (Fig. 21).

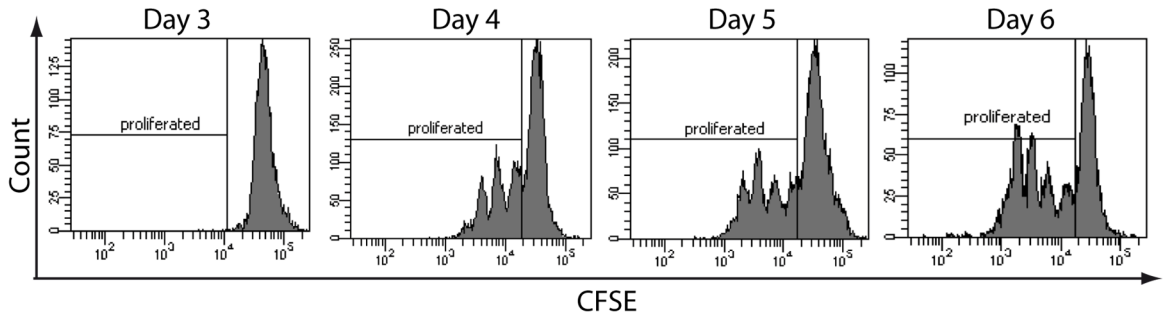

Figure 21 | T-cell proliferation analyses

An example of FACS plots of CFSE labelled T-cells after 3 to 6 days of culture with 10 ng/ml anti-CD3.

All concentrations of anti-CD3 tested, led to an activation of T-cell proliferation, ranging from 25 to 54% (Fig. 22) and except for 25 ng/ml anti-CD3 the amount of proliferated cells was highest on day 6 (Fig. 22). For the following experiments we used 10 ng/ml anti-CD3 and analysed on day 6, because T-cells were nicely stimulated, but not over stimulated, at these conditions.

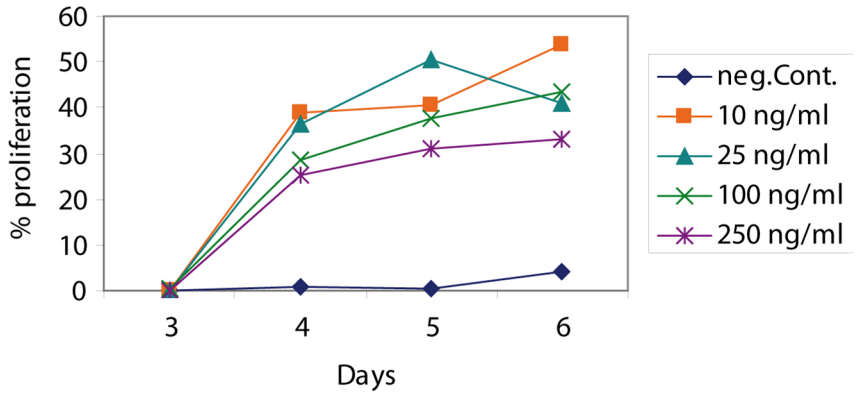

Figure 22 | Titration of anti-CD3 concentration and time-course of CFSE based proliferation assay
CFSE labelled T-cells were activated with different concentrations of anti-CD3 as shown and incubated for 3, 4, 5 or 6 days before they were analysed by flow cytometry. The percentage of CFSE negative (proliferating) cells was determined.

4.3.2 Co-culture of T-cells and neuroblastoma cells

To study whether NB-cells (control, spontaneous senescent, HU treated senescent, CPT treated senescent and BrdU treated senescent cells) modulate the proliferation of T-cells, these cell types were co-cultured and T-cell proliferation was determined. NB-cells were mixed with T-cells at a ratio of 1:1, 1:5 and 1:10 in a 96-well plate. Different ratios were used to see if the effect is concentration dependent. The maximum proliferation of T-cells was achieved 6 days after activation with 10 ng/ml anti-CD3 (as shown in chapter 1.2.1; Fig. 22). As for subsequent experiments we aimed at analysing a possible immune-modulatory effect of NB-cells on T-cells, an even lower concentration of 5 ng/ml antiCD3 was selected and cultures were harvested and FACS analysed at day 6. For FACS analysis, we first gated for single cells, then we excluded cell debris before gating for DAPI negative cells (as described in Fig. 20). In a next step gates were set on $CD4^+$ and $CD8^+$ cells and within these two populations the percentage of $CFSE^-$ (proliferating) cells was determined. The experiment was accomplished two times. The first experiment contained all types of drug induced senescent NB-cells (Fig. 23 A) whereas in the second experiment CPT induced senescent cells were not included (Fig. 23 B).

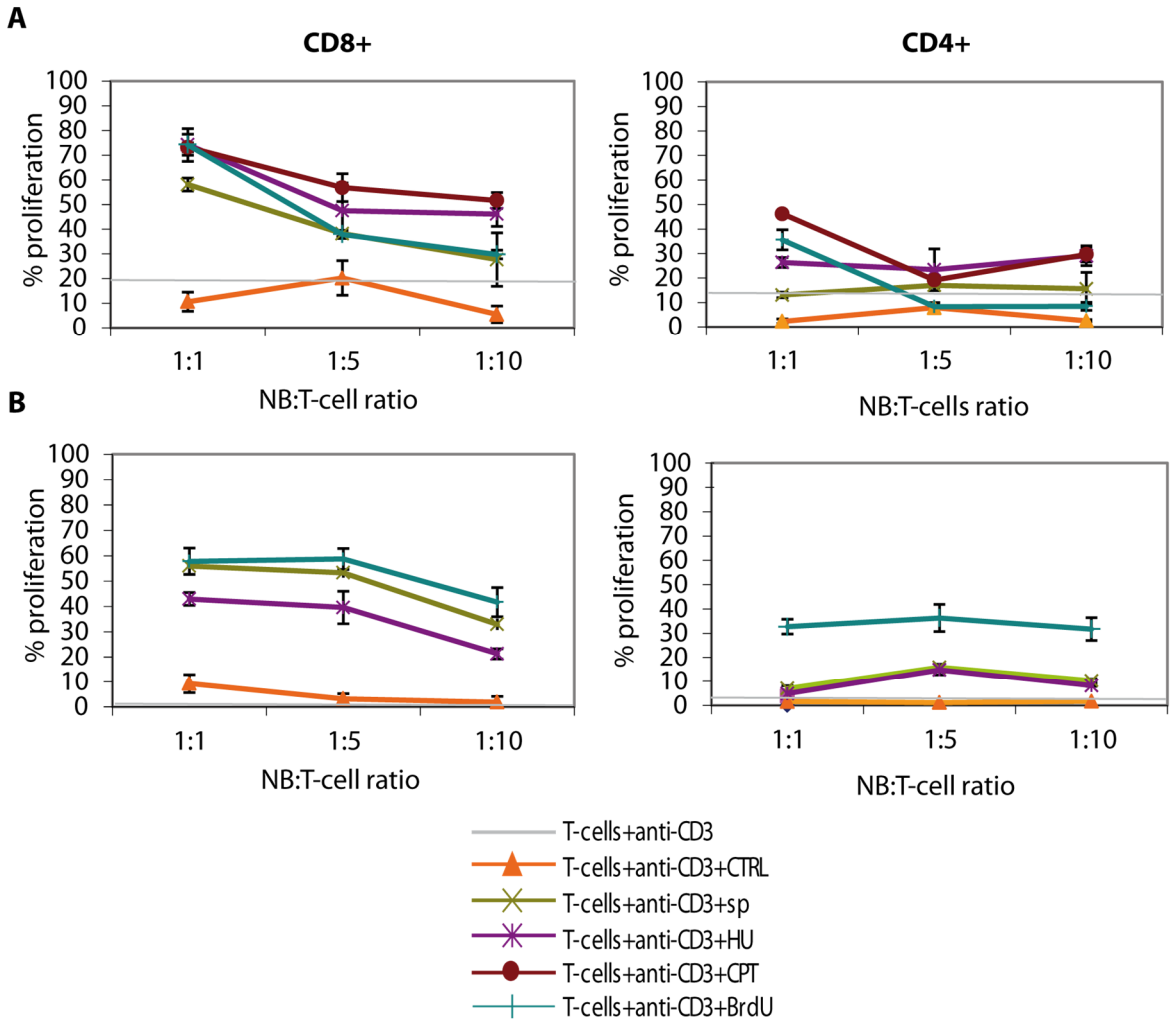

Figure 23 | Proliferation of CD8$^+$ and CD4$^+$ T-cells after 6 days in co-culture with different treated NB-cells. NB-cells generated under different culture conditions were compared for their capacity to stimulate T-cell proliferation. Analysis was done on day 6 of co-culture. 5ng/ml anti-CD3 was used for activation of T-cells. Results of two independent co-culture experiments (A and B) are shown.

T-cells activated with anti-CD3 alone (negative control) showed 14-19% proliferation in experiment 1 (Fig. 23 A) and almost no proliferation (1-4%) in experiment 2 (Fig. 23 B). In both experiments the proliferation of T-cells (both CD4$^+$ and CD8$^+$) was higher when they were cultivated together with senescent cells compared to control cells (Fig. 23). At the 1:1 NB to T-cell ratio 58-74% of CD8$^+$ cells proliferated in the presence of senescent cells in experiment 1 (Fig. 23 A) and 43-58% in experiment 2 (Fig. 23 B), whereas the proliferation rate of CD8$^+$ cells co-cultivated with control cells was only around 10%. CD8$^+$ cells had a considerable higher proliferation rate than CD4$^+$ cells in both experiments. At a ratio of 1:1 around 2% of CD4$^+$ cells co-cultured with control cells proliferated. In co-cultures with senescent NB-cells CD4$^+$ cells showed a proliferation of 13-26% in experiment 1 (Fig. 23 A)

and 5-33% in experiment 2 (Fig. 23 B). The level of $CD8^+$ T-cell proliferation in the presence of senescent cells (which were induced by different drugs) slightly varied between experiments, but they all presented the same trend in up-modulating the $CD8^+$ proliferation. The proliferation was always highest in wells with the 1:1 NB:T-cell ratio. With a decreased cell number of senescent NB-cells (1:5 and 1:10 NB:T-cell ratio) there was also a decline of $CD8^+$ proliferation (Fig. 23 A). $CD4^+$ cells generally proliferated less in the presence of senescent NB-cells compared to $CD8^+$ cells, however the same trend was observed. In summary, senescent NB-cells facilitate T-cell proliferation and this effect is cell number dependent.

4.3.3 T-cells cultured with conditioned medium from neuroblastoma cells

To test whether the effect of NB-cells on T-cell proliferation is cell contact dependent or independent we looked for the proliferation of T-cells in the presence of conditioned medium produced by control or senescent NB-cells (control, spontaneous senescent, HU treated senescent, CPT treated senescent and BrdU treated senescent cells). The experiment was set up as in the co-culture experiment aforementioned in a 6-day assay except that NB-cell conditioned medium was used instead of NB-cells.

Experiment A and B were performed in parallel to the co-culture experiment 1 (Fig. 23A), which means that parallel approaches included NB-cells from the same flasks/preparations and T-cells from the same batch. For each condition triplicates were done, except for some cases in which the cell number of NB-cells was insufficient. In those cases duplicate wells were set up. $5x10^4$ cells/well were seeded. After one day control or senescent NB-cell conditioned medium was transferred onto T-cells either one time or daily.

In experiment A (Fig. 24 A) anti-CD3 activated T-cells and T-cells with control-cell conditioned medium achieved almost the same percentage of CFSE negative T-cells (around 17% of $CD8^+$ and 25% of $CD4^+$).T-cells, including both $CD4^+$ and $CD8^+$ cells, grown in conditioned medium from all types of senescent NB-cells presented a slightly decreased proliferation (between 5-17%). However, in this experiment, cells generally proliferated less than previously observed.

NB-cells produce and secret cytokines continuously when they are in direct co-culture with T-cells. Therefore, we wanted to know whether these factors affect the proliferation of T-cells. However, transfer of NB-cell conditioned medium (CM) only on day 0 does not expose the T-cells continuously to factors produced by NB-cells as they would encounter in a direct co-culture. To compensate for this problem, CM produced by control or senescent NB-cells

(control, spontaneous senescent, HU treated senescent, CPT treated senescent and BrdU treated senescent cells) was transferred daily to T-cells in experiment B (Fig. 24B). In the positive control (T-cells + anti-CD3) 67-72% T-cells proliferated. T-cells treated with CM from all NB-cell types (CTRL, Fsp, HU, CPT and BrdU) displayed only slight differences in proliferation (between 75-92%). $CD4^+$ cells generally showed a proliferation rate comparable to those of $CD8^+$ cells (Fig. 24B).

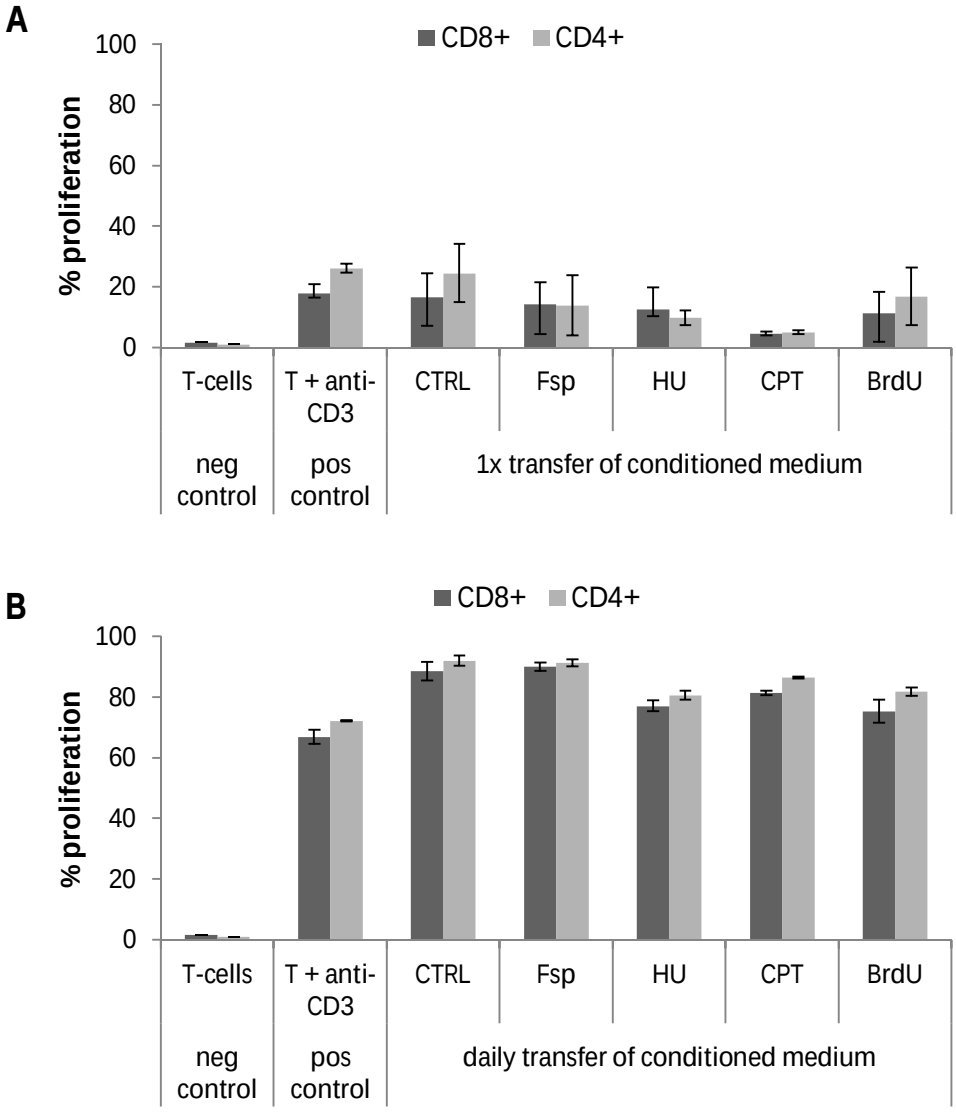

Figure 24| T-cell proliferation after transfer of conditioned media from NB-cells to T-cells

Two experiments are shown. Conditioned medium either from control cells (CTRL), spontaneous senescent F-cells (Fsp), HU treated senescent, CPT treated senescent or BrdU treated senescent cells was transferred to T-cells. For negative and positive control normal medium was used. In experiment (A) conditioned medium was transferred only one time (on day 0). In experiment (B) daily transfer of conditioned medium and anti-CD3 was carried out. Reactions were set up in duplicates or triplicate, respectively. NB-cells of exp. (A) and exp. (B) are from the same flasks/preparations and T-cells from the same batch. Experiments were done in parallel.

Both experiments showed similar results. There was almost no difference in T-cell proliferation when co-cultured with control cells or senescent NB-cells. However, experiment A and experiment B differed in the proliferation efficiency of T-cells, probably because in experiment A cells were stimulated only once with anti-CD3 on day 0, whereas cells in experiment B were stimulated every day by daily addition of anti-CD3, which caused a higher proliferation rate.

4.3.4 Co-culture of T-cells and neuroblastoma cells in a transwell plate

None of the previously described supernatant transfer experiments could mimic a co-culture situation where NB-cells and T-cells do not have the possibility of direct cell contact, because additional steps had to be done like supernatant transfer, which dilutes components that are produced by T-cells, or anti-CD3 addition to maintain the original concentration. A more accurate method to prove if the effect on T-cell proliferation is cell-cell contact dependent or cell contact independent is the cultivation of T-cells and NB-cells (CTRL, Fsp, HU, CPT or BrdU) in a transwell assay. Therefore, T-cells and NB-cells were either separated by a transwell membrane or grew without transwell separation in a direct co-culture for comparison. The NB:T-cell ratio was 1:2 and cells were cultivated for 6 days (described in detail in chapter 2.1.4.7).
For FACS data evaluation, we gated for single cells, excluded cell debris and then gated for DAPI negative cells. Further $CD4^+$ and $CD8^+$ cells were gated separately and analysed for CFSE. Within these two populations the percentage of cells having proliferated was determined via a CFSE intensity and activation of $CD4^+$ and $CD8^+$ cells was measured by determining the percentage of cells positive for CD25, a marker present on activated T-cells.

The positive control displayed very weak T-cell proliferation (2%). T-cells in direct co-culture with control cells showed 6% and separated through a transwell about 2% proliferation. In direct co-culture with senescent NB-cells 50-64% T-cells proliferated whereas in transwells there were only 2-3%. Both, proliferation and activation, of $CD8^+$ cells are highly increased in wells with direct co-culture of T-cells and all types of senescent NB-cells (Fsp, HU, CPT and BrdU) whereas the same combination of cells in transwells showed similar proliferation and activation values as the positive control containing only T-cells and anti-CD3 without NB-cells (Fig. 25 and Fig. 26).
The bars for the activation marker CD25 presented the same trend as the proliferation bars. 14% of T-cells in the positive control showed CD25 expression, in co-culture with control cells 19% were activated and in trans-wells only 13%. In direct co-culture with senescent NB-cells 55-66% of T-cells expressed CD25 compared to only 10-14% under transwell conditions.

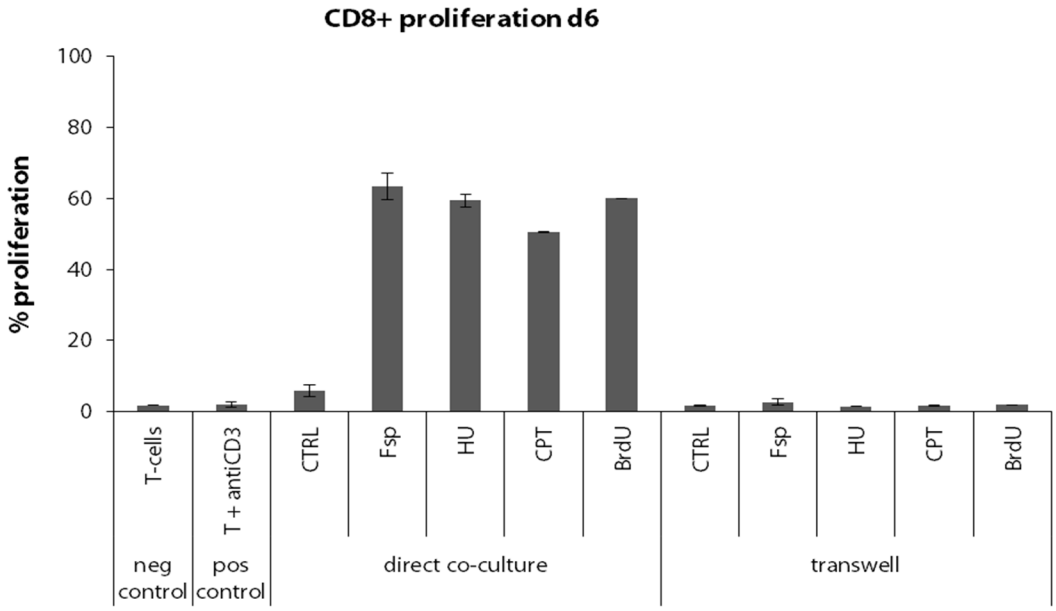

Figure 25 | Proliferation of CD8$^+$ cells after direct co-culture and co-culture in transwells of NB-cells and T-cells. Senescent NB-cells (Fsp, HU, CPT and BrdU) permitted strong proliferation of CD8$^+$ cells in direct co-culture but not in transwells.

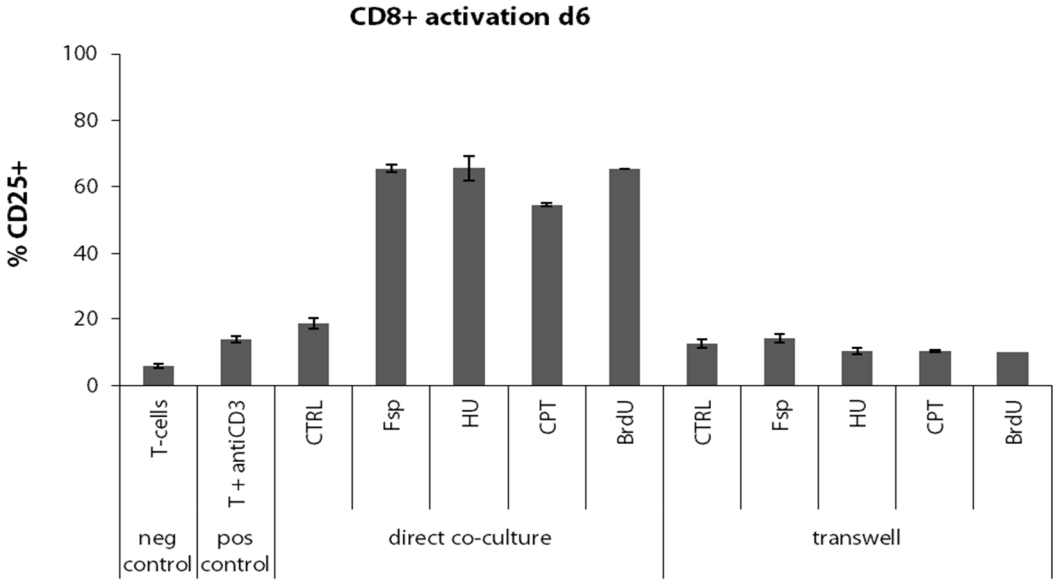

Figure 26 | Activation of CD8$^+$ cells after direct co-culture and co-culture in transwells of NB-cells and T-cells. Senescent NB-cells (Fsp, HU, CPT and BrdU) led to strong CD25 expression of CD8$^+$ cells in direct co-culture but not in transwells.

The same tendency in proliferation and activation was visible for CD4$^+$ cells as for CD8$^+$ cells, but the values were lower (Fig. 27 and Fig. 28). 20-32% of CD4$^+$ T-cells in direct co-culture proliferated, only around half as many as in CD8$^+$ cells. 29-44% CD4$^+$ T-cells expressed CD25 compared to over 55% in CD8$^+$ cells. In general, CPT induced senecent

NB-cells permitted a little bit less proliferation and activation of both $CD8^+$ and $CD4^+$ T-cells compared to spontaneous senescent F-cells, HU- and BrdU induced senescent cells.
Taken together, T-cells proliferated and showed the activation marker CD25 only in direct co-culture with senescent NB-cells, but not in the respective trans-well assay.

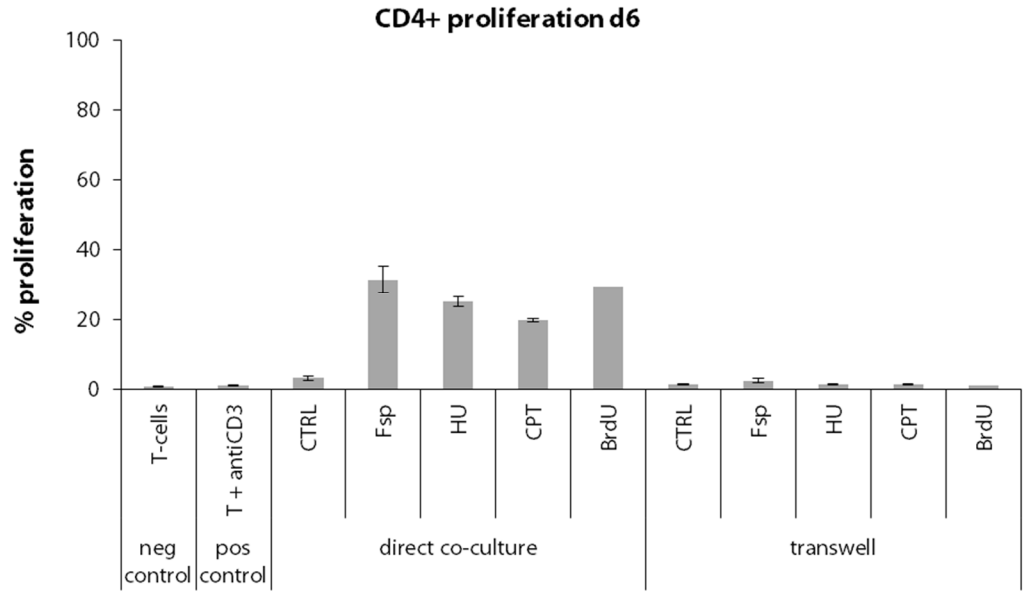

Figure 27 | Proliferation of $CD4^+$ cells after direct co-culture and co-culture in transwells of NB-cells and T-cells. Senescent NB-cells (Fsp, HU, CPT and BrdU) permitted proliferation of $CD4^+$ cells in direct co-culture but not in transwells.

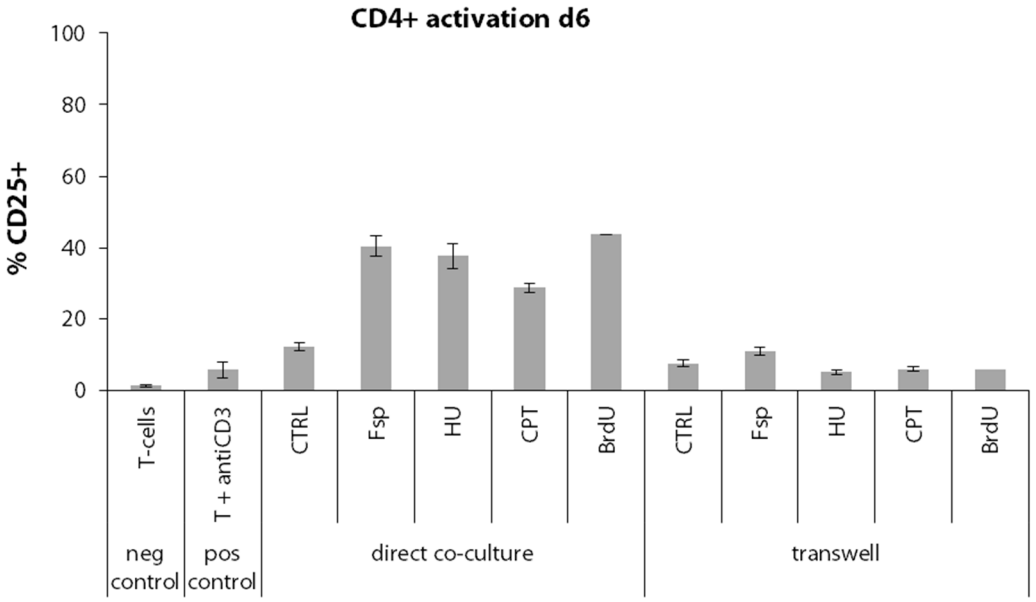

Figure 28 | Activation of $CD4^+$ cells after direct co-culture and co-culture in transwells of NB-cells and T-cells. Senescent NB-cells (Fsp, HU, CPT and BrdU) led to strong activation (CD25 expression) of $CD4^+$ cells in direct co-culture but not in transwells

5 Discussion

In this study, we showed that, next to treatment with HU, senescence can also be induced by treating MNA neuroblastoma cells with CPT and BrdU *in vitro* and that triggering senescence with these two drugs is faster compared to HU (only 3 weeks compared to 8-10 weeks). A shorter senescence induction time means, that CPT and BrdU are more efficient compared to HU *in vitro*. Treatment of NB-cells with any of the 3 drugs arrested tumour cell growth and induced senescence, confirmed by SA-β-Gal staining. Moreover, we could show a decrease of *MYCN* copy number and GD2 level and an increase of CD44 and MHC I expression in these drug treated senescent cells and in spontaneous senescent cells compared to control cells. The CD44 and *MYCN* status are similar to less aggressive forms of NB-tumors. Searching for the senescence pathway activated in senescent NB-cells, we found that p16 is increased in spontaneous senescent cells and in CPT and BrdU treated senescent cells, but only slightly in HU treated senescent cells. Therefore we suspect that different drug treatments may induce different senescence pathways. Whether senescent NB-cells alter the proliferation rate of non-senescent NB-cells still remains an open question. Finally, we found that senescent NB-cells were able to modulate the immune system by allowing an increased proliferation of CD8+ cells compared to non-senescent NB-cells. This might play an important role in cancer pathology.

5.1 Characteristics of drug induced senescent neuroblastoma cells *in vitro*

Spontaneously occurring senescent F-cells and HU induced senescent cells demonstrate similar biological characteristics which were previously described by our group [125, 126]. In this study we found that long term treatment with low doses of HU, CPT and BrdU induced senescence in MNA neuroblastoma cells of the cell line STA-NB 10. In NB-Ma HU treatment showed no effect on the cell proliferation, while CPT and BrdU also induced senescence. After induction with CPT more NB-cells died and therefore less senescent cells remained after 2-3 weeks compared with HU and BrdU induction. Furthermore, those remaining cells were strongly granulated. So it is very likely that the amount of DNA damage caused by CPT was more extensive than that caused by HU or BrdU. Comparing the features of spontaneous senescent F-cells, HU-, CPT- and BrdU induced senescent cells we found that all these cells demonstrated a similar senescent morphology. Thus, induction of senescence by HU, CPT and BrdU probably represents an acceleration and increase of the spontaneously occurring senescence taking place in cell culture. However, all three drugs induced, beside senescence and apoptosis, also differentiation in the first weeks of induction. Looking at the SA-β-Gal staining we saw that both spontaneous senescent F-cells and induced senescent cells showed a high percentage of SA-β-Gal positive cells, while control cells had only very few SA-β-Gal positive cells. Comparing spontaneously occurring and drug

induced senescent cells we observed that the percentage of SA-β-Gal positive cells was higher in the latter. Curiously the percentage of SA-β-Gal positive cells in spontaneous senescent cells of the STA-NB 10 cell line was much less (12%) compared to the NB-Ma cell line (86%). This could be explained by the occurrence of morphologically flat cells in the STA-NB-10 cultures that have not yet terminated the senescence process, thus are not efficiently stained by SA-β-Gal staining. In line with this it has been shown by others that the classical SA-β-Gal protocol, which is widely used, is actually not adequate to identify all senescent cells neither *in vitro* nor *in vivo* [176]. Therefore it is advisable to identify senescent cells by more than one method.

MYCN amplification usually indicates an aggressive neuroblastoma tumour with rapid progression and a poor outcome [20]. In our experiments all kind of senescent NB-cells showed a clearly reduced *MYCN* copy number. Thus, senescent NB-cells lost genetic markers associated with aggressive tumour growth through the treatment with HU, CPT and BrdU. Although generally correlating, a low *MYCN* copy number could still be accompanied by high MYCN protein expression and vice versa [177, 178]. Our group showed that extra chromosomally amplified *MYCN* copies can be expulsed spontaneously by micronuclei formation [126] and that this phenomenon can be enhanced through low dose HU treatment [125]. In addition, HU is known to cause DNA ds breaks, thus triggering the DNA-damage repair pathway (DDR) [179]. As CPT and BrdU also induce DNA ds breaks, it is anticipated, that in NB-cells these substances trigger senescence through an impaired DDR. Camptothecin, a topoisomerase inhibitor, is known to induce DNA damage in human colon cancer cells by disrupting the DNA replication machinery. Treatment with low concentrations of CPT causes cells to undergo senescence. For this senescence development p21 has been shown to be required [88]. Recently, it was found that *MYCN* amplified neuroblastoma cells are more sensitive to camptothecin than *MYCN* negative cells and that camptothecin caused selective down-regulation of MYCN expression [180]. Our Western blot showed that control cells displayed not only the highest *MYCN* copy number, as shown by FISH experiments, but also the highest expression of the MYCN protein, while HU, CPT and BrdU-treated senescent cells showed no detectable MYCN expression. Whether CPT treatment in NB-cells preferentially selects for cells with low *MYCN* copy number or leads to a *MYCN*-amplicon reduction or direct down-regulation of MYCN expression remains to be elucidated. However, high numbers of micronuclei containing *MYCN* amplicons have been observed in CPT and BrdU-treated NB-cells (data not shown) which could explain the reduced *MYCN* copy number in senescent NB-cells. Importantly, independent of the underlying mechanism, *MYCN* copy number and MYCN protein expression are both low in HU, CPT as well as in BrdU-treated senescent NB-cells.

BrdU is a thymidine analogue that incorporates into DNA and is commonly used in the detection of proliferating cells in tissues [181]. Moreover, BrdU has been shown to increase

the sensitivity of treated cells to ionizing radiation [169]. BrdU is suggested to increase the risk of mutations and double-strand breaks by altering the stability of DNA [182], but it should be mentioned that most of these effects appear only when BrdU treatment is combined with secondary stressors, such as ionizing radiation. In the absence of secondary stressors BrdU is thought to operate relatively mild as a thymidine analogue [181]. Recently it was published that a single brief *in vitro* treatment with BrdU induces an intense and constant reduction in the proliferation rate of all cancer cells examined (e.g. human cutaneous T-cell lymphoma, human osteosarcoma, rat glioma) and that those cancer cells show some signs consistent with senescence (e.g. SA-β-Gal activity) as they arrest in the G1 phase of the cell cycle [181]. Despite of this, BrdU is currently not considered as alternative drug to be included in NB treatment protocols because of high toxicity expected in young children.
Together with the expression of SA-β-Gal and the *MYCN* copy number reduction, the number of CD44 positive cells increased in cells treated with HU, CPT and BrdU and in cells with spontaneous senescent F-cells. Neuroblastomas positive for CD44 are usually low stage tumours with favourable prognosis [138]. Thus, drug treatment with HU, CPT and BrdU reduces the aggressive characteristics of neuroblastoma cells and up-regulate CD44 and MHC I.

When cells enter senescence, they become flattened, enlarged and multinucleated. Moreover many vacuoles can be found in the cytoplasm which leads to an increased cellular complexity. It is published that this distinctive senescent morphology can be seen by flow cytometry as increased side scatter [124]. This change was also visible in our experiments where spontaneous and treated senescent cells showed an increased side scatter. Further, analysis of GD2, CD44 and MHC I by FACS showed that spontaneous senescent-cells and CPT, HU and BrdU treated cultures contained a higher percentage of MHC I^+ $CD44^+$ cells compared to control cells. In line with the results of the GD2/CD44 immunofluorescence staining, $GD2^+$ cells were decreased in all senescent cultures compared to control cells. All MHC I^+ cells were also $CD44^+$, but not all MHC I^- cells were $CD44^-$. The percentage of CD44-cells within the MHC I^- $GD2^{+/-}$ cells was reduced in drug treated cells. It can be speculated that those $CD44^+$ cells started already their senescence program after drug treatment, while their MHC I expression was still low. Quantification clearly shows that the frequency of MHC $I^+/CD44^+$ cells was high and the frequency of MHC I^- $GD2^{+/-}$ cells is low in both cell lines in spontaneous senescent-cells and upon treatment with CPT, HU and BrdU.
So far, our findings demonstrated no remarkable difference between spontaneously occurring and CPT-, BrdU- and HU induced senescent cells in MNA NB-cells. All senescent cells resembled in morphology, SA-β-Gal staining, *MYCN* copy number and showed high expression of the markers CD44 and MHC I and low levels of GD2. Thus, CPT-, BrdU- and

HU treatment of MNA NB-cells *in vitro* induces characteristics similar to a non-aggressive form of NB-tumours in these cells.

Generally tumour rejection is mediated most notably by CTL, but human cancer cells usually try to escape CTL-mediated immune surveillance by low/absent expression of MHC I molecules. Thereby they evade to present target epitopes on the cell surface which are important for the immune recognition by CTL [183]. As long term low dose treatment of MNA neuroblastoma cells with CPT, HU and BrdU leads to up-regulation of MHC I molecules in our experiments, these senescent cells should be more efficiently recognized by CTL. This strategy of senescence induction could therefore reduce or prevent tumour progression especially in the minimal residual disease setting. An autologous cytotoxicity assay using senescent versus control NB-cells as target cells and autologous CTL as effector cells would clarify this issue.

In search of the senescence pathways activated in drug induced senescent NB-cells, we found that different drugs induce either the p16 or an alternative senescence pathway. Western blot results show that p16 is overexpressed in BrdU- and CPT treated senescent cells and in spontaneous senescent cells, but only slightly in HU treated senescent cells compared to control cells. Thus, p16 seems to play a role in senescence induction after treatment with CPT, BrdU and probably HU and in spontaneous senescent cell.

Moreover, CDK2 and MYCN are down-regulated in all senescent cells compared to control cells. MYC oncoproteins (including c-Myc and N-Myc) are known to be involved in development of several types of cancer. *MYC* encodes a pleiotropic transcription factor that primarily induces apoptosis by induction of p19Arf, which stabilizes p53 [184]. Wu et al. recently showed that the suppression of the c-Myc oncogene induces cellular senescence in several tumour types (e.g. lymphoma, osteosarcoma, hepatocellular carcinoma) [97].

Further, it was shown that depletion or inhibition of Cdk2 forced cells expressing Myc/Ras into cellular senescence [185]. Molenaar et al. demonstrated that silencing of Cdk2 by RNA interference induced apoptosis in *MYCN* amplified NB-cell lines, but no apoptosis was observed 48h after MYCN silencing [186]. Based on these studies it can be speculated, that cells may go into senescence when MYCN and CDK2 are down-regulated. This assumption fits to our Western blot results showing that Cdk2 and MYCN were low/absent in spontaneous and drug-induced senescent NB-cells.

Total p53 was similar in control and senescent NB-cells, but significantly lower as compared to a Ewing sarcoma cell line, SK-N-MC. Similarly, phospho-p53 levels were equally low in control and senescent NB-cells and high in the SK-N-MC cell line. From previous experiments we know however, that HU-treatment induces total p53 levels and concomitant p53 phosphorylation at Ser15 3-5 days after treatment start. At later time points (4 weeks, 8 weeks) no phospho-p53 was detectable. This fits to a senescence model published by

Roninson et al. which suggests that p53 is up-regulated early upon senescence induction and is then down-regulated, whereas p16 is upregulated later and is then required for maintaining the senescence phenotype, e.g. the SASP [124].

In human erythroleukemia K562 cells it is published, that HU treatment for 7 days or more changed the morphology of these tumour cells into a senescent like phenotype. Further, those HU treated cells possessed a positive SA-β-Gal staining and an accumulation of cdk inhibitors, such as p16, p21 and p27 [90]. One of those findings, the p16 accumulation after HU treatment, is in contrast to our experiment, which showed only weak p16 accumulation in HU treated senescent NB-cells. The two other cdk inhibitors, p21 and p27, should be analysed in further studies in treated and untreated MNA NB-cells. However the effect of the same drug may vary in tumour cells derived from different tissues.

It has been shown that low concentrations of CPT induce DNA damage in human colon cancer cells causing cells to senesce [88]. Further it is known that molecular events caused by treatment with CPT mostly deal with stress response and pathways for cell survival activated by DNA damage [187]. In response to the Topo I inhibition, caused by CPT, two pathways have been described to play a role: the ATM/Chk2 DNA damage checkpoint pathway and the ATR-Chk1 response [188]. CPT has also been shown to activate NF-kB, an important transcriptional factor regulating the survival response [189]. Independently, after CPT exposure p16 has also been shown to accumulate quickly *in vitro* and *in vivo* [190]. The last finding is in line with our western blot results, which show p16 accumulation also in CPT treated senescent NB-cells.

A study in lung cancer cells, that express wild-type p53, but no p16, showed that BrdU induces phenotypic changes that resemble senescence. BrdU treatment evoked a DNA damage response which involved the activation of Chk1, Chk2 and p53. Further an up-regulation of p27 has been found [191]. Thus BrdU is able to induce senescence also independent of the p16 pathway, which we assume to be one of the crucial pathways underlying drug-induced senescence in MNA neuroblastoma cells.

5.2 Functional Analysis: Co-culture of senescent and non-senescent neuroblastoma cells

In preliminary experiments of our group the growth rate and GD2 level were found to be reduced in co-cultures of senescent together with non-senescent NB-cell lines compared to non-senescent cells alone. However, due to technical problems we could not reproduce these results in this study. First, N-cells easily detached from the bottom of the wells after seeding and always required some days to recover from manipulation during cell seeding. In general control cells grew much better in culture flasks than in 96-, 24- or 12-well plates. In order to improve attachment, wells were coated with fibronectin, but still attachment was not

comparable with the situation in culture flasks. In general N-type-cells started to proliferate faster after seeding in the presence of some spontaneous senescent F-cells, probably because senescent cells produce more extracellular matrix proteins which improve attachment of both cell types. In contrast to control cells, senescent cells quickly attach to the plastic surface of all kind of plates or flasks. Thus, control cultures containing a higher percentage of spontaneous senescent cells had an initial advantage in proliferation due to faster attachment. Second, control cells were not completely free of senescent cells and drug-treated cultures contained small, but varying amounts of N-type cells, which made it difficult to prepare repeated co-cultures with the same ratio of N-type and senescent cells. Third, we were not able to continue the co-culture experiment over a period longer than 2 weeks, because thereafter viability in control cells dropped and they had to be re-seeded. Another critical point was the CPD staining which was done to track senescent cells and therewith their expression changes of MHC I. Unfortunately, it was not possible to separate senescent and non-senescent cells with this staining, as the CPD intensity dropped in senescent cells already after a few days, without having proliferated. Thus, our plan to monitor CPD negative control cells and learn if they acquire MHC I or CD44 during co-cultivation with senescent cells was not feasible.

As senescent cells produce ROS and secret various factors, such as interleukins, growth factors and enzymes that degrade extracellular matrix, it has been proposed that they can shape their local microenvironment and stimulate (tumour) cell growth, invasiveness and angiogenesis [65, 192, 193]. However a recently published study demonstrated the effect of senescent fibroblasts on their normal (proliferation-competent) corresponding cells. Via cell-cell contact through gap junctions and ROS involving processes senescent fibroblasts induce a DNA damage response in nearby fibroblasts *in vitro*. As a result those bystander cells become also senescent. This effect, which describes the spreading of senescence towards neighbouring senescent cells, was named senescence-induced senescence [194].

Due to the experimental setup and technical difficulties, we could not study this effect of senescence-induced senescence in our co-cultures. Therefore the experimental setup must be optimized for future studies.

5.3 Functional Analysis: Immunomodulation of T-cells through neuroblastoma cells

We could clearly demonstrate that the senescent NB-cells allow T-cells to proliferate much better than they do in co-culture with control cells. This effect could be seen with all kinds of senescent cells (spontaneous F-cells, HU- , CPT-, and BrdU induced cells) and it was most pronounced in the $CD8^+$ T-cells. There are two possibilities how NB-cells could influence T-cell proliferation: either senescent cells activate proliferation actively or non-senescent cells

inhibit proliferation. Previous studies using diphtheria-toxin, an antigen-dependent T-cell activation model, has shown that components of NB-cells, i.e. GD2, can inhibit T-cell proliferation [195]. Thus, control cells, which produce high levels of GD2 may actively suppress T-cell activation, whereas senescent cells, having reduced GD2 may allow T-cell activation or even facilitate T-cell activation by an additional, unknown mechanism. Furthermore we could detect a NB to T-cell ratio dependent decline of $CD8^+$ T-cell proliferation from 1:1 to 1:5 and further to 1:10. Thus, the influence on T-cell proliferation is dependent on the cell number of NB-cells.

By transwell experiments we could clearly see that direct contact of NB-cells and T-cells is required to induce efficient $CD8^+$ and $CD4^+$ T-cell activation and proliferation. The effect on $CD4^+$ T cells was considerably below that on $CD8^+$ T-cells. Moreover, we proved again that senescent NB-cells enhance T-cell proliferation compared to control cells.

In our first attempts to analyse the role of secreted factors on T-cell activation, we either once or daily transferred NB-cell conditioned medium to T-cells. After one time transfer of NB conditioned medium (CM) on day 0, proliferation of T-cells was lower than previously observed, and CM from senescent cells led to a slight decrease of proliferating T-cells. When CM from NB-cells was transferred daily to T-cells, proliferation of T-cells was very high (up to 88%) for all conditions and control cells showed similar results as senescent cells. These results suggest that the conditions in experiment A with one time transfer of NB conditioned medium (CM) on day 0,were not sufficient for T-cell proliferation and in experiment B daily transfer of NB conditioned medium plus daily replenished anti-CD3 led to an overstimulation of T-cells. Furthermore, in the assay with the daily transfer of conditioned medium T-cells could also secrete factors which can influence the proliferation, but those were diluted in our experiment through the process of medium transfer. In general, the situation in a co-culture cannot be imitated by transfer of conditioned medium. Consequently we decided to use transwell plates, which allow co-culturing of cells without cell-cell contact. Finally, further experiments should clarify if those T-cells that have proliferated are cytotoxic T lymphocytes (CTLs) or may contain $CD8^+$ regulatory T-cells (Tregs). It would be also of interest how effective CTLs can kill senescent NB-cells compared to control cells in an allogeneic setting.

In the co-cultivation experiments with T-cells and NB-cells, T-cells activated with anti-CD3 showed generally a very low proliferation (~1-20%) compared to the anti-CD3 titration results (54%). Actually, the percentage of proliferating T-cells should be similar, because the experimental setup was the same. One explanation for the observed discrepancies could be the fact that the IgG antibody for coating of wells was re-used and was therefore less efficient in the second experiment. Thus always fresh IgG should be used for coating.

In conclusion, these functional assays suggest that promoting cellular senescence could be beneficial for the clearance of non-senescent cells in tumours and may result in a reduction

of the tumour. It still remains to be investigated how mouse models with neuroblastoma tumours and beyond that, patients respond to treatment with low dose HU or CPT.

The importance of senescence, a stress response blocking the proliferation of the cell, is increasingly recognized. Transformation of pre-malignant cells to tumours requires evading senescence. Surprisingly, many malignant tumour cells are still able to senesce either spontaneously or in response to stress stimuli from outside. Senescent cells are not only affecting themselves, rather they influence their microenvironment and their neighbouring cells through secretory and cell bound factors. Senescence seems to have specific physiological functions (e.g. aging) and pathological consequences (e.g. tumour suppression). Importantly, immune cells can clear senescent tumour cells and hence induce tumour regression. Furthermore chemotherapeutic drugs have been shown to lead to cellular senescence which may be a reason for the therapeutic success. Moreover, studies suggest that therapeutics which target molecules required for tumour growth may lead to induction of senescence and tumour regression [196]. These points make senescence inducing therapeutics a promising option in the fight against cancer. The challenge is to translate these concepts into clinical oncology.

With respect to our study, the future experiments should analyse CPT- and HU-treatment *in vivo*, e.g. to clarify whether low dose treatment in xeno-transplanted mice leads to reduced neuroblastic tumour growth. If successful, one of these drugs could be included into a clinical trial protocol in high-risk NB-patients. Future research in the field of molecular mechanisms of senescence and in particular induction of cellular senescence in neuroblastoma cells will hopefully contribute to improve treatment of high-risk NB-patients and thereby their survival rate.

References

1. Gurney, J.G., et al., *Infant cancer in the U.S.: histology-specific incidence and trends, 1973 to 1992.* Journal of pediatric hematology/oncology, 1997. **19**(5): p. 428-32.
2. Brodeur, G.M., *Neuroblastoma.* Principles and Practice of Pediatric Oncology, 2001: p. 895-937.
3. Pearson, A., Pinkerton, R., *Neuroblastoma.* Paediatric oncology, 2004: p. 386-415.
4. Alexander, F., *Neuroblastoma.* The Urologic clinics of North America, 2000. **27**(3): p. 383-92, vii.
5. Brodeur, G.M., *Neuroblastoma: biological insights into a clinical enigma.* Nature reviews. Cancer, 2003. **3**(3): p. 203-16.
6. Carachi, R., *Perspectives on neuroblastoma.* Pediatric surgery international, 2002. **18**(5-6): p. 299-305.
7. Ambros, I.M., et al., *Role of ploidy, chromosome 1p, and Schwann cells in the maturation of neuroblastoma.* The New England journal of medicine, 1996. **334**(23): p. 1505-11.
8. Maris, J.M. and K.K. Matthay, *Molecular biology of neuroblastoma.* Journal of clinical oncology : official journal of the American Society of Clinical Oncology, 1999. **17**(7): p. 2264-79.
9. Lastowska, M., et al., *Comprehensive genetic and histopathologic study reveals three types of neuroblastoma tumors.* Journal of clinical oncology : official journal of the American Society of Clinical Oncology, 2001. **19**(12): p. 3080-90.
10. Look, A.T., et al., *Clinical relevance of tumor cell ploidy and N-myc gene amplification in childhood neuroblastoma: a Pediatric Oncology Group study.* Journal of clinical oncology : official journal of the American Society of Clinical Oncology, 1991. **9**(4): p. 581-91.
11. Kaneko, Y., et al., *Different karyotypic patterns in early and advanced stage neuroblastomas.* Cancer research, 1987. **47**(1): p. 311-8.
12. Ambros, P.F., et al., *Regression and progression in neuroblastoma. Does genetics predict tumour behaviour?* European journal of cancer, 1995. **31A**(4): p. 510-5.
13. Maris, J.M., et al., *Significance of chromosome 1p loss of heterozygosity in neuroblastoma.* Cancer research, 1995. **55**(20): p. 4664-9.
14. Caron, H., et al., *Allelic loss of chromosome 1p as a predictor of unfavorable outcome in patients with neuroblastoma.* The New England journal of medicine, 1996. **334**(4): p. 225-30.
15. Attiyeh, E.F., et al., *Chromosome 1p and 11q deletions and outcome in neuroblastoma.* The New England journal of medicine, 2005. **353**(21): p. 2243-53.
16. Fong, C.T., et al., *Loss of heterozygosity for the short arm of chromosome 1 in human neuroblastomas: correlation with N-myc amplification.* Proceedings of the National Academy of Sciences of the United States of America, 1989. **86**(10): p. 3753-7.
17. Caron, H., *Allelic loss of chromosome 1 and additional chromosome 17 material are both unfavourable prognostic markers in neuroblastoma.* Medical and pediatric oncology, 1995. **24**(4): p. 215-21.

18. Bown, N., et al., *Gain of chromosome arm 17q and adverse outcome in patients with neuroblastoma.* The New England journal of medicine, 1999. **340**(25): p. 1954-61.
19. Spitz, R., et al., *Gain of distal chromosome arm 17q is not associated with poor prognosis in neuroblastoma.* Clinical cancer research : an official journal of the American Association for Cancer Research, 2003. **9**(13): p. 4835-40.
20. Brodeur, G.M., et al., *Amplification of N-myc in untreated human neuroblastomas correlates with advanced disease stage.* Science, 1984. **224**(4653): p. 1121-4.
21. Seeger, R.C., et al., *Association of multiple copies of the N-myc oncogene with rapid progression of neuroblastomas.* The New England journal of medicine, 1985. **313**(18): p. 1111-6.
22. Caron, H., et al., *Allelic loss of the short arm of chromosome 4 in neuroblastoma suggests a novel tumour suppressor gene locus.* Human genetics, 1996. **97**(6): p. 834-7.
23. Thompson, P.M., et al., *Homozygous deletion of CDKN2A (p16INK4a/p14ARF) but not within 1p36 or at other tumor suppressor loci in neuroblastoma.* Cancer research, 2001. **61**(2): p. 679-86.
24. Schleiermacher, G., et al., *Chromosomal CGH identifies patients with a higher risk of relapse in neuroblastoma without MYCN amplification.* British journal of cancer, 2007. **97**(2): p. 238-46.
25. Brodeur, G.M., et al., *Revisions of the international criteria for neuroblastoma diagnosis, staging, and response to treatment.* Journal of clinical oncology : official journal of the American Society of Clinical Oncology, 1993. **11**(8): p. 1466-77.
26. Haase, G.M., C. Perez, and J.B. Atkinson, *Current aspects of biology, risk assessment, and treatment of neuroblastoma.* Seminars in surgical oncology, 1999. **16**(2): p. 91-104.
27. Park, J.R., A. Eggert, and H. Caron, *Neuroblastoma: biology, prognosis, and treatment.* Pediatric clinics of North America, 2008. **55**(1): p. 97-120, x.
28. Modak, S. and N.K. Cheung, *Neuroblastoma: Therapeutic strategies for a clinical enigma.* Cancer treatment reviews, 2010. **36**(4): p. 307-17.
29. Johnson, E., S.M. Dean, and P.M. Sondel, *Antibody-based immunotherapy in high-risk neuroblastoma.* Expert reviews in molecular medicine, 2007. **9**(34): p. 1-21.
30. Castel, V., V. Segura, and A. Canete, *Treatment of high-risk neuroblastoma with anti-GD2 antibodies.* Clinical & translational oncology : official publication of the Federation of Spanish Oncology Societies and of the National Cancer Institute of Mexico, 2010. **12**(12): p. 788-93.
31. Schwab, M., et al., *Amplified DNA with limited homology to myc cellular oncogene is shared by human neuroblastoma cell lines and a neuroblastoma tumour.* Nature, 1983. **305**(5931): p. 245-8.
32. Kohl, N.E., et al., *Transposition and amplification of oncogene-related sequences in human neuroblastomas.* Cell, 1983. **35**(2 Pt 1): p. 359-67.
33. Schwab, M., et al., *Chromosome localization in normal human cells and neuroblastomas of a gene related to c-myc.* Nature, 1984. **308**(5956): p. 288-91.
34. Corvi, R., et al., *MYCN is retained in single copy at chromosome 2 band p23-24 during amplification in human neuroblastoma cells.* Proceedings of the National Academy of Sciences of the United States of America, 1994. **91**(12): p. 5523-7.
35. Brodeur, G.M. and C.T. Fong, *Molecular biology and genetics of human neuroblastoma.* Cancer genetics and cytogenetics, 1989. **41**(2): p. 153-74.

36. Reiter, J.L. and G.M. Brodeur, *MYCN is the only highly expressed gene from the core amplified domain in human neuroblastomas.* Genes, chromosomes & cancer, 1998. **23**(2): p. 134-40.
37. Scott, D., et al., *Genes co-amplified with MYCN in neuroblastoma: silent passengers or co-determinants of phenotype?* Cancer letters, 2003. **197**(1-2): p. 81-6.
38. De Preter, K., et al., *Quantification of MYCN, DDX1, and NAG gene copy number in neuroblastoma using a real-time quantitative PCR assay.* Modern pathology : an official journal of the United States and Canadian Academy of Pathology, Inc, 2002. **15**(2): p. 159-66.
39. Lee, W.H., A.L. Murphree, and W.F. Benedict, *Expression and amplification of the N-myc gene in primary retinoblastoma.* Nature, 1984. **309**(5967): p. 458-60.
40. Nisen, P.D., et al., *Enhanced expression of the N-myc gene in Wilms' tumors.* Cancer research, 1986. **46**(12 Pt 1): p. 6217-22.
41. Rouah, E., et al., *N-myc amplification and neuronal differentiation in human primitive neuroectodermal tumors of the central nervous system.* Cancer research, 1989. **49**(7): p. 1797-801.
42. Seeger, R.C., et al., *Expression of N-myc by neuroblastomas with one or multiple copies of the oncogene.* Progress in clinical and biological research, 1988. **271**: p. 41-9.
43. Wenzel, A. and M. Schwab, *The mycN/max protein complex in neuroblastoma. Short review.* European journal of cancer, 1995. **31A**(4): p. 516-9.
44. Dang, C.V., et al., *The c-Myc target gene network.* Seminars in cancer biology, 2006. **16**(4): p. 253-64.
45. Hirvonen, H., et al., *Expression of the myc proto-oncogenes in developing human fetal brain.* Oncogene, 1990. **5**(12): p. 1787-97.
46. Zimmerman, K.A., et al., *Differential expression of myc family genes during murine development.* Nature, 1986. **319**(6056): p. 780-3.
47. Grady, E.F., M. Schwab, and W. Rosenau, *Expression of N-myc and c-src during the development of fetal human brain.* Cancer research, 1987. **47**(11): p. 2931-6.
48. Hirning, U., et al., *A comparative analysis of N-myc and c-myc expression and cellular proliferation in mouse organogenesis.* Mechanisms of development, 1991. **33**(2): p. 119-25.
49. Stanton, B.R., et al., *Loss of N-myc function results in embryonic lethality and failure of the epithelial component of the embryo to develop.* Genes & development, 1992. **6**(12A): p. 2235-47.
50. Malynn, B.A., et al., *N-myc can functionally replace c-myc in murine development, cellular growth, and differentiation.* Genes & development, 2000. **14**(11): p. 1390-9.
51. Alam, G., et al., *MYCN promotes the expansion of Phox2B-positive neuronal progenitors to drive neuroblastoma development.* The American journal of pathology, 2009. **175**(2): p. 856-66.
52. Hayflick, L. and P.S. Moorhead, *The serial cultivation of human diploid cell strains.* Experimental cell research, 1961. **25**: p. 585-621.
53. Sherwood, S.W., et al., *Defining cellular senescence in IMR-90 cells: a flow cytometric analysis.* Proceedings of the National Academy of Sciences of the United States of America, 1988. **85**(23): p. 9086-90.
54. Vojta, P.J. and J.C. Barrett, *Genetic analysis of cellular senescence.* Biochimica et biophysica acta, 1995. **1242**(1): p. 29-41.

55. Cristofalo, V.J., et al., *Alterations in the responsiveness of senescent cells to growth factors.* Journal of gerontology, 1989. **44**(6): p. 55-62.
56. Goldstein, S., *Replicative senescence: the human fibroblast comes of age.* Science, 1990. **249**(4973): p. 1129-33.
57. Matsumura, T., Z. Zerrudo, and L. Hayflick, *Senescent human diploid cells in culture: survival, DNA synthesis and morphology.* Journal of gerontology, 1979. **34**(3): p. 328-34.
58. Hampel, B., et al., *Differential regulation of apoptotic cell death in senescent human cells.* Experimental gerontology, 2004. **39**(11-12): p. 1713-21.
59. Marcotte, R., C. Lacelle, and E. Wang, *Senescent fibroblasts resist apoptosis by downregulating caspase-3.* Mechanisms of ageing and development, 2004. **125**(10-11): p. 777-83.
60. Jackson, J.G. and O.M. Pereira-Smith, *p53 is preferentially recruited to the promoters of growth arrest genes p21 and GADD45 during replicative senescence of normal human fibroblasts.* Cancer research, 2006. **66**(17): p. 8356-60.
61. Dimri, G.P., et al., *A biomarker that identifies senescent human cells in culture and in aging skin in vivo.* Proceedings of the National Academy of Sciences of the United States of America, 1995. **92**(20): p. 9363-7.
62. Lee, B.Y., et al., *Senescence-associated beta-galactosidase is lysosomal beta-galactosidase.* Aging cell, 2006. **5**(2): p. 187-95.
63. Zhang, H., K.H. Pan, and S.N. Cohen, *Senescence-specific gene expression fingerprints reveal cell-type-dependent physical clustering of up-regulated chromosomal loci.* Proceedings of the National Academy of Sciences of the United States of America, 2003. **100**(6): p. 3251-6.
64. Kuilman, T. and D.S. Peeper, *Senescence-messaging secretome: SMS-ing cellular stress.* Nature reviews. Cancer, 2009. **9**(2): p. 81-94.
65. Coppe, J.P., et al., *Senescence-associated secretory phenotypes reveal cell-nonautonomous functions of oncogenic RAS and the p53 tumor suppressor.* PLoS biology, 2008. **6**(12): p. 2853-68.
66. Coppe, J.P., et al., *The senescence-associated secretory phenotype: the dark side of tumor suppression.* Annual review of pathology, 2010. **5**: p. 99-118.
67. Narita, M., et al., *Rb-mediated heterochromatin formation and silencing of E2F target genes during cellular senescence.* Cell, 2003. **113**(6): p. 703-16.
68. Narita, M., et al., *A novel role for high-mobility group a proteins in cellular senescence and heterochromatin formation.* Cell, 2006. **126**(3): p. 503-14.
69. Zhang, R., et al., *Formation of MacroH2A-containing senescence-associated heterochromatin foci and senescence driven by ASF1a and HIRA.* Developmental cell, 2005. **8**(1): p. 19-30.
70. Di Micco, R., et al., *Interplay between oncogene-induced DNA damage response and heterochromatin in senescence and cancer.* Nature cell biology, 2011. **13**(3): p. 292-302.
71. Collado, M., M.A. Blasco, and M. Serrano, *Cellular senescence in cancer and aging.* Cell, 2007. **130**(2): p. 223-33.
72. Campisi, J., *Cellular senescence as a tumor-suppressor mechanism.* Trends in cell biology, 2001. **11**(11): p. S27-31.
73. Vijg, J. and J. Campisi, *Puzzles, promises and a cure for ageing.* Nature, 2008. **454**(7208): p. 1065-71.
74. Freund, A., C.K. Patil, and J. Campisi, *p38MAPK is a novel DNA damage response-independent regulator of the senescence-associated secretory phenotype.* The EMBO journal, 2011. **30**(8): p. 1536-48.

75. Chan, S.W., et al., *Altering telomere structure allows telomerase to act in yeast lacking ATM kinases.* Current biology : CB, 2001. **11**(16): p. 1240-50.
76. de Lange, T., *Shelterin: the protein complex that shapes and safeguards human telomeres.* Genes & development, 2005. **19**(18): p. 2100-10.
77. Blasco, M.A., *Telomeres and human disease: ageing, cancer and beyond.* Nature reviews. Genetics, 2005. **6**(8): p. 611-22.
78. von Zglinicki, T., et al., *Human cell senescence as a DNA damage response.* Mechanisms of ageing and development, 2005. **126**(1): p. 111-7.
79. Harley, C.B., A.B. Futcher, and C.W. Greider, *Telomeres shorten during ageing of human fibroblasts.* Nature, 1990. **345**(6274): p. 458-60.
80. Stewart, S.A. and R.A. Weinberg, *Telomeres: cancer to human aging.* Annual review of cell and developmental biology, 2006. **22**: p. 531-57.
81. Muntoni, A. and R.R. Reddel, *The first molecular details of ALT in human tumor cells.* Human molecular genetics, 2005. **14 Spec No. 2**: p. R191-6.
82. Bodnar, A.G., et al., *Extension of life-span by introduction of telomerase into normal human cells.* Science, 1998. **279**(5349): p. 349-52.
83. Robles, S.J. and G.R. Adami, *Agents that cause DNA double strand breaks lead to p16INK4a enrichment and the premature senescence of normal fibroblasts.* Oncogene, 1998. **16**(9): p. 1113-23.
84. Di Leonardo, A., et al., *DNA damage triggers a prolonged p53-dependent G1 arrest and long-term induction of Cip1 in normal human fibroblasts.* Genes & development, 1994. **8**(21): p. 2540-51.
85. Chen, Q. and B.N. Ames, *Senescence-like growth arrest induced by hydrogen peroxide in human diploid fibroblast F65 cells.* Proceedings of the National Academy of Sciences of the United States of America, 1994. **91**(10): p. 4130-4.
86. Finkel, T. and N.J. Holbrook, *Oxidants, oxidative stress and the biology of ageing.* Nature, 2000. **408**(6809): p. 239-47.
87. Wahl, G.M. and A.M. Carr, *The evolution of diverse biological responses to DNA damage: insights from yeast and p53.* Nature cell biology, 2001. **3**(12): p. E277-86.
88. Han, Z., et al., *Role of p21 in apoptosis and senescence of human colon cancer cells treated with camptothecin.* The Journal of biological chemistry, 2002. **277**(19): p. 17154-60.
89. Shay, J.W. and I.B. Roninson, *Hallmarks of senescence in carcinogenesis and cancer therapy.* Oncogene, 2004. **23**(16): p. 2919-33.
90. Park, J.I., et al., *Hydroxyurea induces a senescence-like change of K562 human erythroleukemia cell.* Journal of cancer research and clinical oncology, 2000. **126**(8): p. 455-60.
91. Chang, B.D., et al., *A senescence-like phenotype distinguishes tumor cells that undergo terminal proliferation arrest after exposure to anticancer agents.* Cancer research, 1999. **59**(15): p. 3761-7.
92. Sherr, C.J. and R.A. DePinho, *Cellular senescence: mitotic clock or culture shock?* Cell, 2000. **102**(4): p. 407-10.
93. Lu, T. and T. Finkel, *Free radicals and senescence*. Experimental cell research, 2008. **314**(9): p. 1918-22.
94. Wei, S. and J.M. Sedivy, *Expression of catalytically active telomerase does not prevent premature senescence caused by overexpression of oncogenic Ha-Ras in normal human fibroblasts.* Cancer research, 1999. **59**(7): p. 1539-43.
95. Serrano, M., et al., *Oncogenic ras provokes premature cell senescence associated with accumulation of p53 and p16INK4a.* Cell, 1997. **88**(5): p. 593-602.

96. Kuilman, T., et al., *The essence of senescence.* Genes & development, 2010. **24**(22): p. 2463-79.
97. Wu, C.H., et al., *Cellular senescence is an important mechanism of tumor regression upon c-Myc inactivation.* Proceedings of the National Academy of Sciences of the United States of America, 2007. **104**(32): p. 13028-33.
98. Hydbring, P., et al., *Phosphorylation by Cdk2 is required for Myc to repress Ras-induced senescence in cotransformation.* Proceedings of the National Academy of Sciences of the United States of America, 2010. **107**(1): p. 58-63.
99. Chen, Z., et al., *Crucial role of p53-dependent cellular senescence in suppression of Pten-deficient tumorigenesis.* Nature, 2005. **436**(7051): p. 725-30.
100. Courtois-Cox, S., et al., *A negative feedback signaling network underlies oncogene-induced senescence.* Cancer cell, 2006. **10**(6): p. 459-72.
101. Ben-Porath, I. and R.A. Weinberg, *The signals and pathways activating cellular senescence.* The international journal of biochemistry & cell biology, 2005. **37**(5): p. 961-76.
102. Vandenberk, B., et al., *p16INK4a: A central player in cellular senescence and a promising aging biomarker in elderly cancer patients.* 2011. **2**(4): p. 259-269.
103. Canepa, E.T., et al., *INK4 proteins, a family of mammalian CDK inhibitors with novel biological functions.* IUBMB life, 2007. **59**(7): p. 419-26.
104. Ciccia, A. and S.J. Elledge, *The DNA damage response: making it safe to play with knives.* Molecular cell, 2010. **40**(2): p. 179-204.
105. Campisi, J., *Suppressing cancer: the importance of being senescent.* Science, 2005. **309**(5736): p. 886-7.
106. Bringold, F. and M. Serrano, *Tumor suppressors and oncogenes in cellular senescence.* Experimental gerontology, 2000. **35**(3): p. 317-29.
107. Li, D.M. and H. Sun, *PTEN/MMAC1/TEP1 suppresses the tumorigenicity and induces G1 cell cycle arrest in human glioblastoma cells.* Proceedings of the National Academy of Sciences of the United States of America, 1998. **95**(26): p. 15406-11.
108. Tresini, M., et al., *A phosphatidylinositol 3-kinase inhibitor induces a senescent-like growth arrest in human diploid fibroblasts.* Cancer research, 1998. **58**(1): p. 1-4.
109. Lloyd, R.V., et al., *p27kip1: a multifunctional cyclin-dependent kinase inhibitor with prognostic significance in human cancers.* The American journal of pathology, 1999. **154**(2): p. 313-23.
110. Collado, M. and M. Serrano, *Senescence in tumours: evidence from mice and humans.* Nature reviews. Cancer, 2010. **10**(1): p. 51-7.
111. Adams, P.D., *Healing and hurting: molecular mechanisms, functions, and pathologies of cellular senescence.* Molecular cell, 2009. **36**(1): p. 2-14.
112. Hanahan, D. and R.A. Weinberg, *The hallmarks of cancer.* Cell, 2000. **100**(1): p. 57-70.
113. Kim, W.Y. and N.E. Sharpless, *The regulation of INK4/ARF in cancer and aging.* Cell, 2006. **127**(2): p. 265-75.
114. Campisi, J., *Senescent cells, tumor suppression, and organismal aging: good citizens, bad neighbors.* Cell, 2005. **120**(4): p. 513-22.
115. Morton, J.P., et al., *Mutant p53 drives metastasis and overcomes growth arrest/senescence in pancreatic cancer.* Proceedings of the National Academy of Sciences of the United States of America, 2010. **107**(1): p. 246-51.

116. Ha, L., et al., *ARF functions as a melanoma tumor suppressor by inducing p53-independent senescence.* Proceedings of the National Academy of Sciences of the United States of America, 2007. **104**(26): p. 10968-73.
117. Herbig, U., et al., *Cellular senescence in aging primates.* Science, 2006. **311**(5765): p. 1257.
118. Minamino, T. and I. Komuro, *Vascular cell senescence: contribution to atherosclerosis.* Circulation research, 2007. **100**(1): p. 15-26.
119. Price, J.S., et al., *The role of chondrocyte senescence in osteoarthritis.* Aging cell, 2002. **1**(1): p. 57-65.
120. Wiemann, S.U., et al., *Hepatocyte telomere shortening and senescence are general markers of human liver cirrhosis.* FASEB journal : official publication of the Federation of American Societies for Experimental Biology, 2002. **16**(9): p. 935-42.
121. Roninson, I.B., *Tumor senescence as a determinant of drug response in vivo.* Drug resistance updates : reviews and commentaries in antimicrobial and anticancer chemotherapy, 2002. **5**(5): p. 204-8.
122. te Poele, R.H., et al., *DNA damage is able to induce senescence in tumor cells in vitro and in vivo.* Cancer research, 2002. **62**(6): p. 1876-83.
123. Roberson, R.S., et al., *Escape from therapy-induced accelerated cellular senescence in p53-null lung cancer cells and in human lung cancers.* Cancer research, 2005. **65**(7): p. 2795-803.
124. Roninson, I.B., *Tumor cell senescence in cancer treatment.* Cancer research, 2003. **63**(11): p. 2705-15.
125. Narath, R., et al., *Induction of senescence in MYCN amplified neuroblastoma cell lines by hydroxyurea.* Genes Chromosomes Cancer, 2007. **46**(2): p. 130-42.
126. Ambros, I.M., et al., *Neuroblastoma cells can actively eliminate supernumerary MYCN gene copies by micronucleus formation--sign of tumour cell revertance?* European journal of cancer, 1997. **33**(12): p. 2043-9.
127. Tumilowicz, J.J., et al., *Definition of a continuous human cell line derived from neuroblastoma.* Cancer research, 1970. **30**(8): p. 2110-8.
128. Biedler, J.L., L. Helson, and B.A. Spengler, *Morphology and growth, tumorigenicity, and cytogenetics of human neuroblastoma cells in continuous culture.* Cancer research, 1973. **33**(11): p. 2643-52.
129. Canute, G.W., et al., *Hydroxyurea accelerates the loss of epidermal growth factor receptor genes amplified as double-minute chromosomes in human glioblastoma multiforme.* Neurosurgery, 1996. **39**(5): p. 976-83.
130. Snapka, R.M. and A. Varshavsky, *Loss of unstably amplified dihydrofolate reductase genes from mouse cells is greatly accelerated by hydroxyurea.* Proceedings of the National Academy of Sciences of the United States of America, 1983. **80**(24): p. 7533-7.
131. Schulz, G., et al., *Detection of ganglioside GD2 in tumor tissues and sera of neuroblastoma patients.* Cancer research, 1984. **44**(12 Pt 1): p. 5914-20.
132. Svennerholm, L., et al., *Gangliosides and allied glycosphingolipids in human peripheral nerve and spinal cord.* Biochimica et biophysica acta, 1994. **1214**(2): p. 115-23.
133. Ponta, H., L. Sherman, and P.A. Herrlich, *CD44: from adhesion molecules to signalling regulators.* Nature reviews. Molecular cell biology, 2003. **4**(1): p. 33-45.

134. Fichter, M., et al., *Expression of CD44 isoforms in neuroblastoma cells is regulated by PI 3-kinase and protein kinase C.* Oncogene, 1997. **14**(23): p. 2817-24.
135. Liu, J. and G. Jiang, *CD44 and hematologic malignancies.* Cellular & molecular immunology, 2006. **3**(5): p. 359-65.
136. Ponti, D., et al., *Isolation and in vitro propagation of tumorigenic breast cancer cells with stem/progenitor cell properties.* Cancer research, 2005. **65**(13): p. 5506-11.
137. Shmelkov, S.V., et al., *CD133 expression is not restricted to stem cells, and both CD133+ and CD133- metastatic colon cancer cells initiate tumors.* The Journal of clinical investigation, 2008. **118**(6): p. 2111-20.
138. Gross, N., et al., *CD44H expression by human neuroblastoma cells: relation to MYCN amplification and lineage differentiation.* Cancer research, 1994. **54**(15): p. 4238-42.
139. Gross, N., K. Balmas, and C.B. Brognara, *Absence of functional CD44 hyaluronan receptor on human NMYC-amplified neuroblastoma cells.* Cancer research, 1997. **57**(7): p. 1387-93.
140. Wolfl, M., et al., *Expression of MHC class I, MHC class II, and cancer germline antigens in neuroblastoma.* Cancer immunology, immunotherapy : CII, 2005. **54**(4): p. 400-6.
141. Prigione, I., et al., *Immunogenicity of human neuroblastoma.* Annals of the New York Academy of Sciences, 2004. **1028**: p. 69-80.
142. Hicklin, D.J., F.M. Marincola, and S. Ferrone, *HLA class I antigen downregulation in human cancers: T-cell immunotherapy revives an old story.* Molecular medicine today, 1999. **5**(4): p. 178-86.
143. Corrias, M.V., et al., *Lack of HLA-class I antigens in human neuroblastoma cells: analysis of its relationship to TAP and tapasin expression.* Tissue antigens, 2001. **57**(2): p. 110-7.
144. Lampson, L.A., C.A. Fisher, and J.P. Whelan, *Striking paucity of HLA-A, B, C and beta 2-microglobulin on human neuroblastoma cell lines.* Journal of immunology, 1983. **130**(5): p. 2471-8.
145. Raffaghello, L., et al., *Multiple defects of the antigen-processing machinery components in human neuroblastoma: immunotherapeutic implications.* Oncogene, 2005. **24**(29): p. 4634-44.
146. Coughlin, C.M., et al., *Immunosurveillance and survivin-specific T-cell immunity in children with high-risk neuroblastoma.* Journal of clinical oncology : official journal of the American Society of Clinical Oncology, 2006. **24**(36): p. 5725-34.
147. Heitger, A. and S. Ladisch, *Gangliosides block antigen presentation by human monocytes.* Biochimica et biophysica acta, 1996. **1303**(2): p. 161-8.
148. Jensen, C., et al., *Complexity of the influence of gangliosides on histamine release from human basophils and rat mast cells.* Agents and actions, 1987. **21**(1-2): p. 79-82.
149. Ladisch, S., H. Becker, and L. Ulsh, *Immunosuppression by human gangliosides: I. Relationship of carbohydrate structure to the inhibition of T cell responses.* Biochimica et biophysica acta, 1992. **1125**(2): p. 180-8.
150. Ladisch, S., et al., *Modulation of the immune response by gangliosides. Inhibition of adherent monocyte accessory function in vitro.* The Journal of clinical investigation, 1984. **74**(6): p. 2074-81.

151. Miller, H.C. and W.J. Esselman, *Modulation of the immune response by antigen-reactive lymphocytes after cultivation with gangliosides.* Journal of immunology, 1975. **115**(3): p. 839-43.
152. Shen, W., et al., *Modulation of CD4 Th cell differentiation by ganglioside GD1a in vitro.* Journal of immunology, 2005. **175**(8): p. 4927-34.
153. Shen, W., et al., *Inhibition of TLR activation and up-regulation of IL-1R-associated kinase-M expression by exogenous gangliosides.* Journal of immunology, 2008. **180**(7): p. 4425-32.
154. Whisler, R.L. and A.J. Yates, *Regulation of lymphocyte responses by human gangliosides. I. Characteristics of inhibitory effects and the induction of impaired activation.* Journal of immunology, 1980. **125**(5): p. 2106-11.
155. Li, R.X. and S. Ladisch, *Shedding of human neuroblastoma gangliosides.* Biochimica et biophysica acta, 1991. **1083**(1): p. 57-64.
156. Rivoltini, L., et al., *Phenotypic and functional analysis of lymphocytes infiltrating paediatric tumours, with a characterization of the tumour phenotype.* Cancer immunology, immunotherapy : CII, 1992. **34**(4): p. 241-51.
157. Airoldi, I., et al., *Expression of costimulatory molecules in human neuroblastoma. Evidence that CD40+ neuroblastoma cells undergo apoptosis following interaction with CD40L.* British journal of cancer, 2003. **88**(10): p. 1527-36.
158. Main, E.K., et al., *Human neuroblastoma cell lines are susceptible to lysis by natural killer cells but not by cytotoxic T lymphocytes.* Journal of immunology, 1985. **135**(1): p. 242-6.
159. Rossi, A.R., et al., *Lysis of neuroblastoma cell lines by human natural killer cells activated by interleukin-2 and interleukin-12.* Blood, 1994. **83**(5): p. 1323-8.
160. Metelitsa, L.S., et al., *Human NKT cells mediate antitumor cytotoxicity directly by recognizing target cell CD1d with bound ligand or indirectly by producing IL-2 to activate NK cells.* Journal of immunology, 2001. **167**(6): p. 3114-22.
161. Seeger, R.C., *Immunology and immunotherapy of neuroblastoma.* Seminars in cancer biology, 2011. **21**(4): p. 229-37.
162. Raffaghello, L. and V. Pistoia, *Immunotherapy of neuroblastoma: present, past and future.* Expert review of neurotherapeutics, 2006. **6**(4): p. 509-18.
163. Tonini, G.P. and V. Pistoia, *Molecularly guided therapy of neuroblastoma: a review of different approaches.* Current pharmaceutical design, 2006. **12**(18): p. 2303-17.
164. Yu, A.L., et al., *Anti-GD2 antibody with GM-CSF, interleukin-2, and isotretinoin for neuroblastoma.* The New England journal of medicine, 2010. **363**(14): p. 1324-34.
165. Rakhra, K., et al., *CD4(+) T cells contribute to the remodeling of the microenvironment required for sustained tumor regression upon oncogene inactivation.* Cancer cell, 2010. **18**(5): p. 485-98.
166. Reimann, M., C.A. Schmitt, and S. Lee, *Non-cell-autonomous tumor suppression: oncogene-provoked apoptosis promotes tumor cell senescence via stromal crosstalk.* Journal of molecular medicine, 2011. **89**(9): p. 869-75.
167. Kang, T.W., et al., *Senescence surveillance of pre-malignant hepatocytes limits liver cancer development.* Nature, 2011. **479**(7374): p. 547-51.
168. Carson, J.P., et al., *Pharmacogenomic identification of targets for adjuvant therapy with the topoisomerase poison camptothecin.* Cancer research, 2004. **64**(6): p. 2096-104.
169. Djordjevic, B. and W. Szybalski, *Genetics of human cell lines. III. Incorporation of 5-bromo- and 5-iododeoxyuridine into the deoxyribonucleic acid of human cells*

and its effect on radiation sensitivity. The Journal of experimental medicine, 1960. **112**: p. 509-31.
170. Michishita, E., et al., *5-Bromodeoxyuridine induces senescence-like phenomena in mammalian cells regardless of cell type or species.* Journal of biochemistry, 1999. **126**(6): p. 1052-9.
171. Minagawa, S., et al., *Early BrdU-responsive genes constitute a novel class of senescence-associated genes in human cells.* Experimental cell research, 2005. **304**(2): p. 552-8.
172. Acosta, S., et al., *Comprehensive characterization of neuroblastoma cell line subtypes reveals bilineage potential similar to neural crest stem cells.* BMC developmental biology, 2009. **9**: p. 12.
173. Miller, J., ed. *Experiments in molecular genetics.* Cold Spring Harbor Laboratory, Cold Spring Harbor, New York.1972.
174. Ambros, P.F., et al., *International consensus for neuroblastoma molecular diagnostics: report from the International Neuroblastoma Risk Group (INRG) Biology Committee.* British journal of cancer, 2009. **100**(9): p. 1471-82.
175. Terman, A. and U.T. Brunk, *Lipofuscin: mechanisms of formation and increase with age.* APMIS : acta pathologica, microbiologica, et immunologica Scandinavica, 1998. **106**(2): p. 265-76.
176. Debacq-Chainiaux, F., et al., *Protocols to detect senescence-associated beta-galactosidase (SA-betagal) activity, a biomarker of senescent cells in culture and in vivo.* Nature protocols, 2009. **4**(12): p. 1798-806.
177. Bordow, S.B., et al., *Prognostic significance of MYCN oncogene expression in childhood neuroblastoma.* Journal of clinical oncology : official journal of the American Society of Clinical Oncology, 1998. **16**(10): p. 3286-94.
178. Tang, X.X., et al., *The MYCN enigma: significance of MYCN expression in neuroblastoma.* Cancer research, 2006. **66**(5): p. 2826-33.
179. Balajee, A.S. and C.R. Geard, *Replication protein A and gamma-H2AX foci assembly is triggered by cellular response to DNA double-strand breaks.* Experimental cell research, 2004. **300**(2): p. 320-34.
180. Sottile, F., et al., *A chemical screen identifies the chemotherapeutic drug topotecan as a specific inhibitor of the B-MYB/MYCN axis in neuroblastoma.* Oncotarget, 2012. **3**(5): p. 535-45.
181. Levkoff, L.H., et al., *Bromodeoxyuridine inhibits cancer cell proliferation in vitro and in vivo.* Neoplasia, 2008. **10**(8): p. 804-16.
182. Taupin, P., *BrdU immunohistochemistry for studying adult neurogenesis: paradigms, pitfalls, limitations, and validation.* Brain research reviews, 2007. **53**(1): p. 198-214.
183. Khanna, R., *Tumour surveillance: missing peptides and MHC molecules.* Immunology and cell biology, 1998. **76**(1): p. 20-6.
184. Zindy, F., et al., *Myc signaling via the ARF tumor suppressor regulates p53-dependent apoptosis and immortalization.* Genes & development, 1998. **12**(15): p. 2424-33.
185. Hydbring, P. and L.G. Larsson, *Cdk2: a key regulator of the senescence control function of Myc.* Aging, 2010. **2**(4): p. 244-50.
186. Molenaar, J.J., et al., *Inactivation of CDK2 is synthetically lethal to MYCN over-expressing cancer cells.* Proceedings of the National Academy of Sciences of the United States of America, 2009. **106**(31): p. 12968-73.

187. Morandi, E., et al., *Gene expression time-series analysis of camptothecin effects in U87-MG and DBTRG-05 glioblastoma cell lines.* Molecular cancer, 2008. **7**: p. 66.
188. Flatten, K., et al., *The role of checkpoint kinase 1 in sensitivity to topoisomerase I poisons.* The Journal of biological chemistry, 2005. **280**(14): p. 14349-55.
189. Huang, T.T., et al., *NF-kappaB activation by camptothecin. A linkage between nuclear DNA damage and cytoplasmic signaling events.* The Journal of biological chemistry, 2000. **275**(13): p. 9501-9.
190. Minderman, H., et al., *In vitro and in vivo irinotecan-induced changes in expression profiles of cell cycle and apoptosis-associated genes in acute myeloid leukemia cells.* Molecular cancer therapeutics, 2005. **4**(6): p. 885-900.
191. Masterson, J.C. and S. O'Dea, *5-Bromo-2-deoxyuridine activates DNA damage signalling responses and induces a senescence-like phenotype in p16-null lung cancer cells.* Anti-cancer drugs, 2007. **18**(9): p. 1053-68.
192. Passos, J.F., et al., *Feedback between p21 and reactive oxygen production is necessary for cell senescence.* Molecular systems biology, 2010. **6**: p. 347.
193. Liu, D. and P.J. Hornsby, *Senescent human fibroblasts increase the early growth of xenograft tumors via matrix metalloproteinase secretion.* Cancer research, 2007. **67**(7): p. 3117-26.
194. Nelson, G., et al., *A senescent cell bystander effect: senescence-induced senescence.* Aging cell, 2012. **11**(2): p. 345-9.
195. Floutsis, G., L. Ulsh, and S. Ladisch, *Immunosuppressive activity of human neuroblastoma tumor gangliosides.* International journal of cancer. Journal international du cancer, 1989. **43**(1): p. 6-9.
196. Kong, Y., et al., *Regulation of senescence in cancer and aging.* Journal of aging research, 2011. **2011**: p. 963172.

List of abbreviations

BrdU	Bromodeoxyuridine
BSA	Bovine Serum Albumin
CD44	Phagocytic Glycoprotein-1
CFSE	Carboxyfluorescein Diacetate Succinimidyl Ester
CM	conditioned medium
CPD	Cell Proliferation Dye
CPT	Camptothecin
CTL	Cytotoxic T lymphocytes
CTRL	control
DAPI	4'-6-Diamidino-2-phenylindole
DDR	DNA damage response
dmin	double minute chromosome
DNA	deoxyribonucleic acid
FACS	fluorescence activated cell sorting
F-cells	flat-cells
FISH	Fluorescence in situ hybridization
FITC	fluorescein isothiocyanate
Fsp	spontaneous F-cell
GD2	GD2 ganglioside
HEPES	(4-(2-hydroxyethyl)-1-piperazineethanesulfonic acid)
hsr	homogenously staining region
HU	Hyroxyurea
IC50	The half maximal inhibitory concentration
ind.	induced
MHC-1	major histocompatibility complex class 1
MNA	MYCN amplification
MTT	methylthiazolyldiphenyl-tetrazolium bromide
MYCN	v-myc myelocytomatosis viral related oncogene, neuroblastoma derived
NB	Neuroblastoma
NB-Ma	Neuroblastoma-Ma
N-cells	neuronal cells
PI	propidium iodide
RT	room temperature
SA-β-Gal	senescence-associated-β-galactosidase
SDS-PAGE	sodium dodecyl sulfate polyacrylamide gel electrophoresis
sp.F	spontaneous F-cell
STA-NB-10	St. Anna Neuroblastoma 10

Curriculum Vitae

Personal data

Name:	Nelli Frank
Date of birth:	05.03.1986
Place of birth:	Karaganda, Kasachstan
Citizenship:	German
Contact:	NelliF@gmx.de

Education

1992 – 1996	Albrecht-Dürer Grundschule Heilbronn, Germany
1996 – 2005	Robert-Mayer-Gymnasium Heilbronn, Germany
Since Oct. 2005	Studies of Molecular Biology at the University of Vienna, Austria

Research Experience

03/2009	Internship at the Max F. Perutz Laboratories (MFPL), University of Vienna Laboratory of Roland Foisner Focus: Lamins in nuclear organization
06/2009 – 07/2009	Internship at the MFPL, University of Vienna Laboratory of Friedrich Propst Focus: Neuronal cytoskeleton in axon guidance
08/2009	Internship at the MFPL, University of Vienna Laboratory of Marcela Hermann Focus: Apolipoproteins
03/2010 – 05/2010	Internship at the Center of Inflammation and Metabolism, Copenhagen, Denmark Laboratory of Bente Klarlund Pedersen Focus: Cytokine production of electrical stimulated muscle cells
Since Oct.2010	Diploma Thesis at the Children's Cancer Research Institute, Vienna, Laboratory of Peter Ambros Focus: Senescence in *MYCN* amplified neuroblastoma cells

Acknowledgements

I want to thank Peter Ambros for giving me the opportunity to do my diploma thesis in his group at the Children's Cancer Research Institute. I would like to thank him and his wife Inge Ambros for their suggestions and for their moral support. Moreover, I am very grateful to my practical supervisor Sabine Taschner-Mandl for her enormous guidance, patience, and support. Thank you, for always taking the time to answer all my questions, for the encouraging discussions and for keeping your cool whatever happened in the lab. Also, I want to thank my colleagues in the lab: Bettina Brunner and Andrea Ziegler, who supported me a lot with their practical knowledge and helped me with FISH and Western Blots. Further, special thanks to Eva Bozsaky and Dominik Bogen for their care and advice.
I also want to thank Julia Stemberger and Dieter Printz for technical support and for answering all FACS related questions. Generally, I also want to thank all members of the CCRI for the great work atmosphere and especially thanks to those people who shared nice moments with me also outside the institute.

Thank you to Roland Foisner for being the supervisor of my diploma thesis at the University of Vienna.

I owe my utmost gratitude to my parents and my sister for helping and encouraging me and for their inspiration and love. Without their great support I would never have been able to start and persevere at my studies in Vienna.